Linköping studies in science and technology. Dissertations.
No. 1409

Sensor Fusion for Automotive Applications

Christian Lundquist

Department of Electrical Engineering
Linköping University, SE–581 83 Linköping, Sweden

Linköping 2011

Cover illustration: The intensity map describes the density of stationary targets along the road edges. A photo of the the driver's view in the green car is shown in Figure 5a on Page 216.

Linköping studies in science and technology. Dissertations.
No. 1409

Sensor Fusion for Automotive Applications

Christian Lundquist

lundquist@isy.liu.se
www.control.isy.liu.se
Division of Automatic Control
Department of Electrical Engineering
Linköping University
SE–581 83 Linköping
Sweden

ISBN 978-91-7393-023-9 ISSN 0345-7524

Printed by LiU-Tryck, Linköping, Sweden 2011

To Nadia

Abstract

Mapping stationary objects and tracking moving targets are essential for many autonomous functions in vehicles. In order to compute the map and track estimates, sensor measurements from radar, laser and camera are used together with the standard proprioceptive sensors present in a car. By fusing information from different types of sensors, the accuracy and robustness of the estimates can be increased.

Different types of maps are discussed and compared in the thesis. In particular, road maps make use of the fact that roads are highly structured, which allows relatively simple and powerful models to be employed. It is shown how the information of the lane markings, obtained by a front looking camera, can be fused with inertial measurement of the vehicle motion and radar measurements of vehicles ahead to compute a more accurate and robust road geometry estimate. Further, it is shown how radar measurements of stationary targets can be used to estimate the road edges, modeled as polynomials and tracked as extended targets.

Recent advances in the field of multiple target tracking lead to the use of finite set statistics (FISST) in a set theoretic approach, where the targets and the measurements are treated as random finite sets (RFS). The first order moment of a RFS is called probability hypothesis density (PHD), and it is propagated in time with a PHD filter. In this thesis, the PHD filter is applied to radar data for constructing a parsimonious representation of the map of the stationary objects around the vehicle. Two original contributions, which exploit the inherent structure in the map, are proposed. A data clustering algorithm is suggested to structure the description of the prior and considerably improving the update in the PHD filter. Improvements in the merging step further simplify the map representation.

When it comes to tracking moving targets, the focus of this thesis is on extended targets, i.e., targets which potentially may give rise to more than one measurement per time step. An implementation of the PHD filter, which was proposed to handle data obtained from extended targets, is presented. An approximation is proposed in order to limit the number of hypotheses. Further, a framework to track the size and shape of a target is introduced. The method is based on measurement generating points on the surface of the target, which are modeled by an RFS.

Finally, an efficient and novel Bayesian method is proposed for approximating the tire radii of a vehicle based on particle filters and the marginalization concept. This is done under the assumption that a change in the tire radius is caused by a change in tire pressure, thus obtaining an indirect tire pressure monitoring system.

The approaches presented in this thesis have all been evaluated on real data from both freeways and rural roads in Sweden.

Populärvetenskaplig sammanfattning

Dagens bilar blir säkrare för varje år. Tidigare var det den passiva säkerheten med bilbälten, krockkuddar och krockzoner som förbättrades. Nu sker de snabbaste förändringarna inom aktiv säkerhet, med förarstödsystem såsom antisladd och nödbromssystem och förarvarningssystem för farliga filbyten och framförvarande hinder.

Förarstödsystem kräver omvärldsuppfattning, och de sensorer för detta som finns i bruk idag är kamera och radar. Kameran ser t.ex. filmarkeringar och kan användas för att detektera fordon och fotgängare. Radarn är mycket bra på att detektera rörliga objekt och på avståndsbedömning, och används idag för att följa bilen framför. Radarn ger en mängd information som idag är outnyttjad, och ett syfte med avhandlingen är att undersöka hur radarinformationen kan användas fullt ut i framtida säkerhetssystem.

Ett bidrag i avhandlingen är att använda radarns mätningar av stillastående objekt på och jämte vägen för att bygga upp en lokal karta. Kartan visar områden som är körbara och hinder som ska undvikas. Ett annat bidrag är att sortera alla de träffar från rörliga objekt som radarn registrerar och ge en noggrann karta över hur många andra fordon det finns, samt deras positioner, hastigheter och storlekar. Tillsammans bildar dessa två kartor en lägesbild som kan användas i nästa generations kollisionsundvikande system som kan kombinera broms och styringrepp för att på ett intelligent, säkert och kontrollerat sätt väja undan i kritiska nödsituationer.

En annan typ av säkerhetssystem är varningssystem till föraren på förändringar i fordonsdynamiska parametrar som kan försämra köregenskaperna. Exempel på sådana parametrar är däcktryck, friktion och fellastning. Ett bidrag i avhandlingen är ett nytt sätt att skatta en sänkning i däcktryck, genom att kombinera sensorer i fordonet med satellitnavigering.

De metoder som presenteras i avhandlingen har utvärderats på verkliga data från bland annat motorvägar och landsvägar i Sverige.

Acknowledgments

It all started in the end of the 80s, when my teacher asked me what I wanted to become when I grow up. I had only one wish, to study at Chalmers; followed by my answer my teacher laughed and told me “you will never make it, you are too stupid". This incentivized me, and encourage by other teachers I managed to finish school and be admitted at Chalmers. Several years later I’m now here and I have finished my thesis, something I would never have managed alone, without the support of many wonderful persons.

I would like to thank my supervisor professor Fredrik Gustafsson for his positive, inspiring, encouraging and relaxed attitude and my co-supervisor Dr. Thomas B. Schön for giving me a speedy start into academic research. Whenever I run into problems Dr. Umut Orguner, who possesses an enormous amount of knowledge about everything beyond least squares, pushed me in the right direction. Thank you for your help and for always having time. Further, I would like to acknowledge professor Svante Gunnarsson, who is a skillful head of the group, and his predecessor professor Lennart Ljung. They have created a wonderful research atmosphere which makes enjoyable going to office.

Part of the work has been performed with colleagues. I would like to mention Lic. Karl Granstöm, since one can’t find a better partner to collaborate with. Further I like to mention Dr. Lars Hammarstrand, at Chalmers, with whom I had very useful and interesting discussions. Finally, I would like to thank Dr. Emre Özkan, who opened the Gaussian window and let me see other distributions.

Andreas Andersson at Nira Dynamics AB and Dr. Andreas Eidehall at Volvo Personvagnar AB have rescued me from the simulation swamp, by supporting me with measurement data from prototype vehicles. Dr. Gustaf Hendeby and Dr. Henrik Tidefelt helped me with latex issues, without their support this thesis would not be in this professional shape. Ulla Salaneck, Åsa Karmelind and Ninna Stensgård have helped with many practical things during the years in the group.

An important part of the PhD studies is the time spent outside the office bunker, i.e., in the *fika* room and in pubs. I would like to thank Lic. Jonas Callmer, Lic. Karl Granström and Lic. Martin Skoglund for sharing *vagnen* with me. Further I would like to thank Lic. Christian Lyzell, Dr. Ragnar Wallin, Dr. Henrik Ohlsson Lic. Zoran Sjanic and Sina Khoshfetrat Pakazad for being generous and good friends.

Dr. Wolfgang Reinelt became a mentor for me, he supported and encouraged me during the time at ZF Lenksysteme GmbH. With him I wrote my first publications. My former boss Gerd Reimann taught me about vehicle dynamics and the importance of good experiments; I will always remember *Sinuslenken*.

One of the most inspiring persons I met is Dr. Peter Bunus. Together with professor Fredrik Gustafsson, Dr. David Törnqvist, Lic. Per Skoglar and Lic. Jonas Callmer we started SenionLab AB. I’m looking forward to keeping on working with all of them in the near future.

I would like to acknowledge the supported from the SEnsor fusion for Safety (SEFS) project within the Intelligent Vehicle Safety Systems (IVSS) program and the support from the Swedish Research Council under the frame project grant Extended Target Tracking.

I would never have been able to fulfill my wish to study without the support from my family, for this I am endlessly thankful. Finally, I would like to thank *amore della mia vita* Nadia, who has brought so much love and joy into my life.

Linköping, October 2011
Christian Lundquist

Contents

II Publications

Notation

Operators

Notation	Meaning
min	minimize
max	maximize
$\arg\min_x A$	the value x that minimizes A
$\arg\max_x A$	the value x that maximizes A
E	expectation
Cov	covariance
Var	variance
$\mathrm{diag}(a, b)$	diagonal matrix with elements a and b
$\mathrm{blkdiag}(A, B)$	Block diagonal matrix with matrices A and B
$\Pr(A)$	probability of event A
A^{T}	transpose of matrix A
Std	standard deviation
$\mathrm{Tr}(A)$	trace of matrix A
$\lvert x\rvert$	absolute value of x (or cardinality if x is a set)
$\hat{x}$	estimate of the stochastic variable x
$\triangleq$	equal by definition
$\sim$	is distributed according to
$\propto$	proportional to
$\in$	belongs to
$\dot{x}$	time derivative of x

Probability theory and Distributions

Notation	Meaning
iW	inverse Wishart distribution
D	intesity or PHD function
$\mathcal{N}$	normal or Gaussian distribution
NiW	normal inverse Wishart distribution
Pois	Poisson ditribution
St	student-t distribution
$\mathcal{U}$	uniform distribution
$p(x)$	density function of x
$p(x, y)$	joint density function of x and y
$p(x\|y)$	conditional density function of x given y

Sets

Notation	Meaning
$\mathbb{N}$	set of natural numbers
$\mathbf{M}$	set of map variables or features
$\mathbb{R}$	set of real numbers
$\mathbf{S}$	set of measurement generating points
$\mathbf{X}$	set of state variables
$\mathbf{Z}$	set of measurements
$N_{\mathbf{x}}$	number of elements in the set $\mathbf{X}$
$\emptyset$	empty set

Random Variables

Notation	Meaning
$\mathbf{x}$	state
$\mathbf{y}$	measurement (no data association needed)
$\mathbf{z}$	measurement (data association needed)
$\mathbf{u}$	input
P	state covariance
$\mathbf{w}$	process noise
Q	process noise covariance
$\mathbf{e}$	measurement noise
R	measurement noise covariance
$\mathbf{m}$	map state
$\mathbf{p}$	point feature
$\mathbf{s}$	state of a measurement generating point
$\boldsymbol{\theta}$	parameter
n_x	dimension of the vector $\mathbf{x}$
$\hat{\mathbf{x}}_{k\|\kappa}$	estimate of $\mathbf{x}$ at time given measurements $\mathbf{y}_{1:\kappa}$

Geometry and dynamics

Notation	Meaning
c	Cartesian representation
p	polar representation
x	Cartesian position x-coordinate (longitudinal)
y	Cartesian position y-coordinate (lateral)
z	Cartesian position z-coordinate (vertical)
w	width
l	length
a	acceleration
v	velocity
u, v	pixel coordinates
$\boldsymbol{d}$	displacement vector
r	range (between sensor and target)
ψ	heading angle, yaw angle or bearing (angle around z-axis)

Miscellaneous

Notation	Meaning
k	discrete time variable
T	sample time
l_b	wheel base (distance between front and rear axle)
l_t	wheel track (distance between left and right wheel)
c_o	road curvature
c_1	road curvature derivative

Abbreviations

Abbreviation	Meaning
ABS	antilock braking system
ACC	adaptive cruise control
C2C	car to car communication
CAN	controller area network
EIV	errors in variables
EIO	errors in output
EKF	extended Kalman filter
ELA	emergency lane assist
ET-GM-PHD	extended target Gaussian mixture probability hypothesis density
FISST	finite set statistics
FMCW	frequency modulated continuous-wave (a radar system)
GM-PHD	gaussian mixture probability hypothesis density
GNN	global nearest neighbor (data association)
GPS	global positioning system
IMU	inertial measurement unit
KF	Kalman filter
LKA	lane keeping assistance
LS	least Squares
MAE	mean absolute error
MAP	maximum a posteriori
MC	Monte Carlo (experiments based on repeated random sampling)
MGP	measurement generating point (reflection point on target)
ML	maximum likelihood
MPF	marginalized particle filter
NN	nearest neighbor (data association)
OGM	occupancy grid map
OLR	optical lane recognition
OSPA	optimal subpattern assignment (multitarget evaluation measure)
PDF	probability density function
PHD	probability hypothesis density
PF	particle Filter
RFS	random finite set
RMSE	root mean square error
SLAM	simultaneous localization and mapping
s.t.	subject to
UKF	unscented Kalman filter
virt	virtual sensor measurement
WLS	weighted least squares

Part I

Background

1

Introduction

This thesis is concerned with the problem of estimating the motion of a vehicle and the characteristics of its surroundings. More specifically, the description of the ego vehicle's surroundings consists of other vehicles and stationary objects as well as the geometry of the road. The signals from several different sensors, including camera, radar and inertial sensor, must be combined and analyzed to compute estimates of various quantities and to detect and classify many objects simultaneously. Sensor fusion allows the system to obtain information that is better than if it was obtained by individual sensors.

Situation awareness is the perception of environmental features, the comprehension of their meaning and the prediction of their status in the near future. It involves being aware of what is happening in and around the vehicle to understand how the subsystems impact on each other.

Sensor fusion is introduced in Section 1.1 and its application within the automotive community is briefly discussed in Section 1.2. The study presented in this thesis was conducted within two Swedish research project, briefly described in Section 1.3 and 1.4. The sensor fusion framework and its components, such as infrastructure, estimation algorithms and various mathematical models, are all introduced in Section 1.5. Finally, the chapter is concluded with an overview of the author's publications in Section 1.6, a statement of the contributions in Section 1.7 and the outline of this thesis given in Section 1.8.

1.1 Sensor Fusion

Sensor fusion is the process of using information from several different sensors to compute an estimate of the state of a dynamic system. The resulting estimate is

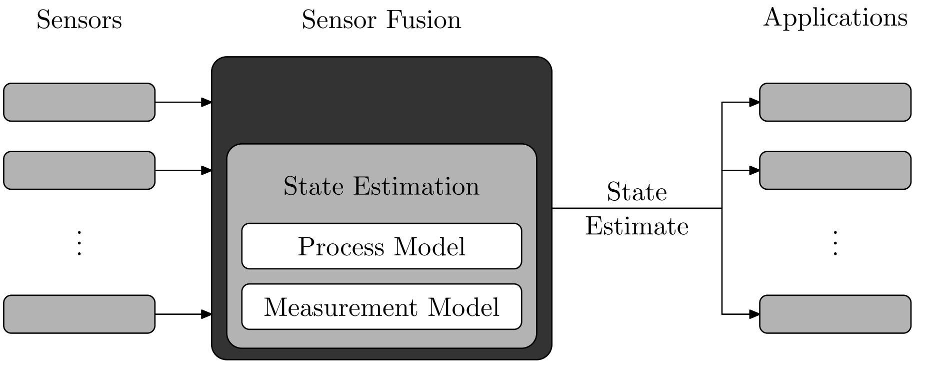

Figure 1.1: The main components of the sensor fusion framework are shown in the middle box. The framework receives measurements from several sensors, fuses them and produces one state estimate, which can be used by several applications.

in some sense better than it would be if the sensors were used individually. The term better can in this case mean more accurate, more reliable, more available and of higher safety integrity. Furthermore, the resulting estimate may in some cases only be possible to obtain by using data from different types of sensors. Figure 1.1 illustrates the basic concept of the sensor fusion framework. Many systems have traditionally been stand alone systems with one or several sensors transmitting information to only one single application. Using a sensor fusion approach it might be possible to remove one sensor and still perform the same tasks, or add new applications without the need to add new sensors.

Sensor fusion is required to reduce cost, system complexity and the number of components involved and to increase accuracy and confidence of sensing.

1.2 Automotive Sensor Fusion

Within the automotive industry there is currently a huge interest in active safety systems. External sensors are increasingly important and typical examples used in this work are radar sensors and camera systems. Today, a sensor is usually connected to a single function. However, all active safety functions need information about the state of the ego vehicle and its surroundings, such as the lane geometry and the position of other vehicles. The use of signal processing and sensor fusion to replace redundant and costly sensors with software attracted recent attention in the IEEE Signal Processing Magazine (Gustafsson, 2009).

The sensors in a modern passenger car can be divided into a number of subgroups; there are internal sensors measuring the motion of the vehicle, external sensors measuring the objects surrounding the vehicle and there are sensors communicating with other vehicles and with the infrastructure. The communication between sensors, fusion framework, actuators and controllers is made possible by the controller area network (CAN). It is a serial bus communication protocol developed by Bosch in the early 1980s and presented by Kiencke et al. (1986) at the SAE international congress in Detroit. An overview of the CAN bus, which has become the *de facto* standard for automotive communication, is given in Johansson et al. (2005).

Internal sensors are often referred to as proprioceptive sensors in the literature. Typical examples are gyroscopes, primarily measuring the yaw rate about the vehicle's vertical axis, and accelerometers, measuring the longitudinal and lateral acceleration of the vehicle. The velocity of the vehicle is measured using inductive wheel speed sensors and the steering wheel position is measured using an angle sensor. External sensors are referred to as exteroceptive sensors in the literature, typical examples are radar (RAdio Detection And Ranging), lidar (LIght Detection And Ranging) and cameras.

An example of how a radar and a camera may be mounted in a passenger car is illustrated in Figure 1.2. These two sensors complement each other very well, since the advantage of the radar is the disadvantage of the camera and vice versa. A summary of the two sensors' properties is presented in Table 1.1 and in e.g., Jansson (2005).

As already mentioned, the topic of this thesis is how to estimate the state variables describing the ego vehicle's motion and the characteristics of its surroundings. The ego vehicle is one subsystem, labeled (E) in this work. The use of data from the vehicle's actuators, e.g., the transmission and the steering wheel, to estimate a change in position over time is referred to as odometry. The ego vehicle's surroundings consists of other vehicles, referred to as targets (T), and stationary objects as well as the shape and the geometry of the road (R). Mapping is the problem of integrating the information obtained by the sensors into a given representation, denoted (M), see Adams et al. (2007) for a recent overview and Thrun (2002) for an older survey. Simultaneous localization and mapping (SLAM) is an approach used by autonomous vehicles to build a map while at the

Table 1.1: *Properties of radar and camera for object detection*

	Camera	**Radar**
Detects	other vehicles, lane markings, pedestrians	other vehicles, stationary objects
Classifies objects	yes	no
Azimuth angle	high accuracy	medium accuracy
Range	low accuracy	very high accuracy
Range rate	not	very high accuracy
Field of View	wide	narrow
Weather Conditions	sensitive to bad visibility	less sensitive

(a) *(b)*

Figure 1.2: *Figure (a) shows the camera and Figure (b) the front looking radar in a Volvo S60 production car. Courtesy of Volvo Car Corporation.*

same time keeping track of their current locations, see e.g., Durrant-Whyte and Bailey (2006); Bailey and Durrant-Whyte (2006). This approach is not treated in this thesis.

1.3 Sensor Fusion for Safety

Parts of the work in this thesis have been performed within the research project *Sensor Fusion for Safety* (SEFS), which is funded by the Swedish *Intelligent Vehicle Safety Systems* (IVSS) program. The project is a collaboration between Volvo Technology, Volvo Cars, Volvo Trucks, Mecel, Chalmers University of Technology and Linköping University.

The overall objective of this project is to obtain sensor fusion competence for automotive safety applications in Sweden by doing research within relevant areas. This goal is achieved by developing a sensor fusion platform, algorithms, modeling tools and a simulation platform. More specifically, the aim is to develop general methods and algorithms for a sensor fusion system utilizing information from all available sensors in a modern passenger car. The sensor fusion will provide a refined description of the vehicle's environment that can be used by a number of different safety functions. The integration of the data flow requires new specifications with respect to sensor signals, hardware, processing, architectures and reliability.

The SEFS work scope is divided into a number of work packages. These include at a top level, fusion structure, key scenarios and the development of requirement methods. The next level consists in work packages such as pre-processing and modeling, the implementation of a fusion platform and research done on fusion algorithms, into which this thesis can be classified. The use-case work package consists of implementation of software and design of prototypes and demonstrators. Finally, there is an evaluation and validation work package.

During the runtime of the SEFS project, i.e., from 2005 until 2009, three PhD theses (Schön, 2006; Gunnarsson, 2007; Danielsson, 2010) and three licentiate theses (Bengtsson, 2008; Danielsson, 2008; Lundquist, 2009) have been produced. An overview of the main results in the project is given in Ahrholdt et al. (2009) and the sensor fusion framework is well described in Bengtsson and Danielsson (2008). Furthermore it is worth mentioning some of the publications produced by the project partners. Motion models for tracked vehicles are covered in Svensson and Gunnarsson (2006); Gunnarsson et al. (2006); Sörstedt et al. (2011). A better sensor model of the tracked vehicle is presented in Gunnarsson et al. (2007). Detection of lane departures and lane changes of leading vehicles is studied in Schön et al. (2006), with the goal to increase the accuracy of the road geometry estimate. Computational complexity for systems obtaining data from sensors with different sampling rates and different noise distributions is studied in Schön et al. (2007).

Paper D in this thesis describes a method to estimate and represent stationary objects along the road edges. This publication is based on data collected from the SEFS prototype car and the work was carried out within the project.

1.4 Extended Target Tracking

The final parts of the work in the thesis have been performed within the frame project grant *Extended Target Tracking* (621-2010-4301), founded by the Swedish Research Council. This research project started in 2011 and lasts until 2014. The overall goal is to study new ways of representing targets and their posterior distribution. The work is performed for different types of imagery sensors, such as camera, radar and laser. More specifically the purpose of the project is to study different options to extend the state vector of the target with specific and unusual features, such as physical size and shape, physical properties, colors etc.

So far only a few articles, which relates to the work presented in this thesis, have been published in the project. It is worth mentioning the following publications. An approach to track bicycles from imagery sensor data is proposed by Ardeshiri et al. (2011). It is based on detecting ellipsoids in the images, and treat these pairwise using a dynamic bicycle model. Wahlström et al. (2011) shows theoretically and experimentally that the position and heading of a moving metallic target can be tracked using two magnetometers placed on the ground, for surveillance and traffic monitoring applications.

The Papers E and F in this thesis are produced within the extended target tracking project. In these papers new approaches are proposed to represent and estimate the position and size of targets which, due to their size, might generate more than one measurement per time step.

1.5 Components of the Sensor Fusion Framework

A systematic approach to handle sensor fusion problems is provided by nonlinear state estimation theory. Estimation problems are handled using discrete-time model based methods. The systems discussed in this thesis are primarily dynamic and they are modeled using stochastic difference equations. More specifically, the systems are modeled using the *discrete-time nonlinear state space model*

$$\mathbf{x}_{k+1} = f_k(\mathbf{x}_k, \mathbf{u}_k, \mathbf{w}_k, \boldsymbol{\theta}_k), \tag{1.1a}$$

$$\mathbf{y}_k = h_k(\mathbf{x}_k, \mathbf{u}_k, \mathbf{e}_k, \boldsymbol{\theta}_k), \tag{1.1b}$$

where (1.1a) describes the evolution of the state variable $\mathbf{x}$ over time and (1.1b) explains how the *state variable* $\mathbf{x}$ relates to the *measurement* $\mathbf{y}$[1]. The state vector at time k is denoted by $\mathbf{x}_k \in \mathbb{R}^{n_x}$, with elements $x_1, \dots, x_{n_x}$ being real numbers. Sensor observations collected at time k are denoted by $\mathbf{y}_k \in \mathbb{R}^{n_y}$, with elements $y_1, \dots, y_{n_y}$ being real numbers. The model f_k in (1.1a) is referred to as the *process model*, the *motion model*, the dynamic model or the system model, and it describes how the state propagates in time. The model h_k in (1.1b) is referred to as the *measurement model* or the *sensor model* and it describes how the state is propagated into the measurement space. The random vector $\mathbf{w}_k$ describes the process noise, which models the fact that the actual state dynamics is usually unknown. The random vector $\mathbf{e}_k$ describes the sensor noise. Furthermore, $\mathbf{u}_k$ denotes the deterministic input signals and $\boldsymbol{\theta}_k$ denotes the possibly unknown parameter vector of the model.

The ego vehicle constitutes an important dynamic system in this thesis. The yaw and lateral dynamics are modeled using the so called single track model. This model will be used as an example throughout the thesis. Some of the variables and parameters in the model are introduced in Example 1.1.

1.1 Example: Single Track Ego Vehicle Model

A so called bicycle model is obtained if the wheels at the front and the rear axle of a passenger car are modeled as single wheels. This type of model is also referred to as a single track model and a schematic drawing is given in Figure 1.3. Some examples of typical variables and parameters are:

State variables x: the yaw rate $\dot{\psi}_E$ and the body side slip angle β, i.e.,

$$\mathbf{x} = \begin{bmatrix} \dot{\psi}_E & \beta \end{bmatrix}^{\mathrm{T}}. \tag{1.2}$$

Measurements y: the yaw rate $\dot{\psi}_E$ and the lateral acceleration $\mathsf{a_y}$, i.e.,

$$\mathbf{y} = \begin{bmatrix} \dot{\psi}_E & \mathsf{a_y} \end{bmatrix}^{\mathrm{T}}, \tag{1.3}$$

which both are measured by an inertial measurement unit (IMU).

Input signals u: the steering wheel angle δ_s, which is measured with an angular sensor at the steering column and the velocity $\dot{\mathsf{v}}$, which is measured by

[1] Note that the measurement vector is denoted $\mathbf{y}$ when the sensor measures one or several specific quantities, e.g., acceleration and yaw rate from an IMU sensor. However, when the number of sensor measurements (observations) depends on the environmental circumstances the measurement vector is denoted $\mathbf{z}$, e.g., for a radar which observes an unknown number of targets. This usually leads to a data association problem.

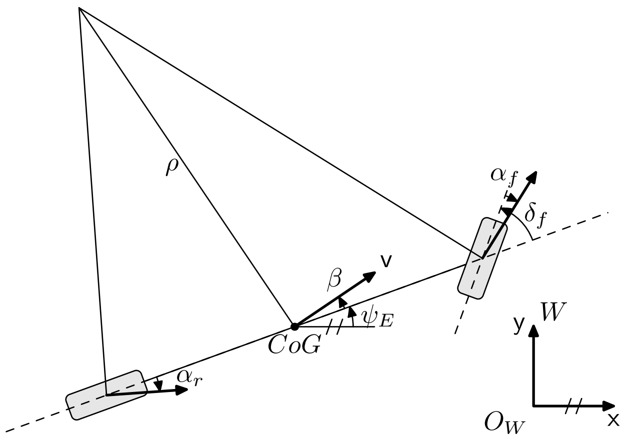

Figure 1.3: *Illustration of the geometry for the single track model, describing the motion of the ego vehicle. The ego vehicle velocity vector* v *is defined from the center of gravity (CoG) and its angle to the longitudinal axis of the vehicle is denoted by β, referred to as the body side slip angle. Furthermore, the slip angles are referred to as α_f and α_r. The front wheel angle is denoted by δ_f and the current driven radius is denoted by ρ.*

wheel speed sensors, i.e.,

$$\mathbf{u} = \begin{bmatrix} \delta_s & \mathsf{v} \end{bmatrix}^{\mathrm{T}}. \tag{1.4}$$

Parameters $\boldsymbol{\theta}$: the vehicle mass m, which is weighed before the tests, the steering ratio i_s between the steering wheel angle and the front wheels, which has to be estimated in advance, and the tire parameter C_α, which is estimated on-line, since the parameter value changes due to different road and weather conditions.

The nonlinear models f and h are specified in Chapter 2.

The model (1.1) must describe the essential properties of the system, but it must also be simple enough to be efficiently used within a state estimation algorithm. Chapter 3 describes algorithms that are used to compute estimates of the state $\mathbf{x}_k$ and the parameter $\boldsymbol{\theta}_k$ in (1.1).

Before describing the individual steps of the sensor fusion framework another important example is presented in Example 1.2.

1.2 Example: Object Tracking

Other objects, such as vehicles or stationary objects on and along the road, are tracked using measurements from a radar mounted in the ego vehicle. A simple model for one such tracked object is given by using the following variables:

State variables x: Cartesian position of tracked targets $i = 1, \dots, N_\mathbf{x}$ in a world fixed coordinate frame W, i.e., $\mathbf{x}^{(i)} = \begin{bmatrix} \mathrm{x}^W & \mathrm{y}^W \end{bmatrix}^\mathrm{T}$.

Measurements z: Range and azimuth angle to objects $m = 1, \dots, N_\mathbf{z}$ measured by the radar in the ego vehicle fixed coordinate frame E, i.e., $\mathbf{z}^{(m)} = \begin{bmatrix} r^E & \psi \end{bmatrix}^\mathrm{T}$.

At every time step k, $N_\mathbf{z}$ observations are obtained by the radar. Hence, the radar delivers $N_\mathbf{z}$ range and azimuth measurements in a multi-sensor set $\mathbf{Z} = \left\{\mathbf{z}^{(1)}, \dots, \mathbf{z}^{(N_\mathbf{z})}\right\}$ to the sensor fusion framework. The sensor fusion framework currently also tracks $N_\mathbf{x}$ targets. The multi-target state is given by the set $\mathbf{X} = \left\{\mathbf{x}^{(1)}, \dots, \mathbf{x}^{(N_\mathbf{x})}\right\}$ where $\mathbf{x}^{(1)}, \dots, \mathbf{x}^{(N_\mathbf{x})}$ are the individual states.

Obviously, the total number of state variables in the present example is $2N_\mathbf{x}$ and the total number of measurements is $2N_\mathbf{z}$. This issue may be compared to Example 1.1, where the size of the $\mathbf{y}$-vector corresponds to the total number of measurements at time k. Typically, the radar also observes false detections, referred to as clutter, or receives several measurements from the same target, i.e., $N_\mathbf{z}$ is seldom equal to $N_\mathbf{x}$ for radar sensors.

The different steps of a typical sensor fusion algorithm, as the central part of the larger framework, are shown in Figure 1.4. The algorithm is initiated using a prior guess of the state $\mathbf{x}_0$ or, if it is not the first iteration, the state estimate $\hat{\mathbf{x}}_{k-1|k-1}$ from the previous time step $k-1$ is used. New measurements $\mathbf{Z}_k$ are collected from the sensors and *preprocessed* at time k. Model (1.1) is used to *predict* the state estimate $\hat{\mathbf{x}}_{k|k-1}$ and the measurement $\hat{\mathbf{z}}_{k|k-1}$. For Example 1.2 it is necessary to *associate* the radar observations $\mathbf{Z}_k$ with the predicted measurements $\widehat{\mathbf{Z}}_{k|k-1}$ of the existing state estimates and to *manage the tracks*, i.e., initiate new states and remove old, invalid states. The data association and track management are further discussed in Section 4.2. Finally, the new measurement $\mathbf{z}_k$ is used to calculate the state estimate $\hat{\mathbf{x}}_{k|k}$ at time k in the so called *measurement update* step. The prediction and measurement update are described in Section 3.2. This algorithm is iterated, $\hat{\mathbf{x}}_{k|k}$ is used to predict $\hat{\mathbf{x}}_{k+1|k}$, new measurements $\mathbf{Z}_{k+1}$ are collected at time $k+1$ and so on. The state estimation theory, as part of the sensor fusion framework, is discussed further in Chapter 3. Note that in Example 1.1, the data association and track management are obviously not needed, since there the data association is assumed fixed. In the example the measurements $\mathbf{y}$ from the pre-processing are fed directly to the measurement update.

1.6 Publications

Published work of the author that are of relevance to this thesis are listed below. The publications are clustered in groups preambled by a short summary. The publications are principally listed in chronological order.

The author has been involved in the development of an active steering system prior to starting his PhD-studies. The active steering system superimposes an

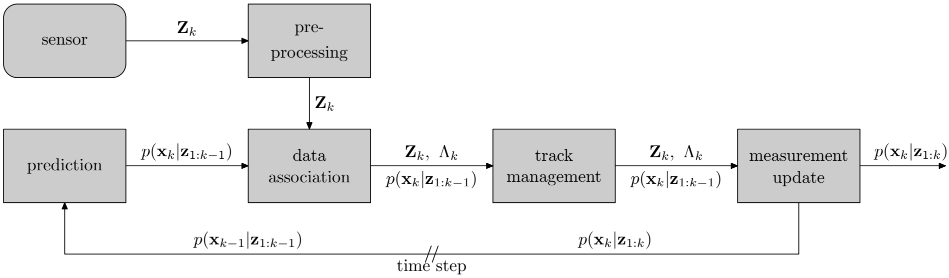

Figure 1.4: *The new measurements* $\mathbf{Z}_k$ *contain new information and are* associated *to the* predicted *states* $\widehat{\mathbf{X}}_{k|k-1}$ *and thereafter used to* update *them to obtain the improved state estimates* $\widehat{\mathbf{X}}_{k|k}$.

electronically controlled angle to the driver's steering input. The aim of the system is to reduce the driver's steering efforts at low velocities, to reduce the vehicle's sensibility at very high velocities and to intervene when the vehicle tends to become unstable. The system is thoroughly described in

W. Reinelt and C. Lundquist. Mechatronische Lenksysteme: Modellbildung und Funktionalität des Active Front Steering. In R. Isermann, editor, *Fahrdynamik Regelung - Modellbildung, Fahrassistenzsysteme, Mechatronik*, pages 213–236. Vieweg Verlag, September 2006a.

W. Reinelt, W. Klier, G. Reimann, C. Lundquist, W. Schuster, and R. Großheim. Active front steering for passenger cars: System modelling and functions. In *Proceedings of the IFAC Symposium on Advances in Automotive Control*, Salerno, Italy, April 2004.

Sensor fusion based monitoring systems are described in

W. Reinelt, C. Lundquist, and H. Johansson. On-line sensor monitoring in an active front steering system using extended Kalman filtering. In *Proceedings of the SAE World Congress*, SAE paper 2005-01-1271, Detroit, MI, USA, April 2005.

W. Reinelt and C. Lundquist. Observer based sensor monitoring in an active front steering system using explicit sensor failure modeling. In *Proceedings of the IFAC World Congress*, Prague, Czech Republic, July 2005.

S. Malinen, C. Lundquist, and W. Reinelt. Fault detection of a steering wheel sensor signal in an active front steering system. In *Preprints of the IFAC Symposium on SAFEPROCESS*, pages 547–552, Beijing, China, August 2006.

C. Lundquist and W. Reinelt. Electric motor rotor position monitoring method for electrically aided steering system e.g. steer by wire,

for motor vehicle, involves outputting alarm when difference between measurement value and estimated value of motor exceeds threshold. German Patent Application DE 102005016514 October 12, 2006, Priority date April 8, 2006.

W. Reinelt, C. Lundquist, and S. Malinen. Automatic generation of a computer program for monitoring a main program to provide operational safety. German Patent Application DE 102005049657 April 19, 2007, Priority date October 18, 2005.

W. Reinelt, W. Schuster, R. Großheim, and C. Lundquist. Operating method for electronic servo steering system of vehicle, involves presetting steering wheel angle by steering mechanism as measure for desired wheel turning angle for steering wheel of vehicle. German Patent Application DE 102006052092 May 8, 2008, Priority date November 4, 2006.

W. Reinelt, W. Schuster, R. Großheim, and C. Lundquist. Electronic servo steering system operating method for motor vehicle, involves recognizing track misalignment of vehicle when forces differentiate around preset value from each other at preset period of time in magnitude and/or direction. German Patent DE 102006043069 December 3, 2009, Priority date September 14, 2006.

W. Reinelt, W. Schuster, R. Großheim, and C. Lundquist. Motor vehicle's electronically regulated servo steering system operating method, involves comparing actual value of measured value with stored practical value of corresponding measured value. German Patent DE 10 2006 040 443 January 27, 2011, Priority date August 29, 2006.

Sensor fusion based utility functions to improve driving comfort, safety or agility are described in

W. Reinelt, W. Schuster, R. Großheim, and C. Lundquist. Operating method for electronic power-assisted steering system of vehicle, involves overlapping additional angle, which is disabled after re-start of utility function. German Patent Application DE 102006041236 Mars 6, 2008, Priority date September 2, 2006a.

W. Reinelt, W. Schuster, R. Großheim, and C. Lundquist. Operating method for electronic power-assisted steering system of vehicle, involves re-starting utility function, and after re-start of utility function superimposition of additional angle is unlatched. German Patent DE 102006041237 December 3, 2009, Priority date September 2, 2006b.

G. Reimann and C. Lundquist. Method for operating electronically controlled servo steering system of motor vehicle, involves determining steering wheel angle as measure for desired steering handle angle by steering handle for steering wheels of motor vehicle. German

Patent Application DE 102006053029 May 15, 2008, Priority date November 10, 2006.

C. Lundquist and R. Großheim. Method and device for determining steering angle information. German Patent Application DE 10 2007 000 958 Mai 14, 2009, International Patent Application WO 2009 047 020 April 16, 2009 and European Patent Application EP 2205478 April 16, 2009, Priority date October 2, 2007.

A reverse driving assistant for passenger cars with trailers based on sensor data of the angle between car and trailer is presented in

C. Lundquist and W. Reinelt. Rückwärtsfahrassistent für PKW mit Aktive Front Steering. In *Proceedings of the AUTOREG (Steuerung und Regelung von Fahrzeugen und Motoren*, VDI Bericht 1931, pages 45–54, Wiesloch, Germany, March 2006b.

C. Lundquist and W. Reinelt. Back driving assistant for passenger cars with trailer. In *Proceedings of the SAE World Congress*, SAE paper 2006-01-0940, Detroit, MI, USA, April 2006a.

W. Reinelt and C. Lundquist. Method for assisting the driver of a motor vehicle with a trailer when reversing. German Patent DE 10 2006 002 294 February 24, 2011, European Patent Application EP 1810913 July 25, 2007 and Japanese Patent Application JP 2007191143 August 2, 2007, Priority date January 18, 2006.

Furthermore, a control system which stabilizes a vehicle trailer combination, based on the same sensor information as the publications listed above, is described in

C. Lundquist. Method for stabilizing a vehicle combination. U.S. Patent US 8010253 August 30, 2011 and German Patent Application DE 102007008342 August 21, 2008, Priority date February 20, 2007.

The functional safety concept for the active steering system, among others including a sensor fusion based monitoring system, is described in

W. Reinelt and C. Lundquist. Controllability of active steering system hazards: From standards to driving tests. In Juan R. Pimintel, editor, *Safety Critical Automotive Systems*, pages 173–178. SAE International, 400 Commonwealth Drive, Warrendale, PA, USA, August 2006b.

During his time as a PhD student the author has been involved in the following publications. Starting with road geometry estimation, i.e., describing the curvature of the lane, which is covered in

C. Lundquist and T. B. Schön. Road geometry estimation and vehicle tracking using a single track model. In *Proceedings of the IEEE Intelligent Vehicles Symposium*, pages 144–149, Eindhoven, The Netherlands, June 2008.

C. Lundquist and T. B. Schön. Joint ego-motion and road geometry estimation. *Information Fusion*, 12:253–263, October 2011.

Road edge estimation primarily aims to estimate the position and shape of stationary objects next to the road. Two approaches have been studied; road edges modeled as extended targets are described in

C. Lundquist and T. B. Schön. Estimation of the free space in front of a moving vehicle. In *Proceedings of the SAE World Congress*, SAE paper 2009-01-1288, Detroit, MI, USA, April 2009a.

C. Lundquist, U. Orguner, and T. B. Schön. Tracking stationary extended objects for road mapping using radar measurements. In *Proceedings of the IEEE Intelligent Vehicles Symposium*, pages 405–410, Xi'an, China, June 2009.

C. Lundquist, U. Orguner, and F Gustafsson. Estimating polynomial structures from radar data. In *Proceedings of the International Conference on Information Fusion*, Edinburgh, UK, July 2010b.

C. Lundquist, U. Orguner, and F. Gustafsson. Extended target tracking using polynomials with applications to road-map estimation. *IEEE Transactions on Signal Processing*, 59(1):15–26, January 2011c.

and an approach where the stationary objects along the road are represented by an intensity map is presented in

C. Lundquist, L. Danielsson, and F. Gustafsson. Random set based road mapping using radar measurements. In *Proceedings of the European Signal Processing Conference*, pages 219–223, Aalborg, Denmark, August 2010a.

C. Lundquist, L. Hammarstrand, and F. Gustafsson. Road intensity based mapping using radar measurements with a probability hypothesis density filter. *IEEE Transactions on Signal Processing*, 59(4):1397–1408, April 2011b.

A method to on-line estimate the cornering stiffness parameters of the tires is presented in

C. Lundquist and T. B. Schön. Recursive identification of cornering stiffness parameters for an enhanced single track model. In *Proceedings of the IFAC Symposium on System Identification*, pages 1726–1731, Saint-Malo, France, July 2009b.

An overview of the results from the SEFS project, and specifically an overview about mapping techniques, is given in

M. Ahrholdt, F. Bengtsson, L. Danielsson, and C. Lundquist. SEFS – results on sensor data fusion system development. In *Proceedings of the World Congress on Intelligent Transportation Systems and Services*, Stockholm, Sweden, September 2009.

C. Lundquist. *Automotive Sensor Fusion for Situation Awareness*. Licentiate Thesis No 1422, Department of Electrical Engineering, Linköping University, Sweden, 2009.

C. Lundquist, T. B. Schön, and F. Gustafsson. Situational awareness and road prediction for trajectory control applications. In A. Eskandarian, editor, *Handbook of Intelligent Vehicles*, chapter 24. Springer, November 2011e.

Extended target tracking with a PHD filter is described in

K. Granström, C. Lundquist, and U Orguner. A Gaussian mixture PHD filter for extended target tracking. In *Proceedings of the International Conference on Information Fusion*, Edinburgh, UK, July 2010.

C. Lundquist, K. Granström, and U. Orguner. Estimating the shape of targets with a PHD filter. In *Proceedings of the International Conference on Information Fusion*, Chicago, IL, USA, July 2011a.

U. Orguner, C. Lundquist, and K. Granström. Extended target tracking with a cardinalized probability hypothesis density filter. In *Proceedings of the International Conference on Information Fusion*, pages 65–72, Chicago, IL, USA, July 2011.

K. Granström, C. Lundquist, and U Orguner. Tracking rectangular and elliptical extended targets using laser measurements. In *Proceedings of the International Conference on Information Fusion*, Chicago, IL, USA, July 2011b.

K. Granström, C. Lundquist, and U. Orguner. Extended target tracking using a Gaussian-mixture PHD filter. *IEEE Transactions on Aerospace and Electronic Systems*, 2011a. Under review.

An approach to use camera data to improve the position estimate of a vehicle is presented in

E. Nilsson, C. Lundquist, T. B. Schön, D. Forslund, and J. Roll. Vehicle motion estimation using an infrared camera. In *Proceedings of the World Congress of the International Federation of Automatic Control*, Milan, Italy, August 2011.

A marginalized particle filter based method to estimate the tire radii, and thereby being able to detect pressure losses is presented in

E. Özkan, C. Lundquist, and F. Gustafsson. A Bayesian approach to jointly estimate tire radii and vehicle trajectory. In *Proceedings of the IEEE Conference on Intelligent Transportation Systems*, Washington DC, USA, October 2011.

C. Lundquist, E. Özkan, and F. Gustafsson. Tire radii estimation using a marginalized particle filter. *IEEE Transactions on Intelligent Transportation Systems*, 2011d. Submitted.

Finally, the pedagogic contribution

C. Lundquist, M. Skoglund, K. Granström, and T. Glad. How peer-review affects student learning. In *Utvecklingskonferens för Sveriges ingenjörsutbildingar*, Norrköping, Sweden, November 2011f.

describes how peer-review can improve student's learning. This work is implemented in a course in sensor fusion.

1.7 Contributions

The main contributions of this thesis are briefly summarized and presented below:

Mapping: An overview of different methods to map stationary objects in the surroundings of the vehicle are summarized in Paper A.

Road curvature estimation: The estimation from camera and radar is improved by using information about the ego vehicle motion. The results are presented in Paper B.

Road edge estimation: Errors in variables methods are applied in order to track the road edges using point measurements, and the results are given in Paper C. The edges are modeled as extended targets.

Intensity based map: An intensity function is used to represent stationary objects along the road. Structures in the road are used to improve the update and representation of the map as described in Paper D.

Extended target tracking: A modification of the GM-PHD filter, which is able to handle extended targets, is presented in Paper E.

Target size estimation: An approach to estimate the size and the shape is introduced in Paper F. The tracking framework contains a hybrid state space where measurement generating points and the measurements are modeled by random finite sets and target states by random vectors.

Tire radii estimation: The marginalized particle filter is applied to the problem of estimating the tire radii of a vehicle. The Bayesian method, presented in Paper G, is efficient and the estimate is more accurate than estimates from comparable methods.

1.8 Thesis Outline

The thesis is divided into two parts. The first part contains an overview of the research area and background theory for the second part, which contains edited versions of published papers.

1.8.1 Outline of Part I

An overview of vehicle, road and target models is given in Chapter 2, as well as some methods to simplify and make the models applicable for automotive applications. The chapter is concerned with the inner part of the model based estimation process i.e., the *process model* and the *measurement model* illustrated by the two white rectangles in Figure 1.1.

Chapter 3 describes estimation and filtering algorithms, which have been applied to derive the results in Part II. The *estimation process* is illustrated by the gray rectangle in Figure 1.1, and the chapter has a tutorial character.

Target tracking is the subject of Chapter 4, and it describes the framework which takes care of incoming measurements. The framework is illustrated by the black rectangle in Figure 1.1.

Chapter 5 describes a filtering framework which propagates the so called PHD, being an approximation of a finite random set of targets. The PHD-filter unifies the track management and the estimation process, i.e., the black and the gray box in Figure 1.1.

Finally, the work is summarized and the next steps for future work are given in Chapter 6.

1.8.2 Outline of Part II

Part II presents a collections of publications where the author of this thesis has been involved. The aim of this section is to give a very brief abstract to the publications, describe how they relate to each other and emphasize the authors contribution.

The first four papers are concerned about estimating and mapping the road and the surroundings of the vehicle.

Paper A,

> C. Lundquist, T. B. Schön, and F. Gustafsson. Situational awareness and road prediction for trajectory control applications. In A. Eskandarian, editor, *Handbook of Intelligent Vehicles*, chapter 24. Springer, November 2011e.

gives an overview of mapping methods for automotive applications. The paper summarizes both standard approaches, of which some have been implemented by the author, and methods developed by the author in other publications. There is a slight overlap of the material presented in the paper with other papers in this thesis. The author has written the major part of this paper, besides the section covering lane tracking using a camera.

Paper B,

C. Lundquist and T. B. Schön. Joint ego-motion and road geometry estimation. *Information Fusion*, 12:253–263, October 2011.

presents early work of the author. It is shown how the road curvature estimate can be improved and made more robust by fusing lane marking information with the position of other vehicles on the road and knowledge about the ego vehicles motion. The lane information is obtained by a camera, the other vehicles are tracked by a radar and the ego vehicle's motion is measured with e.g., an IMU. The authors contribution is the model which connects the ego vehicle's motion to the estimate of the curvature.

Paper C,

C. Lundquist, U. Orguner, and F. Gustafsson. Extended target tracking using polynomials with applications to road-map estimation. *IEEE Transactions on Signal Processing*, 59(1):15–26, January 2011c.

describes a method to track the road edges as extended targets. This is the first article in a series where the author is dealing with extended targets. In this paper the targets are represented by polynomials, which represent e.g., guardrails along the road. The presented ideas are primarily the author's contribution, however, Dr. Umut Orguner has assisted with his knowledge in the area of target tracking to make it possible to implement the ideas.

Paper D,

C. Lundquist, L. Hammarstrand, and F. Gustafsson. Road intensity based mapping using radar measurements with a probability hypothesis density filter. *IEEE Transactions on Signal Processing*, 59(4):1397–1408, April 2011b.

is the last of the four papers describing models and algorithms to represent and estimate the road. In this paper objects along road edges are represented by an intensity function. The intensity in each position of the map describes the density of targets in that position. Dr. Lars Hammarstrand came up with the initial ideas to this paper, the realization of the idea was formed in discussion with the author. The modifications to the standard PHD filter were implemented by the author, who also wrote the major part of the paper.

The next two papers treat methods to track moving targets, e.g., vehicles, which have an extent.

Paper E,

K. Granström, C. Lundquist, and U. Orguner. Extended target tracking using a Gaussian-mixture PHD filter. *IEEE Transactions on Aerospace and Electronic Systems*, 2011a. Under review.

introduces a PHD filter based method to track targets which potentially might give rise to more than one measurement. The authors came up with the idea to this paper at a conference where the mathematical framework was presented.

The contribution of this paper is the implementation, including the necessary assumptions, which must be made to make the theory computationally tractable. All authors of this paper have contributed to the presented approach, however the major part of the implementation and the writing was made by Karl Granström.

Paper F,

> C. Lundquist, K. Granström, and U. Orguner. Estimating the shape of targets with a PHD filter. In *Proceedings of the International Conference on Information Fusion*, Chicago, IL, USA, July 2011a.

presents a new approach to track the size and the shape of a target. Since the output of many off-the-shelf sensors are point observations, a model must be found to relate point measurements to a shape. In this paper a random finite set describes points on the target's surface, which are assumed to have generated the measurements. The idea is mainly developed by the author, also the implementation and writing were primarily performed by the author. However, the results were improved through the valuable advice regarding target tracking given by Dr. Umut Orguner.

The last paper is concerned about the ego vehicle only.

Paper G,

> C. Lundquist, E. Özkan, and F. Gustafsson. Tire radii estimation using a marginalized particle filter. *IEEE Transactions on Intelligent Transportation Systems*, 2011d. Submitted.

is based on theories recently developed by among others the two co-authors Dr. Emre Özkan and Professor Fredrik Gustafsson. In this paper these theories are applied to the problem of estimating the tire radii of a vehicle. The primary aim is to detect tire pressure losses. The author has contributed by implementing these theories, by applying them on real data and by writing major part of the paper. Dr. Emre Özkan has helped to implement the method based on his knowledge in the area.

2

Models of Dynamic Systems

Given measurements from several sensors the objective is to estimate one or several state variables, either by means of improving a measured signal or by means of estimating a signal which is not, or can not, be directly measured. In either case the relationship between the measured signals and the state variable must be described, and the equations describing this relationship is referred to as the *measurement model*. When dealing with dynamic systems, as is commonly the case in automotive applications, the objective might be to predict the value of the state variable at the next time step. The prediction equation is referred to as the *process model*. This section deals with these two types of models.

As mentioned in the introduction in Section 1.5, a general model of dynamic systems is provided by the nonlinear state space model

$$\mathbf{x}_{k+1} = f_k(\mathbf{x}_k, \mathbf{u}_k, \mathbf{w}_k, \boldsymbol{\theta}_k), \tag{2.1a}$$

$$\mathbf{y}_k = h_k(\mathbf{x}_k, \mathbf{u}_k, \mathbf{e}_k, \boldsymbol{\theta}_k). \tag{2.1b}$$

Most mechanical and physical laws are provided in continuous-time, but computer implementations are made in discrete-time, i.e., the process and measurement models are derived in continuous-time t according to

$$\dot{\mathbf{x}}(t) = a(\mathbf{x}(t), \mathbf{u}(t), \mathbf{w}(t), \boldsymbol{\theta}(t), t), \tag{2.2a}$$

$$\mathbf{y}(t) = c(\mathbf{x}(t), \mathbf{u}(t), \mathbf{e}(t), \boldsymbol{\theta}(t), t), \tag{2.2b}$$

and are then discretized. Discretization is the topic of Section 2.2. Special cases of the general state space model (2.1), such as the state space model with additive noise and the linear state space model, are discussed in Section 2.3 and 2.4, respectively.

Several models for various applications are given in the papers in Part II. This chapter therefore begins with an introduction to some of these models in Section 2.1.

2.1 Overview of the Models Used in the Thesis

The single track model was introduced in Example 1.1 and it used as an example throughout the first three chapters of this thesis. Furthermore, the model is a vital part for deriving the results in Paper B. The process and measurement models of the single track model are given in Example 2.1.

2.1 Example: Single Track Model

The state variables $\mathbf{x}$, the input signals $\mathbf{u}$ and the measurement signals $\mathbf{y}$ of the ego vehicle model were defined in Example 1.1, and are repeated here for convenience

$$\mathbf{x} = \begin{bmatrix} \dot{\psi}_E & \beta \end{bmatrix}^{\mathrm{T}}, \tag{2.3a}$$

$$\mathbf{u} = \begin{bmatrix} \delta_f & \mathsf{v} \end{bmatrix}^{\mathrm{T}}, \tag{2.3b}$$

$$\mathbf{y} = \begin{bmatrix} \dot{\psi}_E & \mathsf{a_y} \end{bmatrix}^{\mathrm{T}}. \tag{2.3c}$$

Note that the front wheel angle δ_f is used directly as an input signal to simplify the example. The continuous-time single track process and measurement models are given by

$$\dot{\mathbf{x}} = \begin{bmatrix} -\frac{C_{\alpha f} l_f^2 \cos\delta_f + C_{\alpha r} l_r^2}{I_{zz}\mathsf{v}} \dot{\psi}_E + \frac{-C_{\alpha f} l_f \cos\delta_f + C_{\alpha r} l_r}{I_{zz}} \beta + \frac{C_{\alpha f} l_f \tan\delta_f}{I_{zz}} \\ -\left(1 + \frac{C_{\alpha f} l_f \cos\delta_f - C_{\alpha r} l_r}{\mathsf{v}^2 m}\right) \dot{\psi}_E - \frac{C_{\alpha f}\cos\delta_f + C_{\alpha r}}{m\mathsf{v}} \beta + \frac{C_{\alpha f}\sin\delta_f}{m\mathsf{v}} \end{bmatrix}, \tag{2.4a}$$

$$\mathbf{y} = \begin{bmatrix} \dot{\psi}_E \\ \frac{-C_{\alpha f} l_f \cos\delta_f + C_{\alpha r} l_r}{m\mathsf{v}} \dot{\psi}_E - \frac{C_{\alpha f}\cos\delta_f + C_{\alpha r}}{m} \beta + \frac{C_{\alpha f}\sin\delta_f}{m} \end{bmatrix}, \tag{2.4b}$$

with parameter vector

$$\boldsymbol{\theta} = \begin{bmatrix} l_f & l_r & I_{zz} & m & C_{\alpha f} & C_{\alpha r} \end{bmatrix}, \tag{2.5}$$

where l_f and l_r denotes the distances between the center of gravity of the vehicle and the front and rear axles, respectively. Furthermore, m denotes the mass of the vehicle and I_{zz} denotes the moment of inertia of the vehicle about its vertical axis in the center of gravity. The parameters $C_{\alpha f}$ and $C_{\alpha f}$ are called cornering stiffness and describe the road tire interaction. Typical values for the parameters are given in Table 2.1. The model is derived in many vehicle dynamics books, e.g., Mitschke and Wallentowitz (2004); Wong (2001); Gillespie (1992); Rajamani (2006).

Road models are treated in Paper A to D. A good overview of available and commonly used road models is given in Paper A, and therefore no introduction to road modeling in general is given in this chapter. However, road models are often combined with ego vehicle models and described in one single state space

Table 2.1: *Typical ranges for the vehicle parameters used in the single track model.*

m kg	I_{zz} kgm^2	C_α N/rad	$l_f + l_r$ m
1000 – 2500	850 – 5000	45000 – 75000	2.5 – 3.0

model. One approach is presented in Paper B and compared with two other vehicle models with road interaction, which are described as follows.

The first model is described in Example 2.2 and it is commonly used for autonomous driving and lane keeping. This model is well described by e.g., Dickmanns (2007) and Behringer (1997). Note that the ego vehicle's motion is modeled with respect to a road fixed coordinate frame, unlike the single track model in Example 2.1, which is modeled in a Cartesian world coordinate frame.

2.2 Example: Vehicle Model with Road Interaction

The relative angle between the vehicle's longitudinal axis and the tangent of the road is denoted ψ_{RE}. The notation is illustrated in the Figures 1 to 4 in Paper B (Pages 140-144). Ackermann's steering geometry is used to obtain the relation

$$\dot{\psi}_{RE} = \frac{\mathrm{v}}{l_b}\delta_f - \mathrm{v} \cdot c_0, \tag{2.6}$$

where the current curvature of the road c_0 is the inverse of the road's radius. The lateral displacement of the vehicle in the lane is given by

$$\dot{l}_R = \mathrm{v}(\psi_{RE} + \beta). \tag{2.7}$$

A process model for the body side slip angle was given in (2.4a), but since the yaw rate $\dot{\psi}$ is not part of the model in this section, equation (2.4a) has to be rewritten according to

$$\begin{aligned}\dot{\beta} = &-\frac{C_{\alpha f}\cos\delta_f + C_{\alpha r}}{m\mathrm{v}}\beta \\ &-\left(1 + \frac{C_{\alpha f} l_f \cos\delta_f - C_{\alpha r} l_r}{\mathrm{v}^2 m}\right)\frac{v_x}{l_b}\tan\delta_f + \frac{C_{\alpha f}}{m\mathrm{v}}\sin\delta_f,\end{aligned} \tag{2.8}$$

which is further simplified by assuming small angles, to obtain a linear model according to

$$\dot{\beta} = -\frac{C_{\alpha f} + C_{\alpha r}}{m\mathrm{v}}\beta + \left(\frac{C_{\alpha f}}{m\mathrm{v}} - \frac{\mathrm{v}}{l_b}\right)\delta_f. \tag{2.9}$$

The steering wheel angle might have a bias, for example if the sensor is not calibrated, which leads to an accumulation of the side slip angle β in (2.9). Other reasons for a steering wheel angle bias is track torsion or strong side wind, which the driver compensates for with the steering wheel. The problem is solved by introducing an offset to the front wheel angel as a state variable according to

$$\delta_f^m = \delta_f + \delta_f^{\text{offs}}. \tag{2.10}$$

Note that the curvature c_0 is included in (2.6). The curvature c_0 is usually treated as a state variable and in this example the vehicle motion model is augmented with the simple clothoid road model, see Paper A.

To summarize, the state variable vector is defined as

$$\mathbf{x} = \begin{bmatrix} \psi_{RE} \\ l_R \\ \beta \\ \delta_f \\ \delta_f^{\text{offs}} \\ c_0 \\ c_1 \end{bmatrix} = \begin{bmatrix} \text{relative angle between vehicle and road} \\ \text{lateral displacement of vehicle in lane} \\ \text{vehicle body side slip angle} \\ \text{front wheel angle} \\ \text{front wheel angle bias offset} \\ \text{road curvature at the ego vehicle} \\ \text{curvature derivative} \end{bmatrix} \tag{2.11}$$

and the process model is given by

$$\dot{\mathbf{x}} = \begin{bmatrix} \dot{\psi}_{RE} \\ \dot{l}_R \\ \dot{\beta} \\ \dot{\delta}_f \\ \dot{\delta}_f^{\text{offs}} \end{bmatrix} = \begin{bmatrix} \frac{v_x}{l_b}\delta_f - \mathsf{v}c_0 \\ \mathsf{v}(\psi_{RE} + \beta) \\ -\frac{C_{\alpha f} + C_{\alpha r}}{m\mathsf{v}}\beta + \left(\frac{C_{\alpha f}}{m\mathsf{v}} - \frac{\mathsf{v}}{l_b}\right)\delta_f \\ w_{\delta_f} \\ 0 \\ \mathsf{v}c_0 \\ w_{c_1} \end{bmatrix}. \tag{2.12}$$

With the camera it is possible mo measure ψ_{RE}, l_R and c_0. The front wheel angle δ_f can be derived from the steering wheel angle δ_s if the steering geometry is known; i.e., the measurement vector is

$$\mathbf{y} = \begin{bmatrix} \psi_{RE} & l_R & c_0 & \delta_s \end{bmatrix}^{\mathrm{T}} \tag{2.13}$$

and the measurement model is trivial. This model is used in the approach referred to as “fusion 3” in Paper B.

Another and simpler vehicle model is obtained if the side slip angle is omitted and the ego vehicle’s yaw rate $\dot{\psi}_E$ is used instead of the steering wheel angle. The model is summarized in Example 2.3, and thoroughly described together with results in Eidehall (2007); Eidehall et al. (2007); Eidehall and Gustafsson (2006); Gern et al. (2000, 2001); Zomotor and Franke (1997).

More advanced vehicle models with more degrees of freedom, including the two track model, are described by Schofield (2008).

2.3 Example: Simplified Vehicle Model with Road Interaction

The state variable vector is here defined as

$$\mathbf{x} = \begin{bmatrix} \psi_{RE} & l_R & \dot{\psi}_E & c_0 & c_1 \end{bmatrix}^{\mathrm{T}}, \tag{2.14}$$

and the process model is simply given by

$$\dot{\mathbf{x}} = \begin{bmatrix} \dot{\psi}_{RE} \\ \dot{l}_E \\ \dot{c}_0 \\ \dot{c}_1 \end{bmatrix} = \begin{bmatrix} v_x c_0 + \dot{\psi}_E \\ v_x \psi_{RE} \\ w_{\dot{\psi}_{RE}} \\ \mathrm{v} c_0 \\ w_{c_1} \end{bmatrix}. \tag{2.15}$$

The measurement vector is

$$\mathbf{y} = \begin{bmatrix} \psi_{RE} & l_R & c_0 & \dot{\psi}_E \end{bmatrix}^{\mathrm{T}} \tag{2.16}$$

where the yaw rate is measured by the vehicle's IMU. This model is used in the approach referred to as "fusion 2" in Paper B.

In this work, only measurements from the ego vehicle's sensors are available; that is the target's motion is measured using the ego vehicle's radar and camera. This is the reason for why the target model is simpler than the ego vehicle model. The targets play an important role in the sensor fusion framework presented in this work, but little effort has been spent modeling their motion. Instead standard models from target tracking literature are used. A survey of different process models and measurement models are given by Rong Li and Jilkov (2003) and Rong Li and Jilkov (2001), respectively. The subject is also covered in the books by Blackman and Popoli (1999) and Bar-Shalom et al. (2001). One typical target model is given in Example 2.4. This model is used in the Papers F and G, and a somewhat similar model, called constant velocity model, is used in Paper E.

2.4 Example: Coordinated Turn Model

The coordinated turn model is commonly used to model moving targets. The ego vehicle's radar and camera measures the range $r_{T_i E_s}$ and the azimuth angle $\psi_{T_i E_s}$ to target number i as described in the introduction in Example 1.2. The states of the coordinated turn model in polar velocity are given by

$$\mathbf{x} = \begin{bmatrix} \mathrm{x}^W_{T_i W} \\ \mathrm{y}^W_{T_i W} \\ \mathrm{v}^{T_i} \\ \psi_{T_i} \\ \dot{\psi}_{T_i} \end{bmatrix} = \begin{bmatrix} \text{x-position in } W\text{-frame} \\ \text{y-position in } W\text{-frame} \\ \text{longitudinal velocity} \\ \text{heading angle} \\ \text{yaw rate} \end{bmatrix}. \tag{2.17}$$

The process and measurement models are given by

$$\dot{\mathbf{x}} = \begin{bmatrix} \dot{\mathrm{x}}_{T_iW}^{W} \\ \dot{\mathrm{y}}_{T_iW}^{W} \\ \dot{\mathrm{v}}^{T_i} \\ \dot{\psi}_{T_i} \\ \ddot{\psi}_{T_i} \end{bmatrix} = \begin{bmatrix} \mathrm{v}^{T_i} \cos \psi_{T_i} \\ \mathrm{v}^{T_i} \sin \psi_{T_i} \\ 0 \\ \dot{\psi}_{T_i} \\ 0 \end{bmatrix} + \begin{bmatrix} 0 \\ 0 \\ w_{\dot{\mathrm{v}}^{T_i}} \\ 0 \\ w_{\ddot{\psi}_{T_i}} \end{bmatrix} \tag{2.18a}$$

$$\mathbf{z} = \begin{bmatrix} r_{T_iE_s} \\ \psi_{T_iE_s} \end{bmatrix} = \begin{bmatrix} \sqrt{\left(\mathrm{x}_{T_iW}^{W} - \mathrm{x}_{EW}^{W} - \mathrm{x}_{E_sE}^{E}\right)^2 + \left(\mathrm{y}_{T_iW}^{W} - \mathrm{y}_{EW}^{W} - \mathrm{y}_{E_sE}^{E}\right)^2} \\ \arctan \frac{\mathrm{y}_{T_iW}^{W}}{\mathrm{x}_{T_iW}^{W}} - \psi_E - \psi_{E_sE} \end{bmatrix} + \mathbf{e} \tag{2.18b}$$

where $(\mathrm{x}_{E_sE}^{E}, \mathrm{y}_{E_sE}^{E}, \psi_{E_sE})$ represents the sensor mounting position and orientation in the ego vehicle coordinate frame E. The ego vehicle's position in the world frame $(\mathrm{x}_{EW}^{W}, \mathrm{y}_{EW}^{W})$ is included in the measurement model of the target. To be able to estimate the ego vehicles position the single track ego vehicle state variable vector and state space model (2.4) has to be augmented with the ego vehicle's position. Note that the ego vehicle's heading angle is denoted ψ_E here to differentiate it from the heading angle of the target.

2.2 Discretizing Continuous-Time Models

The measurements dealt with in this work are sampled and handled as discrete-time variables in computers and electronic control units (ECU). All sensor signals are transferred in sampled form from different sensors to the log-computer using the so called CAN-Bus (Controller Area Network). Hence, the systems discussed in this thesis must also be described using discrete-time models according to the state space model in (2.1). Nevertheless, since physical relations commonly are given in continuous-time, the various systems presented in this thesis, such as the single track model in Example 2.1, are derived and represented using continuous-time state space models in the form (2.2). Thus, all continuous-time models in this thesis have to be discretized in order to describe the measurements. Only a few of the motion models can be discretized exactly by solving the sampling formula

$$\mathbf{x}_{k+1} = \mathbf{x}_k + \int_{k}^{k+T} a(\mathbf{x}(t), \mathbf{u}(t), \mathbf{w}(t), \boldsymbol{\theta}(t)) dt, \tag{2.19}$$

analytically, where T denotes the sampling time.

2.5 Example: Exact Sampling of the Coordinated Turn Model

Consider the continuous-time coordinate turn model in Example 2.4. The analytic solution of (2.19) is

$$\mathsf{x}^W_{T_iW,k+1} = \mathsf{x}^W_{T_iW,k} + \frac{2\mathsf{v}^{T_i}_k}{\dot\psi_{T_i,k}} \sin\frac{\dot\psi_{T_i,k}T}{2}\cos\left(\psi_{T_i,k} + \frac{\dot\psi_{T_i,k}T}{2}\right) \tag{2.20a}$$

$$\mathsf{y}^W_{T_iW,k+1} = \mathsf{y}^W_{T_iW,k} + \frac{2\mathsf{v}^{T_i}_k}{\dot\psi_{T_i,k}} \sin\frac{\dot\psi_{T_i,k}T}{2}\sin\left(\psi_{T_i,k} + \frac{\dot\psi_{T_i,k}T}{2}\right) \tag{2.20b}$$

$$\mathsf{v}^{T_i}_{k+1} = \mathsf{v}^{T_i}_k \tag{2.20c}$$

$$\psi_{T_i,k+1} = \psi_{T_i,k} + T\dot\psi_{T_i,k} \tag{2.20d}$$

$$\dot\psi_{T_i,k+1} = \dot\psi_{T_i,k}. \tag{2.20e}$$

Simpler than using the exact sampling formula (2.19) is it to make use of the standard forward Euler method, which approximates (2.2a) according to

$$\mathbf{x}_{k+1} \approx \mathbf{x}_k + Ta(\mathbf{x}_k, \mathbf{u}_k, \mathbf{w}_k, \boldsymbol{\theta}_k) \triangleq f_k(\mathbf{x}_k, \mathbf{u}_k, \mathbf{w}_k, \boldsymbol{\theta}_k). \tag{2.21}$$

This is a very rough approximation with many disadvantages, but it is frequently used due to its simplicity. Example 2.6 shows the Euler approximation of the coordinated turn model.

2.6 Example: Euler Sampling of the Coordinated Turn Model

Consider the continuous-time coordinate turn model in Example 2.4. The solution of (2.21) is

$$\mathsf{x}^W_{T_iW,k+1} = \mathsf{x}^W_{T_iW,k} + T\mathsf{v}^{T_i}_k\cos\psi_{T_i,k} \tag{2.22a}$$

$$\mathsf{y}^W_{T_iW,k+1} = \mathsf{y}^W_{T_iW,k} + T\mathsf{v}^{T_i}_k\sin\psi_{T_i,k} \tag{2.22b}$$

$$\mathsf{v}^{T_i}_{k+1} = \mathsf{v}^{T_i}_k \tag{2.22c}$$

$$\psi_{T_i,k+1} = \psi_{T_i,k} + T\dot\psi_{T_i,k} \tag{2.22d}$$

$$\dot\psi_{T_i,k+1} = \dot\psi_{T_i,k}. \tag{2.22e}$$

Sampling of linear systems is thoroughly described by Rugh (1996). Moreover, different options to sample and linearize non-linear continuous-time systems are described by Gustafsson (2000). The linearization problem is treated in Chapter 3, in a discussion of approximative model based filters such as the extended Kalman filter.

2.3 Linear State Space Model

An important special case of the general state space model (2.1) is the linear Gaussian state space model, where f and h are linear functions and the noise is Gaussian,

$$\mathbf{x}_{k+1} = F_k(\boldsymbol{\theta})\mathbf{x}_k + G_k^{\mathbf{u}}(\boldsymbol{\theta})\mathbf{u}_k + G_k^{\mathbf{w}}\mathbf{w}_k(\boldsymbol{\theta}), \tag{2.23a}$$

$$\mathbf{y}_k = H_k(\boldsymbol{\theta})\mathbf{x}_k + H_k^{\mathbf{u}}(\boldsymbol{\theta})\mathbf{u}_k + \mathbf{e}_k(\boldsymbol{\theta}), \tag{2.23b}$$

where $\mathbf{w}_k \sim \mathcal{N}(0, Q_k)$ and $\mathbf{e}_k \sim \mathcal{N}(0, R_k)$. Note that the single track model (2.4) is linear in the state variables, as shown in Example 2.7.

2.7 Example: Linearized Single Track Model

The front wheel angle is usually quite small at higher velocities and the assumptions $\cos\delta_f \approx 1$, $\tan\delta_f \approx \sin\delta_f \approx \delta_f$ therefore applies. The continuous-time single track model (2.4) may first be discretized using Euler sampling and can then be written on the linear form (2.23) according to

$$\dot{\mathbf{x}}_{k+1} = \begin{bmatrix} 1 - T\frac{C_{\alpha f}l_f^2 + C_{\alpha r}l_r^2}{I_{zz}\mathrm{v}_t} & T\frac{-C_{\alpha f}l_f + C_{\alpha r}l_r}{I_{zz}} \\ -T - T\frac{C_{\alpha f}l_f - C_{\alpha r}l_r}{\mathrm{v}_k^2 m} & 1 - T\frac{C_{\alpha f} + C_{\alpha r}}{m\mathrm{v}_k} \end{bmatrix}\mathbf{x}_k + \begin{bmatrix} \frac{C_{\alpha f}l_f}{I_{zz}} \\ \frac{C_{\alpha f}}{m\mathrm{v}} \end{bmatrix}\delta_{f,k} + \mathbf{w}_k, \tag{2.24a}$$

$$\mathbf{y}_k = \begin{bmatrix} 1 & 0 \\ \frac{-C_{\alpha f}l_f + C_{\alpha r}l_r}{m\mathrm{v}_k} & -\frac{C_{\alpha f} + C_{\alpha r}}{m} \end{bmatrix}\mathbf{x}_k + \begin{bmatrix} 0 \\ \frac{C_{\alpha f}}{m} \end{bmatrix}\delta_{f,k} + \mathbf{e}_k. \tag{2.24b}$$

The model is linear in the input $\delta_{f,k}$. However, the input v_k is implicitly modeled in the matrices $F_k(\mathrm{v}_k, \boldsymbol{\theta}_k)$, $G_k^{\mathbf{u}}(\mathrm{v}_k, \boldsymbol{\theta}_k)$ and $H_k(\mathrm{v}_k, \boldsymbol{\theta}_k)$.

Linear state space models and linear system theory in general are thoroughly described by Rugh (1996) and Kailath (1980).

2.4 Nonlinear State Space Model with Additive Noise

A special case of the general state space model (2.1) is given by assuming that the noise enters additively and the input signals are subsumed in the time-varying dynamics, which leads to the form

$$\mathbf{x}_{k+1} = f_k(\mathbf{x}_k, \boldsymbol{\theta}_k) + \mathbf{w}_k, \tag{2.25a}$$

$$\mathbf{y}_t = h_k(\mathbf{x}_k, \boldsymbol{\theta}_k) + \mathbf{e}_k. \tag{2.25b}$$

In Example 1.1 an ego vehicle model was introduced, where the steering wheel angle and the vehicle velocity were modeled as deterministic input signals. This consideration can be motivated by claiming that the driver controls the vehicle's lateral movement with the steering wheel and the longitudinal movement with the throttle and brake pedals. Furthermore, the steering wheel angle and the velocity are measured with less noise than the other measurement signals, and they are often pre-processed to improve the accuracy and remove bias. With these arguments the resulting model, given in Example 2.1, may be employed. The model is in some sense simpler than the case when these two signals are assumed to be stochastic measurements, as shown in Example 2.8.

2.8 Example: Single Track Model without Deterministic Input Signals

In classical signal processing it is uncommon to allow deterministic input signals, at least not if these are measured by sensors. The input signals in Example 1.1 should instead be modeled as stochastic measurements. Hence, the measurement vector and the state vector are augmented and the system is remodeled. One example is given by the state space model

$$\begin{bmatrix} \dot{\psi}_{E,k+1} \\ \beta_{k+1} \\ \delta_{f,k+1} \\ \mathsf{v}_{k+1} \end{bmatrix} = \begin{bmatrix} \dot{\psi}_{E,k} + T\left(-\frac{C_{\alpha f} l_f^2 + C_{\alpha r} l_r^2}{I_{zz} \mathsf{v}_k} \dot{\psi}_{E,k} + \frac{-C_{\alpha f} l_f + C_{\alpha r} l_r}{I_{zz}} \beta_k + \frac{C_{\alpha f} l_f \delta_{f,k}}{I_{zz}}\right) \\ \beta_k + T\left(-\left(1 + \frac{C_{\alpha f} l_f - C_{\alpha r} l_r}{\mathsf{v}_k^2 m}\right) \dot{\psi}_{E,k} - \frac{C_{\alpha f} + C_{\alpha r}}{m \mathsf{v}_k} \beta_k + \frac{C_{\alpha f} \delta_{f,k}}{m \mathsf{v}_k}\right) \\ \delta_{f,k} \\ \mathsf{v}_k \end{bmatrix} + \mathbf{w}_k, \tag{2.26a}$$

$$\begin{bmatrix} \dot{\psi}_t \\ \mathsf{a}_{\mathsf{y},k} \\ \delta_{s,k} \\ \mathsf{v}_k \end{bmatrix} = \begin{bmatrix} \dot{\psi}_{E,k} + e_{\dot{\psi},k} \\ \frac{-C_{\alpha f} l_f + C_{\alpha r} l_r}{m \mathsf{v}_k} \dot{\psi}_{E,k} - \frac{C_{\alpha f} + C_{\alpha r}}{m} \beta_k \\ h_{\delta_f}(\dot{\psi}_k, \beta_k, \delta_{f,k}, \boldsymbol{\theta}) \\ \mathsf{v}_{x,t} \end{bmatrix} + \mathbf{e}_k, \tag{2.26b}$$

where T is the sample time. The first two rows of the process and measurement models are the discretized versions of the model given in (2.4). In the second row in the measurement model the simplification $\cos \delta_f \approx 1$ and $\sin \delta_f \approx 0$ is made to not let the measurement model be dependent on the measurement δ_f. The third measurement signal is the steering wheel angle δ_s, but the third state is the front wheel angle δ_f. A possible measurement model h_{δ_f} will be discussed in Example 3.1. Finally, a random walk is assumed for the front wheel angle δ_f and the velocity v in the process model.

Another way to represent the state space model is given by considering the probability density function (PDF) of different signals or state variables of a system. The *transition density* $p(\mathbf{x}_{k+1}|\mathbf{x}_k)$ models the dynamics of the system and if the process noise is assumed additive, the transition model is given by

$$p(\mathbf{x}_{k+1}|\mathbf{x}_k) = p_{\mathbf{w}}(\mathbf{x}_{k+1} - f(\mathbf{x}_k, \mathbf{u}_k, \boldsymbol{\theta}_k)), \tag{2.27}$$

where $p_{\mathbf{w}}$ denotes the PDF of the process noise $\mathbf{w}$. The density describes the state at time $k+1$ given that information about the state at the previous time step k is known. A fundamental property of the process model is the Markov property,

$$p(\mathbf{x}_{k+1}|\mathbf{x}_1, \ldots, \mathbf{x}_k) = p(\mathbf{x}_{k+1}|\mathbf{x}_k). \tag{2.28}$$

This means that the state of the system at time k contains all necessary information about the past, which is needed to predict the future behavior of the system.

Furthermore, if the measurement noise is assumed additive then the *likelihood function*, which describes the measurement model, is given by

$$p(\mathbf{y}_k|\mathbf{x}_k) = p_{\mathbf{e}}(\mathbf{y}_k - h(\mathbf{x}_k, \mathbf{u}_k, \boldsymbol{\theta}_k)), \tag{2.29}$$

where $p_{\mathbf{e}}$ denotes the PDF of the sensor noise $\mathbf{e}$. The measurement $\mathbf{z}_k$ received by the sensor are described by the likelihood function given that information about the state $\mathbf{x}_k$ at the same time step k is known. The two density functions in (2.27) and (2.29) are often referred to as a hidden Markov model (HMM) according to

$$\mathbf{x}_{k+1} \sim p(\mathbf{x}_{k+1}|\mathbf{x}_k), \tag{2.30a}$$

$$\mathbf{y}_k \sim p(\mathbf{y}_k|\mathbf{x}_k), \tag{2.30b}$$

since $\mathbf{x}_k$ is not directly visible in $\mathbf{y}_k$. It is a statistical model where one Markov process, that represents the system, is observed through another stochastic process, the measurement model.

3

Estimation Theory

This thesis is concerned with estimation problems, i.e. given measurements $\mathbf{y}$ the aim is to estimate the parameter $\boldsymbol{\theta}$ or the state $\mathbf{x}$ in (1.1). Both problems rely on the same theoretical basis and the same algorithms can be used. The parameter estimation problem is a part of the system identification process, which also includes the derivation of the model structure, discussed in the previous chapter. The state estimation problem utilizes the model and its parameters to solve for the states. When estimating $\mathbf{x}$ it is assumed that $\boldsymbol{\theta}$ is known and vice versa. The parameter is estimated in advance if $\boldsymbol{\theta}$ is time invariant or in parallel with the state estimation problem if $\boldsymbol{\theta}$ is assumed to be time varying. Example 3.1 illustrates how the states and parameters may be estimated.

3.1 Example: Parameter and State Estimation

Consider the single track model, which was introduced in Example 1.1 and the equations were given in Example 2.1. The front wheel angle δ_f is considered to be a state variable in Example 2.8 and the steering wheel angle δ_s is treated as a measurement. The measurement equation is in its simplest form a constant ratio given by

$$\delta_{s,k} = h(\delta_{f,k}, \theta) = i_s \delta_{f,k}. \tag{3.1}$$

The parameter $\theta = i_s$ is assumed to be time invariant. The state δ_f must be known in order to identify the parameter θ. Usually the parameter is estimated off-line in advance using a test rig, where the front wheel angle is measured using highly accurate external sensors. The parameter is then used within the model in order to estimate the states on-line while driving.

The tire parameter C_α is assumed to change with weather and road conditions, hence it is a time varying parameter. It has to be identified on-line at time k using the state estimates from the previous time step $k-1$, which in turn were estimated using the parameter estimate from time step $k-1$.

For various reasons some systems are only modeled by a likelihood function. Often these systems are static and there exists no Markov transition density. However, most systems in this thesis are modeled using both a prediction and a likelihood function. In system identification, the model parameter is estimated without physically describing the parameter's time dependency, hence static estimation theory is used. The state can be estimated in more or less the same way. However, the process model (1.1a) is often given and its time transition information is exploited to further improve the state estimate.

The origins of the estimation research field can be traced back to the work by Gauss in 1795 on least squares (Abdulle and Wanner, 2002) and Bayes (1763) on conditional probabilities. Bayes introduced an important theorem which has come to be referred to as *Bayes' theorem*,

$$p(\mathbf{x}, \boldsymbol{\theta}|\mathbf{y}) = \frac{p(\mathbf{y}|\mathbf{x}, \boldsymbol{\theta})p(\mathbf{x}, \boldsymbol{\theta})}{p(\mathbf{y})}, \tag{3.2}$$

with which it is possible to calculate the *posterior probability* $p(\mathbf{x}, \boldsymbol{\theta}|\mathbf{y})$ given a *prior probability* $p(\mathbf{x}, \boldsymbol{\theta})$ and the *likelihood function* $p(\mathbf{y}|\mathbf{x}, \boldsymbol{\theta})$. Note that both the measurement and the state or parameter are treated as random variables. Another view of the estimation problem was introduced by Fisher (1922), who claimed that the probability of an estimate should be seen as a relative frequency of the state or parameter, given data from long-run experiments. Fisher also treats the measurement as a random variable. The main difference to Bayes' approach is that in Fisher's approach there is a true state or parameter which is treated as deterministic, but unknown. To accentuate the different views, the likelihood is often written using $\ell(\mathbf{x}, \boldsymbol{\theta})$ to emphasize that the likelihood is regarded as a function of the state $\mathbf{x}$ and the parameter $\boldsymbol{\theta}$.

After this brief historical background, the remainder of this chapter is outlined as follows. In Section 3.1, static estimation methods based on both Fishers and Bayes theories, are discussed. These methods can be used for both state and parameter estimation. In Section 3.2, dynamic estimation methods are discussed. These methods are, within the scope of this thesis, only used for state estimation and are based solely on Bayes' theories.

3.1 Static Estimation Theory

The general estimation problem consists of finding the estimates $\hat{\mathbf{x}}$ and $\hat{\boldsymbol{\theta}}$ that minimize a given loss function $V(\mathbf{x}, \boldsymbol{\theta}; \mathbf{y})$. This problem is separated into a parameter estimation problem and a state estimation problem according to

$$\widehat{\boldsymbol{\theta}} = \arg\min_{\boldsymbol{\theta}} \; V(\boldsymbol{\theta}; \mathbf{x}, \mathbf{y}), \tag{3.3a}$$

$$\widehat{\mathbf{x}} = \arg\min_{\mathbf{x}} \; V(\mathbf{x}; \boldsymbol{\theta}, \mathbf{y}). \tag{3.3b}$$

How to separate a typical estimation problem into these two parts is shown Example 3.2.

General estimation techniques are covered by most textbooks on this topic, e.g., Kay (1993); Kailath et al. (2000); Ljung (1999). There are many estimation methods available, however, in this section the focus is on the methods used in Part II of this thesis.

3.2 Example: Parameter and State Estimation

Consider the linear single track model in Example 2.7. Suppose that the state variables are measured with external and highly accurate sensors. The yaw rate is measured with an extra IMU and the body side slip angle β is measured with a so called Correvit® sensor, which uses correlation technology to compute the optical flow. The vehicle in Figure 2 on Page 297 is equipped with this type of sensor at the front. Now, the parameter $\boldsymbol{\theta}$ can be estimated, according to (3.3a). This approach has been used to find some of the vehicle parameters in Papers B and G.

Conversely, if $\boldsymbol{\theta}$ is known and $\mathbf{y}$ is measured, the state variables $\mathbf{x}$ can be estimated using (3.3b).

This section covers estimation problems without any process model $f(\cdot)$, where a set of measurements is related to a parameter only via the measurement model $h(\cdot)$. Furthermore, only an important and special case where the measurement model is linear in $\mathbf{x}$ is considered. The linear measurement model was given in (2.23b) and is repeated here for convenience

$$\mathbf{y}_k = H_k(\boldsymbol{\theta})\mathbf{x}_k + \mathbf{e}_k. \tag{3.4}$$

3.1.1 Least Squares Estimator

The *least squares* (LS) estimate is defined as the solution to the optimization problem, where the squared errors between the predicted measurements and the actual measurements are minimized according to,

$$\hat{\mathbf{x}}_k^{LS} = \arg\min_{\mathbf{x}} \sum_{\tau=1}^{k} \|\mathbf{y}_\tau - H_\tau(\boldsymbol{\theta})\mathbf{x}_\tau\|_2^2. \tag{3.5}$$

The solution for the linear case is given in Algorithm 1.

If the measurement covariance $R = \mathrm{Cov}(\mathbf{e})$ is known, or in practice at least assumed to be known, then the *weighted least squares* (WLS) estimate is given by the optimization problem

$$\hat{\mathbf{x}}_k^{WLS} = \arg\min_{\mathbf{x}} \sum_{\tau=1}^{k} (\mathbf{y}_\tau - H_\tau(\boldsymbol{\theta})\mathbf{x}_\tau)^{\mathrm{T}} R_\tau^{-1} (\mathbf{y}_\tau - H_\tau(\boldsymbol{\theta})\mathbf{x}_\tau). \tag{3.6}$$

The solution for the linear case is given in Algorithm 2, and Example 3.3 illustrates how the single track vehicle model can be reformulated to estimate the

Algorithm 1 Least Squares

The least squares estimate and its covariance are given by

$$\hat{\mathbf{x}}_k^{LS} = \left(\sum_{\tau=1}^{k} H_\tau^{\mathrm{T}} H_\tau\right)^{-1} \sum_{\tau=1}^{k} H_\tau^{\mathrm{T}} \mathbf{y}_\tau = \left(\boldsymbol{H}^{\mathrm{T}}\boldsymbol{H}\right)^{-1} \boldsymbol{H}^{\mathrm{T}}\boldsymbol{Y}, \tag{3.7a}$$

$$\mathrm{Cov}\,(\hat{\mathbf{x}}^{LS}) = (\boldsymbol{H}^{\mathrm{T}}\boldsymbol{H})^{-1}(\boldsymbol{H}^{\mathrm{T}}\boldsymbol{R}\boldsymbol{H})(\boldsymbol{H}^{\mathrm{T}}\boldsymbol{H})^{-1} \triangleq P^{LS}. \tag{3.7b}$$

The last equality is the batch solution, where $\boldsymbol{H}$ and $\boldsymbol{Y}$ are augmented measurement models and measurement vectors, respectively. Furthermore, the measurement noises $R_\tau = \mathrm{Cov}\,(\mathbf{e}_\tau)$ form the main diagonal of $\boldsymbol{R}$ according to $\boldsymbol{R} = \mathrm{diag}(R_1, \ldots, R_k)$.

Algorithm 2 Weighted Least Squares

The weighted least squares estimator and its covariance matrix are given by

$$\hat{\mathbf{x}}_k^{WLS} = \left(\sum_{\tau=1}^{t} H_\tau^{\mathrm{T}} R_\tau^{-1} H_\tau\right)^{-1} \sum_{\tau=1}^{k} H_\tau^{\mathrm{T}} R_\tau^{-1} \mathbf{y}_\tau = \left(\boldsymbol{H}^{\mathrm{T}}\boldsymbol{R}^{-1}\boldsymbol{H}\right)^{-1} \boldsymbol{H}^{\mathrm{T}}\boldsymbol{R}^{-1}\boldsymbol{Y}, \tag{3.8a}$$

$$\mathrm{Cov}\,(\hat{\mathbf{x}}^{WLS}) = (\boldsymbol{H}^{\mathrm{T}}\boldsymbol{R}^{-1}\boldsymbol{H})^{-1} \triangleq P^{WLS}, \tag{3.8b}$$

where the weighting matrix is the noise covariance $\boldsymbol{R}$.

parameters using the WLS.

Another example, where both the LS and the WLS estimators are applied, is given in Paper C. The left and right borders of a road are modeled by polynomials and the coefficients are the parameters which are estimated given a batch of measurements from a radar.

3.3 Example: Parameter and State Estimation

Consider the linear single track model in Example 2.7 and the separation of the parameter and the state estimation problems in Example 3.2. Suppose that the vehicle's mass m and the dimensions l_f and l_r are known. Furthermore, suppose that the state variable $\mathbf{x}$ may be measured as described in Example 3.2. Consider the measurement equation (2.24b); the parameter estimation problem can now be formulated in the form (3.4) with

$$\mathbf{y} = H(\mathbf{x}, \mathbf{u}, l_f, l_r, m) \begin{bmatrix} C_{\alpha f} \\ C_{\alpha r} \end{bmatrix} + \mathbf{e}, \tag{3.9}$$

and the parameters $C_{\alpha f}, C_{\alpha r}$ can be solved for using e.g., WLS in (3.6). Furthermore, the inverse of the moment of inertia $1/I_{zz}$ may be estimated off-line by writing the process model (2.24a) in the form (3.4) according to

$$\mathbf{x}_{t+1} = H(\mathbf{x}_t, \mathbf{u}, l_v, l_f, m, C_{\alpha f}, C_{\alpha r}) \cdot \frac{1}{I_{zz}} + \mathbf{w}. \tag{3.10}$$

3.1.2 Probabilistic Point Estimates

The *maximum likelihood* (ML) estimate, first introduced by Fisher (1912, 1922), is defined by

$$\hat{\mathbf{x}}_k^{ML} = \arg\max_{\mathbf{x}_k} \; p(\mathbf{y}_{1:k}|\mathbf{x}_k). \tag{3.11}$$

Put into words, the estimate is chosen to be the parameter most likely to produce the obtained measurements.

The posterior $p(\mathbf{x}_k|\mathbf{y}_{1:k})$, when $\mathbf{x}_k$ is random, contains all known information about the state of the target at time k. The *maximum a posteriori* (MAP) estimator is defined by

$$\hat{\mathbf{x}}_k^{MAP} = \arg\max_{\mathbf{x}_k} \; p(\mathbf{x}_k|\mathbf{y}_{1:k}) = \arg\max_{\mathbf{x}_k} \; p(\mathbf{y}_{1:k}|\mathbf{x}_k)p(\mathbf{x}_k), \tag{3.12}$$

or put in words, find the most likely estimate of the parameter given the measurements $\mathbf{y}_{1:k}$. Bayes' theorem (3.2) and the fact that the maximization is performed over $\mathbf{x}_k$ is used in the second equality of (3.12). The ML estimate is for instance used in Paper E.

3.2 Filter Theory

The topic of this section is recursive state estimation based on dynamic models. The iteration process of the state space estimation was briefly described in words in Section 1.5. The state estimation theory is influenced by the Bayesian view, which implies that the solution to the estimation problem is provided by the filtering PDF $p(\mathbf{x}_k|\mathbf{y}_{1:k})$. The introduction to this section will be rather general using the model defined in (2.30). Bayes' theorem was introduced in (3.2) and is used to derive the recursive *Bayes filter equations*

$$p(\mathbf{x}_{k+1}|\mathbf{y}_{1:k}) = \int p(\mathbf{x}_{k+1}|\mathbf{x}_k)p(\mathbf{x}_k|\mathbf{y}_{1:k})d\mathbf{x}_k, \tag{3.13a}$$

$$p(\mathbf{x}_k|\mathbf{y}_{1:k}) = \frac{p(\mathbf{y}_k|\mathbf{x}_k)p(\mathbf{x}_k|\mathbf{y}_{1:k-1})}{p(\mathbf{y}_k|\mathbf{y}_{1:k-1})}, \tag{3.13b}$$

with the denominator

$$p(\mathbf{y}_k|\mathbf{y}_{1:k-1}) = \int p(\mathbf{y}_k|\mathbf{x}_k)p(\mathbf{x}_k|\mathbf{y}_{1:k-1})d\mathbf{x}_k. \tag{3.13c}$$

These equations describe the time evolution

$$\cdots \to \mathbf{x}_{k|k} \to \mathbf{x}_{k+1|k} \to \mathbf{x}_{k+1|k+1} \to \cdots \tag{3.14}$$

of the random state vector $\mathbf{x}$. The Bayes posterior density function $p(\mathbf{x}_k|\mathbf{y}_{1:k})$ conditioned on the time sequence $\mathbf{y}_{1:k} = \{\mathbf{y}_1, \ldots, \mathbf{y}_k\}$ of measurements accumulated at time k is the probability density function of $\mathbf{x}_k$ given measurements $\mathbf{y}_{1:k}$. The probability density function $p(\mathbf{x}_{k+1}|\mathbf{y}_{1:k})$ is the time prediction of the posterior $p(\mathbf{x}_k|\mathbf{y}_{1:k})$ to the time step of the next measurement $\mathbf{y}_{k+1}$. Note that the Bayes normalization factor given by (3.13c) is independent of $\mathbf{x}$. In practice the numerator of (3.13b) is calculated and then simply normalized, since the integral of the posterior density function must be equal to one. The single target Bayes filter recursion is illustrated with a flow chart as follows

$$
\begin{array}{ccccccc}
\cdots \longrightarrow p_{k|k}(\mathbf{x}_k|\mathbf{z}_{1:k}) & \overset{\text{prediction}}{\longrightarrow} & p_{k+1|k}(\mathbf{x}_{k+1}|\mathbf{z}_{1:k}) & \overset{\text{update}}{\longrightarrow} & p_{k+1|k+1}(\mathbf{x}_{k+1}|\mathbf{z}_{1:k+1}) \longrightarrow \cdots \\
 & & \uparrow & & \uparrow \\
 & & \text{Transition density} & & \text{Likelihood function} \\
 & & p(\mathbf{x}_{k+1}|\mathbf{x}_k) & & p(\mathbf{z}_{k+1}|\mathbf{x}_{k+1}) \\
 & & \uparrow & & \uparrow \\
 & & \text{Motion model} & & \text{Measurement model} \\
 & & \mathbf{x}_{k+1} = f(\mathbf{x}_k) + \mathbf{w}_k & & \mathbf{z}_{k+1} = h(\mathbf{x}_{k+1}) + \mathbf{e}_{k+1}
\end{array}
$$

After the update step is made the algorithm continues recursively, i.e., a new prediction is performed and thereafter a update or *correction* with the likelihood of the new measurements.

If $p(\mathbf{y}_k|\mathbf{x}_k)$, $p(\mathbf{x}_{k+1}|\mathbf{x}_k)$ and $p(\mathbf{x}_k)$ are Gaussian and their corresponding process and senor models are linear, as in (2.23), then (3.13a) and (3.13b) reduce to the Kalman filter prediction and measurement update, respectively. The Kalman filter is treated in Section 3.2.1. In contrast, if $p(\mathbf{y}_k|\mathbf{x}_k)$, $p(\mathbf{x}_{k+1}|\mathbf{x}_k)$ and $p(\mathbf{x}_k)$ can be approximated by a Gaussian and their corresponding process and sensor models are nonlinear (2.1), several approximations of (3.13a) and (3.13b) exist. The two most common filters are the extended Kalman Filter and the unscented Kalman filter, which are outlined in Sections 3.2.2 and 3.2.3, respectively. Other methods, including methods that approximate other density functions than Gaussian, are neatly covered by Hendeby (2008) and Schön (2006). The most popular approaches are the particle filter, which is covered in Section 3.2.4, and the marginalized particle filter, see e.g., Arulampalam et al. (2002); Cappe et al. (2007); Djuric et al. (2003); Karlsson (2005); Schön et al. (2005).

3.2.1 The Kalman Filter

The linear state space representation subject to Gaussian noise, which was given in (2.23), is the simplest special case when it comes to state estimation. The model is repeated here for convenience;

$$
\begin{aligned}
\mathbf{x}_{k+1} &= F_k(\boldsymbol{\theta})\mathbf{x}_k + G_k^{\mathbf{u}}(\boldsymbol{\theta})\mathbf{u}_k + G_k^{\mathbf{w}}\mathbf{w}_k, & \mathbf{w}_k &\sim \mathcal{N}(0, Q_k), & \text{(3.15a)}\\
\mathbf{y}_k &= H_k(\boldsymbol{\theta})\mathbf{x}_k + H_k^{\mathbf{u}}(\boldsymbol{\theta})\mathbf{u}_k + \mathbf{e}_k, & \mathbf{e}_k &\sim \mathcal{N}(0, R_k). & \text{(3.15b)}
\end{aligned}
$$

The linear model (3.15) has two important properties. All density functions involved in the model and state estimation are Gaussian and a Gaussian density function is completely parametrized by the mean and the covariance, i.e. the first and second order moment. Hence, the Bayesian recursion (3.13) is simplified into only propagating the mean and covariance of the involved probability den-

Algorithm 3 Kalman Filter

Consider the linear state space model (3.15). The Kalman filter is given by the two following steps.

Prediction

$$\hat{\mathbf{x}}_{k|k-1} = F_{k-1}\hat{\mathbf{x}}_{k-1|k-1} + G^{\mathbf{u}}_{k-1}\mathbf{u}_{k-1} \tag{3.16a}$$

$$P_{k|k-1} = F_{k-1}P_{k-1|k-1}F^{\mathrm{T}}_{k-1} + G^{\mathbf{w}}_{k-1}Q_{k-1}G^{\mathbf{w}\mathrm{T}}_{k-1} \tag{3.16b}$$

Measurement Update

$$K_k = P_{k|k-1}H^{\mathrm{T}}_k(H_kP_{k|k-1}H^{\mathrm{T}}_k + R_k)^{-1} \tag{3.17a}$$

$$\hat{\mathbf{x}}_{k|k} = \hat{\mathbf{x}}_{k|k-1} + K_k(\mathbf{y}_k - H_k\hat{\mathbf{x}}_{k|k-1} - H^u_k\mathbf{u}_k) \tag{3.17b}$$

$$P_{k|k} = (I - K_kH_k)P_{k|k-1} \tag{3.17c}$$

sity functions, as illustrated in the following flow chart

$$\cdots \longrightarrow \mathcal{N}(\mathbf{x}_{k|k}, P_{k|k}) \xrightarrow{\text{prediction}} \mathcal{N}(\mathbf{x}_{k+1|k}, P_{k+1|k}) \xrightarrow{\text{update}} \mathcal{N}(\mathbf{x}_{k+1|k+1}, P_{k+1|k+1}) \longrightarrow \cdots$$

Transition density	Likelihood function
$\mathcal{N}(\mathbf{x}_{k+1}; F\mathbf{x}_k, Q_k)$	$\mathcal{N}(\mathbf{z}_{k+1}; H\mathbf{x}_{k+1}, R_{k+1})$
$\uparrow$	$\uparrow$
Motion model	Measurement model
$\mathbf{x}_{k+1} = F\mathbf{x}_k + \mathbf{w}_k$	$\mathbf{z}_{k+1} = H\mathbf{x}_{k+1} + \mathbf{e}_{k+1}$

The most well known estimation algorithm is the Kalman Filter (KF), derived by Kalman (1960), and shown in Algorithm 3. Example 3.4 shows how the single track vehicle model, introduced in Example 1.1, may be rewritten to be used with the Kalman filter, which in turn is used to estimate the states.

3.4 Example: Linearized Single Track Model

The single track vehicle model was introduced in Example 1.1 and the model equations were posed in Example 2.1. The process model (2.4a) and the measurement model (2.4b) are linear in the state variables and can be written in the form

$$\begin{bmatrix}\dot{\psi}_{k+1}\\ \beta_{k+1}\end{bmatrix} = F_k(\mathsf{v_x}, \boldsymbol{\theta})\begin{bmatrix}\dot{\psi}_k\\ \beta_k\end{bmatrix} + G^{\mathbf{u}}_k(\mathsf{v_x}, \boldsymbol{\theta})\delta_f + \mathbf{w}, \qquad \mathbf{w} \sim \mathcal{N}(0, Q), \tag{3.18a}$$

$$\begin{bmatrix}\dot{\psi}^m_k\\ a_{\mathsf{y},k}\end{bmatrix} = H_k(\mathsf{v_x}, \boldsymbol{\theta})\begin{bmatrix}\dot{\psi}_k\\ \beta_k\end{bmatrix} + H^u_k(\boldsymbol{\theta})\delta_f + \mathbf{e}, \qquad \mathbf{e} \sim \mathcal{N}(0, R), \tag{3.18b}$$

as shown in Example 2.7. Since the input $\mathsf{v_x}$ is present in F_k, $G^{\mathbf{u}}_k$ and H_k, these matrices must be recalculated at each time step before being used in the Kalman filter (Algorithm 3) to estimate the states.

3.2.2 The Extended Kalman Filter

In general, most complex automotive systems tend to be nonlinear. When it comes to solving state estimation problems in a sensor fusion framework, nonlinear models are commonly applied. This holds also for the work presented in this thesis, but the problems are restricted by the assumption that the process and measurement noise are Gaussian. The most common representation of nonlinear systems is the state space model given in (1.1), repeated here for convenience;

$$\mathbf{x}_{k+1} = f_k(\mathbf{x}_k, \mathbf{u}_k, \mathbf{w}_k, \boldsymbol{\theta}), \qquad \mathbf{w}_k \sim \mathcal{N}(0, Q_k), \tag{3.19a}$$

$$\mathbf{y}_k = h_k(\mathbf{x}_k, \mathbf{u}_k, \mathbf{e}_k, \boldsymbol{\theta}), \qquad \mathbf{e}_k \sim \mathcal{N}(0, R_k). \tag{3.19b}$$

The basic idea underlying the extended Kalman filter (EKF) is to approximate the nonlinear model (3.19) by a local linear model and apply the Kalman filter to this approximation. This local linear approximation is obtained by computing a first order Taylor expansion around the current estimate. The result is the extended Kalman filter, which is given in Algorithm 4. Early practical applications and examples of the EKF are described in the works by Smith et al. (1962); Schmidt (1966). An early reference where the EKF is treated is Jazwinski (1970), other standard references are Anderson and Moore (1979); Kailath et al. (2000) .

The linearization used in the EKF assumes that all second and higher order terms in the Taylor expansion are negligible. This is certainly true for many systems, but for some systems this assumption can significantly degrade the estimation performance. Higher order EKF are discussed by Roth and Gustafsson (2011); Bar-Shalom and Fortmann (1988); Gustafsson (2000). This problem will be revisited in the next section.

Algorithm 4 Extended Kalman Filter

Consider the state space model (3.19). The extended Kalman filter is given by the two following steps.

Prediction

$$\hat{\mathbf{x}}_{k|k-1} = f_{k-1}(\hat{\mathbf{x}}_{k-1|k-1}, \mathbf{u}_{k-1}, 0, \boldsymbol{\theta}) \tag{3.20a}$$

$$P_{k|k-1} = F_{k-1} P_{k-1|k-1} F_{k-1}^{\mathrm{T}} + G_{k-1} Q_{k-1} G_{k-1}^{\mathrm{T}} \tag{3.20b}$$

where

$$F_k = \left.\frac{\partial f_k(\mathbf{x}_k, \mathbf{u}_k, 0, \boldsymbol{\theta})}{\partial \mathbf{x}_k}\right|_{\mathbf{x}_k = \hat{\mathbf{x}}_{k|k}} \qquad G_k = \left.\frac{\partial f_k(\hat{\mathbf{x}}_{k|k}, \mathbf{u}_k, \mathbf{w}_k, \boldsymbol{\theta})}{\partial \mathbf{w}_t}\right|_{\mathbf{w}_k = 0} \tag{3.20c}$$

Measurement Update

$$K_k = P_{k|k-1} H_k^{\mathrm{T}} (H_k P_{k|k-1} H_k^{\mathrm{T}} + R_k)^{-1} \tag{3.21a}$$

$$\hat{\mathbf{x}}_{k|k} = \hat{\mathbf{x}}_{k|k-1} + K_k(\mathbf{y}_k - h_k(\hat{\mathbf{x}}_{k|k-1}, \mathbf{u}_t, 0, \boldsymbol{\theta})) \tag{3.21b}$$

$$P_{k|k} = (I - K_k H_k) P_{k|k-1} \tag{3.21c}$$

where

$$H_k = \left.\frac{\partial h_k(\mathbf{x}_k, \mathbf{u}_k, 0, \boldsymbol{\theta})}{\partial \mathbf{x}_k}\right|_{\mathbf{x}_k = \hat{\mathbf{x}}_{k|k-1}} \tag{3.21d}$$

3.2.3 The Unscented Kalman Filter

The EKF is sufficient for many applications. However, to use an EKF the gradients of $f_k(\cdot)$ and $h_k(\cdot)$ must be calculated, which in some cases is either hard to do analytically or computationally expensive to do numerically. An alternative approach, called the unscented Kalman filter (UKF) was proposed by Julier et al. (1995); Julier and Uhlmann (1997) and further refined by e.g., Julier and Uhlmann (2002, 2004); Julier (2002). Instead of linearizing $f_k(\cdot)$ and $h_k(\cdot)$, the unscented transform (UT) is used to approximate the moments of the predicted and updated states. Thereby the UKF to some extent also considers the second order terms of the models, which is not done by the EKF.

The principle of the unscented transform is to carefully and deterministically select a set of points, called sigma points, of the initial stochastic variable $\mathbf{x}$, such that their mean and covariance are equal to those of $\mathbf{x}$. Then the sigma points are passed through the non-linear function and based on the output the resulting mean and covariance are derived. In case the process noise and measurement noise are not additive, sigma points are selected from an augmented state space, which includes the state $\mathbf{x}$, the process noise $\mathbf{w}$ and the measurement noise $\mathbf{e}$ in one augmented state vector

$$\hat{\mathbf{x}}^a_{k|k} = \begin{bmatrix} \hat{\mathbf{x}}_{k|k} \\ \mathrm{E}(\mathbf{w}_k) \\ \mathrm{E}(\mathbf{e}_{k+1}) \end{bmatrix}, \tag{3.22}$$

with dimension $n_a = n_\mathbf{x} + n_\mathbf{w} + n_\mathbf{e}$ and the corresponding covariance matrix

$$P^a_{k|k} = \begin{bmatrix} P_{k|k} & 0 & 0 \\ 0 & Q_k & 0 \\ 0 & 0 & R_{k+1} \end{bmatrix}. \tag{3.23}$$

If the noise is additive, then the noise covariances can be added directly to the estimated covariances of the non-augmented sigma points.

There exist many possibilities to choose the sigma points, a thorough discussion about different alternatives is presented by Julier and Uhlmann (2004). In the present work only the standard form is reproduced. The basic principle is to choose one sigma point in the mean of $\mathbf{x}^a$ and $2n_a$ points symmetrically on a given contour, described by the state covariance P^a. The sigma points χ^i and the associated weights $w^{(i)}$ are chosen as

$$\chi^{(0)} = \hat{\mathbf{x}}^a \qquad w^{(0)} = w^{(0)} \tag{3.24a}$$

$$\chi^{(i)} = \chi^{(0)} + \left(\sqrt{\frac{n_a}{1 - w^{(0)}} P^a}\right)_i \qquad w^{(i)} = \frac{1 - w^{(0)}}{2n_a} \tag{3.24b}$$

$$\chi^{(i+n_a)} = \chi^{(0)} - \left(\sqrt{\frac{n_a}{1 - w^{(0)}} P^a}\right)_i \qquad w^{(i+n_a)} = \frac{1 - w^{(0)}}{2n_a} \tag{3.24c}$$

for $i = 1, \ldots, n_a$, where $(\sqrt{A})_i$ is the i^{th} column of any matrix B, such that $A = BB^\mathrm{T}$. The augmented state vector makes it possible to propagate and estimate nonlin-

Algorithm 5 Unscented Kalman Filter

Consider the state space model (3.19). The unscented Kalman filter is given by the following steps, which are iterated in the filter.

Choose sigma points according to (3.24)

Prediction

$$\hat{\mathbf{x}}_{k|k-1} = \sum_{i=0}^{2n_a} w^{(i)} \chi^{\mathbf{x},(i)}_{k|k-1} \tag{3.25a}$$

$$P_{k|k-1} = \sum_{i=0}^{2n_a} w^{(i)} \left(\chi^{\mathbf{x},(i)}_{k|k-1} - \hat{\mathbf{x}}_{k|k-1}\right)\left(\chi^{\mathbf{x},(i)}_{k|k-1} - \hat{\mathbf{x}}_{k|k-1}\right)^{\mathrm{T}} \tag{3.25b}$$

where

$$\chi^{\mathbf{x},(i)}_{k|k-1} = f_{k-1}\left(\chi^{\mathbf{x},(i)}_{k-1|k-1}, \mathbf{u}_{k-1}, \chi^{\mathbf{w},(i)}_{k-1|k-1}, \boldsymbol{\theta}\right) \tag{3.25c}$$

Measurement Update

$$\hat{\mathbf{x}}_{k|k} = \hat{\mathbf{x}}_{k|k-1} + P_{\mathbf{xy}} P_{\mathbf{yy}}^{-1} (\mathbf{y}_k - \hat{\mathbf{y}}_{k|k-1}) \tag{3.26a}$$

$$P_{k|k} = P_{k|k-1} - P_{\mathbf{xy}} P_{\mathbf{yy}}^{-1} P_{\mathbf{xy}}^{\mathrm{T}} \tag{3.26b}$$

where

$$\mathbf{y}^{(i)}_{k|k-1} = h_k\left(\chi^{\mathbf{x},(i)}_{k|k-1}, \mathbf{u}_k, \chi^{\mathbf{e},(i)}_{k|k-1}, \boldsymbol{\theta}\right) \tag{3.26c}$$

$$\hat{\mathbf{y}}_{k|k-1} = \sum_{i=0}^{2n_a} w^{(i)} \mathbf{y}^{(i)}_{k|k-1} \tag{3.26d}$$

$$P_{\mathbf{yy}} = \sum_{i=0}^{2n_a} w^{(i)} \left(\mathbf{y}^{(i)}_{k|k-1} - \hat{\mathbf{y}}_{k|k-1}\right)\left(\mathbf{y}^{(i)}_{k|k-1} - \hat{\mathbf{y}}_{k|k-1}\right)^{\mathrm{T}} \tag{3.26e}$$

$$P_{\mathbf{xy}} = \sum_{i=0}^{2n_a} w^{(i)} \left(\chi^{\mathbf{x},(i)}_{k|k-1} - \hat{\mathbf{x}}_{k|k-1}\right)\left(\mathbf{y}^{(i)}_{k|k-1} - \hat{\mathbf{y}}_{k|k-1}\right)^{\mathrm{T}} \tag{3.26f}$$

---

ear influences that the process noise and the measurement noise have on the state vector and the measurement vector, respectively. The weight on the mean $w^{(0)}$ is used for tuning and according to Julier and Uhlmann (2004) preferable properties for Gaussian density functions are obtained by choosing $w^{(0)} = 1 - \frac{n_a}{3}$. After the sigma points have been acquired, the augmented state vector can be partitioned according to

$$\chi^a_{k|k} = \begin{bmatrix} \chi^{\mathbf{x}}_{k|k} \\ \chi^{\mathbf{w}}_{k} \\ \chi^{\mathbf{e}}_{k+1} \end{bmatrix}. \tag{3.24d}$$

The rest of the UKF is summarized in Algorithm 5.

An advantage of the UKF, compared to the EKF, is that the second order bias correction term is implicitly incorporated in the mean estimate. Example 3.5 shows an important problem where the second order term should not be neglected.

3.5 Example: Tracked Radar Object

The radar target tracking problem was introduced in Example 1.2 and the model was defined in Example 2.4. The sensor model converts the Cartesian state variables to polar measurements. This is one of the most important and commonly used transformations for sensors measuring range and azimuth angle. Usually the azimuth angle error of these type of sensors is significantly larger than the range error. This also holds for the sensors used in this thesis.

Let the sensor be located at the origin and the target at $(\mathrm{x}, \mathrm{y}) = (0, 1)$ in this simple, and commonly used example (Julier and Uhlmann, 2004). Measurements may be simulated by adding Gaussian noise to the actual polar value $(r, \psi) = (1, \pi/2)$ of the target localization. A plot of several hundred state estimates, produced in a Monte Carlo simulation, forms a banana shaped arc around the true value $(\mathrm{x}, \mathrm{y}) = (0, 1)$, as shown in Figure 3.1. The azimuth error causes this band of Cartesian points to be stretched around the circumference of a circle, with the result that the mean of these points lies somewhat closer to the origin than the point $(0, 1)$. In the figure it is clearly shown that that the UT estimate $(\times)$ lies close to the mean of the measurements $(\circ)$. Furthermore, it is shown that the linearized state estimate $(+)$ produced by the EKF is biased and the variance in the y component is underestimated.

As a result of the linearization in the EKF, the second order terms are neglected, which produces a bias error in the mean as shown in Example 3.5. In Julier and Uhlmann (2004) it is shown how the UT in some cases calculates the projected mean and covariance correctly to the second order terms.

The unscented Kalman filter is applied in Papers C and D.

3.2.4 The Particle Filter

Numerical approximations of distribution function used in the Bayes equations (3.13) are necessary since analytical solutions to the filtering problems do not exist in most cases. A stochastic method called sequential Monte Carlo (SMC) or particle filter (PF), which is based on Monte Carlo integration, has become popular during the last years. It was introduced by Gordon et al. (1993) and theory is well described by e.g., Doucet et al. (2001, 2000); Ristic et al. (2004); Gustafsson (2010). The idea is to approximate the PDF with a number of samples, called particles, $\{\mathbf{x}_k^{(i)}\}_{i=1}^N$ with associated weights $\{w_{k|k-1}^{(i)}\}_{i=1}^N$ such that

$$p(\mathbf{x}_k|\mathbf{y}_{1:k-1}) \approx \sum_{i=1}^{N} w_{k|k-1}^{(i)} \delta(\mathbf{x}_k - \mathbf{x}_k^{(i)}). \tag{3.27}$$

The particles are selected to be identically and independently distributed samples from a so called proposal distribution $q(\mathbf{x}_{k+1}|\mathbf{x}_k^{(i)}, \mathbf{y}_{1:k+1})$ and the weights are called importance weights. Using Monte Carlo integration the mean value of the

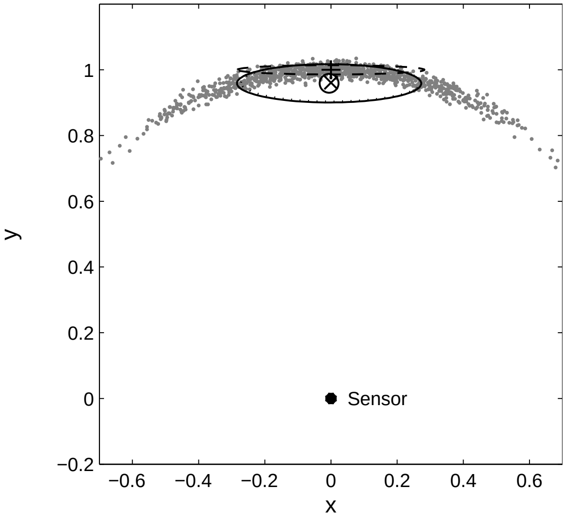

(a)

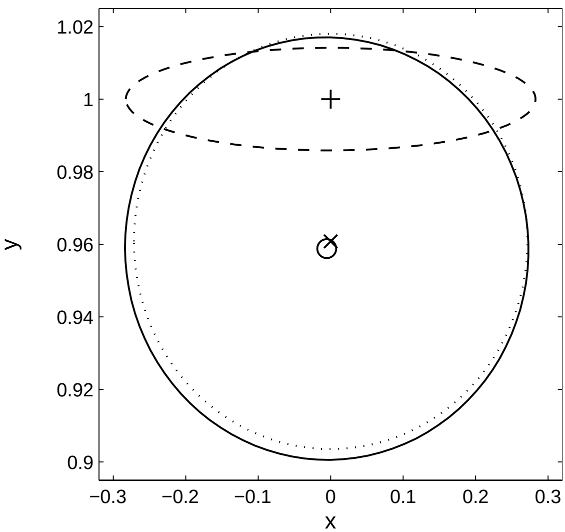

(b)

Figure 3.1: *A Monte Carlo simulation of the problem in Example 3.5 is shown in Figure (a). The sensor, for example a radar, is in the position* $(0, 0)$ *and the true position of the target is in the position* $(0, 1)$*. The mean of the measurements is at* $\circ$ *and the uncertainty ellipse is solid. The linearized mean is at* $+$ *and its ellipse is dashed. The UT mean is at* $\times$ *and its uncertainty ellipse is dotted. Figure (b) is a zoom. Note that the scaling in the* x *and the* y *axis are different.*

Algorithm 6 Particle Filter

1: Initiate $\{\mathbf{x}_0^{(i)}\}_{i=1}^N \sim p_{\mathbf{x}_0}$ and $\{w_0^{(i)}\}_{i=1}^N = \frac{1}{N}$ for $i = 1, \ldots, N$
2: $k = 0$
3: **loop**
4: **for** $i = 1$ **to** N **do**
5: Time Update: generate the sample, $\mathbf{x}_{k|k-1}^{(i)} \sim q(\mathbf{x}_k|\mathbf{x}_{k-1|k-1}^{(i)}, \mathbf{y}_k)$
6: Update importance weights

$$w_{k|k-1}^{(i)} = w_{t-1|t-1}^{(i)} \frac{p(\mathbf{x}_{k|k-1}^{(i)}|\mathbf{x}_{k-1|k-1}^{(i)})}{q(\mathbf{x}_{k|k-1}^{(i)}|\mathbf{x}_{k-1|k-1}^{(i)}, \mathbf{y}_k)}$$

{Note, if $q(\mathbf{x}_k|\mathbf{x}_{k-1|k-1}^{(i)}, \mathbf{y}_{1:k}) = p(\mathbf{x}_k|\mathbf{x}_{k-1|k-1}^{(i)})$ this simplifies to $w_{k|k-1}^{(i)} = w_{t-1|t-1}^{(i)}$}
7: Measurement update: $\bar{w}_{k|k}^{(i)} = p(\mathbf{y}_k|\mathbf{x}_{k|k}^{(i)}) w_{k|k-1}^{(i)}$
8: **end for**
9: Normalize weights $w_{k|k}^{(i)} = \frac{\bar{w}_{k|k}^{(i)}}{\sum_j \bar{w}_{k|k}^{(j)}}$ for $i = 1, \ldots, N$
10: Resample
11: **end loop**

distribution can easily be calculated according to

$$\hat{\mathbf{x}}_{k|k-1} = \mathrm{E}(\mathbf{x}_k) \approx \sum_{i=1}^{N} w_{k|k-1}^{(i)} \mathbf{x}_k^{(i)}. \tag{3.28}$$

The PF is described in Algorithm 6.

The resampling in Line 10 rejuvenates the particles used to represent the PDF. There exist different methods to resample, and it will not be discussed further here; the reader is referred to Hendeby (2008); Schön (2006) instead.

The PF is used in Paper C to track extended targets. In Paper G, the PF is used since the mean and covariance of the process noise are unknown and must be estimated together with the states. In that case the particles are drawn from a Student-t distribution.

4 Target Tracking

The process of estimating over time the location and characteristics of one or more objects of interest, denoted *targets*, using one or several sensors is referred to as target *tracking*. The aim of the tracking algorithm is to detect the true targets, collect observations that originate from them and to estimate quantities of interest, such as target position, velocity and other object characteristics. Typical sensors for these applications, such as radar, laser and vision, report noisy measurements. Besides the fact that the measurements are noisy another difficulty for the algorithm is that the sensor measurements not only originate from the targets, but also from clutter or spurious detections. The target tracking area is well covered in the literature and recommended books are Blackman and Popoli (1999); Bar-Shalom and Fortmann (1988); Bar-Shalom et al. (2001); Ristic et al. (2004); Liggins et al. (2009).

This chapter begins by putting the filter, introduced in the last chapter about estimation theory, into the target tracking framework. In Section 4.1 the focus is on the filter and therefore only the single target case is considered. An automotive target tracking system, must obviously be able to handle multiple targets, because potentially more than one vehicle are surrounding the own vehicle. Therefore the chapter is continued by discussing the extension to *multi target tracking* in Section 4.2. When reading the first two sections, compare with the block diagram of the target tracking framework illustrated in the introduction in Figure 1.4. Finally, in Section 4.3 the system is further enlarged to also be able to track the shape and size of the the targets. This research area is called *extended target tracking*.

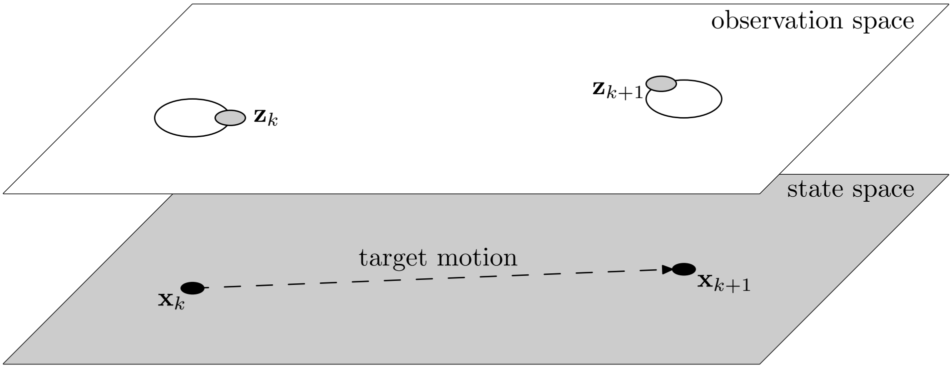

Figure 4.1: *Single target tracking problem. The upper layer is the observation space with the measurements and the lower layer is the state space with the state variables.*

4.1 Single Target Tracking

The complete information required to describe the system at time k is summarized in the state vector $\mathbf{x}_k \in \mathbb{R}^{n_x}$. At each time step the tracking algorithm is supplied with a measurement vector $\mathbf{z} \in \mathbb{R}^{n_z}$. The aim of the filter, as part of a target tracking algorithm, is to find the *posterior density* $p(\mathbf{x}_k|\mathbf{z}_{1:k})$, given a sequence of noisy measurement vectors up to and including time k, collected in

$$\mathbf{z}_{1:k} = \{\mathbf{z}_1, \mathbf{z}_2, \dots \mathbf{z}_k\}. \tag{4.1}$$

From the posterior it is possible to calculate an estimate $\hat{\mathbf{x}}_k$ of the state $\mathbf{x}_k$. Typically, the targets or the sensors are moving and the system changes over time. The motion of the targets in time is modeled with a Markov density, given in (2.27), and the PDF is specified with a motion model (2.1a). The measurement $\mathbf{z}_k$ received by the sensor is modeled by a likelihood function (2.29), which is specified by a measurement model (2.1b). Both the process and measurement noise variables are assumed to be white and independent. Figure 4.1 illustrates the filtering problem. The upper layer represents the *observation space*, where one measurement $\mathbf{z}_k$ is observed at each time step k and another measurement is observed at time step $k + 1$. The lower layer represents the *state space*, with the values of the state vector $\mathbf{x}_k$ at each time step.

The single target Bayes filter recursion consists of two steps, the *prediction* step and the *correction* step. Since all variables are assumed to be unknown stochastic variables in the Bayesian framework it is necessary to describe *a priori* information about the state in the form of a prior density $p_0(\mathbf{x}_0)$. The recursion was illustrated with a flow chart in Section 3.2. A special case is the Kalman filter, where the densities are assumed to be Gaussian.

4.2 Extension to Multitarget Tracking

In this chapter until now only single targets have been considered. This scenario is quite unusual, in most target tracking applications more than one target may appear and must be handled by the target tracking system. A multi target tracking system must not only provide estimates of the state variables

$$\left\{ \mathbf{x}_k^{(1)}, \mathbf{x}_k^{(2)}, \ldots, \mathbf{x}_k^{(N_\mathbf{x})} \right\} \tag{4.2}$$

it must also estimate the number of targets $N_\mathbf{x}$, and find likely associations of the measurements to the tracks. The latter uncertainty is known as the data association problem.

A typical multi target system is shown in Figure 4.2, where several targets exist at each time step. Aspects to consider in a multitarget tracking filter are listed below:

- The number of targets $N_\mathbf{x}$ changes over time, for instance there are probably more vehicles on the roads during rush hour than in the night.
- New targets appear and old targets disappear, as they enter or leave the field of view of the sensor. Compare with Figure 4.2, where target $\mathbf{x}^{(4)}$ appears at time $k+1$.
- The system fails to detect targets because they are temporarily occluded or because the sensor data is very noisy.
- The sensors receive a set of spurious measurements, also denoted *clutter*, stemming from false reflections or from other type of objects in the field of view, etc. In Figure 4.2 there are more observations than targets at each time step.

In this section first the data association problem is treated in Section 4.2.1 and thereafter an overview of the track management, which takes care of the problems in the list above is given in Section 4.2.2.

4.2.1 Data Association

This section would not be needed if only the state variables of the ego vehicle, introduced in Example 1.1 are estimated, because in that case it is obvious how the measurements are associated with the state variables. In the object tracking problem, introduced in Example 1.2, it is no longer obvious which measurement should update which track. There are many methods available for finding likely measurement-to-track associations, i.e., for solving the data association problem, see e.g., Bar-Shalom and Fortmann (1988); Blackman and Popoli (1999). However, the task is seldom easy, due to noisy measurements, multiple reflections on each target and erroneous detections caused by spurious reflections.

The first step in the data association process is called *gating*. Gates are constructed around the predicted measurement $\hat{\mathbf{z}}_{k|k-1}^{(i)}$ of each track i to eliminate

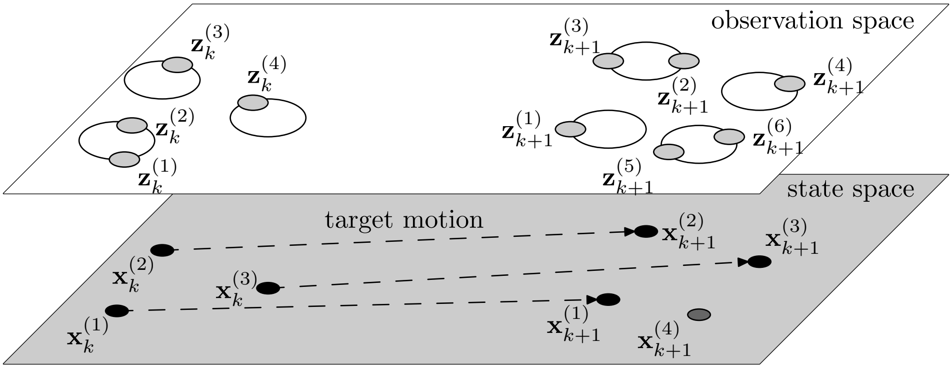

Figure 4.2: *Multi target tracking system, several state vectors are present at each time step and producing more than one observation. Note that there are more observations than targets. A new target* $\mathbf{x}^{(4)}$ *appears at time* $k+1$.

unlikely pairings and thereby to limit the number of measurement-to-track associations. This reduces the number of measurements that are examined by the data association algorithm and reduces the computational load. The residual, which is also called innovation, between a measurement $\mathbf{z}_k^{(j)}$ and a predicted measurement $\hat{\mathbf{z}}_{k|k-1}^{(i)}$ is

$$\tilde{\mathbf{z}}_{k|k-1}^{(i,j)} = \mathbf{z}_k^{(j)} - \hat{\mathbf{z}}_{k|k-1}^{(i)}, \tag{4.3}$$

and it is assumed Gaussian distributed according to

$$\tilde{\mathbf{z}}_{k|k-1}^{(i,j)} \sim \mathcal{N}(0, S_k^{(i)}), \tag{4.4}$$

where $S_k^{(i)}$ is the innovation covariance. Further, under this assumption, the statistical distance between the measurement and the predicted measurement, given by the norm of the residuals according to

$$d_{i,j}^2 = (\tilde{\mathbf{z}}_{k|k-1}^{(i,j)})^{\mathrm{T}} S_{i,k}^{-1} (\tilde{\mathbf{z}}_{k|k-1}^{(i,j)}), \tag{4.5}$$

is a $\chi_{n_y}^2$ random variable. The elliptical gate $\mathcal{G}_i$ is defined as the region

$$\mathcal{G}_i \triangleq \left\{ \mathbf{z} \middle| (\tilde{\mathbf{z}}_{k|k-1}^{(i,j)})^{\mathrm{T}} S_{i,k}^{-1} (\tilde{\mathbf{z}}_{k|k-1}^{(i,j)}) \leq \gamma_{\mathcal{G}} \right\}, \tag{4.6}$$

where $\gamma_{\mathcal{G}}$ is the gating threshold or gate size. Given a certain probability that a true measurement produced by a target i will fall inside its gate, and that the assumption $d_{i,j}^2 \sim \chi_{n_y}^2$ holds, a suitable gate threshold can be determined. The measurements $\mathbf{z}_k^{(j)} \in \mathcal{G}_i$ are considered as candidates for updating the track $\mathbf{x}_k^{(i)}$ in the data association algorithm. In other words the gating is a hard decision about which measurements are feasible measurements for a target.

Now, different conflicts occur. There are several measurements falling within the same gate and there are also measurements falling within more than one gate. There exist many techniques to solve these conflicts, which are considered to be the main part of the data association process. The simplest association algorithm is called *nearest neighbor* (NN). This approach searches for a unique pairing, i.e., one track $\mathbf{x}_k^{(i)}$ is only updated by at most one observation $\mathbf{z}_k^{(j)}$. There are some possibilities to decide which measurement actually is the nearest. Common approaches are to choose the measurement with the smallest error $\tilde{\mathbf{z}}_{k|k-1}^{(i,j)}$ or the smallest statistical distance $d^2(\tilde{\mathbf{z}}_{k|k-1}^{(i,j)})$, defined in (4.5), which is also known as the Mahalanobis distance, see e.g., Bar-Shalom et al. (2001). The association distance for each individual track is locally minimized separately with the NN approach, which could lead to that two tracks are associated with the same measurement. To avoid this problem it would be more beneficial to find the global minimum distance considering all tracks simultaneously, and restrict that a measurement can only be associated with one track. This approach is referred to as global nearest neighbor (GNN), and its aim is to solve

$$\min_{\lambda} = \sum_{i}^{N_k} d_{i,\lambda_i}^2 \tag{4.7}$$

where $\lambda_i \in \{0, 1, \ldots, N\}$ indicates which measurement has been assigned to track i. Note that the value $\lambda_i = 0$ means that track i has not been associated with any measurement. The so called auction algorithm is the most well known method to solve this problem, see Bertsekas (1990). Example 4.1 illustrated gating and a comparison between NN and GNN.

4.1 Example: Gating and Nearest Neighbor Data Association

Consider the target tracking example introduced in Example 1.2. Assume that two vehicles are currently tracked. Their predicted measurements $\hat{\mathbf{z}}_{k|k-1}^{(1)}$ and $\hat{\mathbf{z}}_{k|k-1}^{(2)}$ are shown in blue and green in Figure 4.3. Six measurements $\mathbf{z}_k^{(j)}$, $j = 1, \ldots, 6$ are collected at time k and shown as red stars in the figure. The measurements 2, 4 and 6 fall outside the gates, which are illustrated with ellipses. Measurement 1 and 3 may be obtained from target 1 since they are both in its gate. However, measurement 3 is also in the gate of target 2. The NN data association considers each track individually, and since measurement 3 is the closes measurements of both targets it is used to update both targets as shown in Figure 4.3a. The GNN data association avoids this problem and considers all tracks simultaneously. The result is shown in Figure 4.3b, where target 2 is associated with measurement 5 instated.

There exist a further group of association methods, which uses all measurements that fall inside the gate. In these methods each measurement j is weighted in accordance with the probability that it originates from track i. The two most well known algorithms are probabilistic data association (PDA) (Bar-Shalom and Tse, 1975) and joint probabilistic data association (JPDA) (Fortmann et al., 1983),

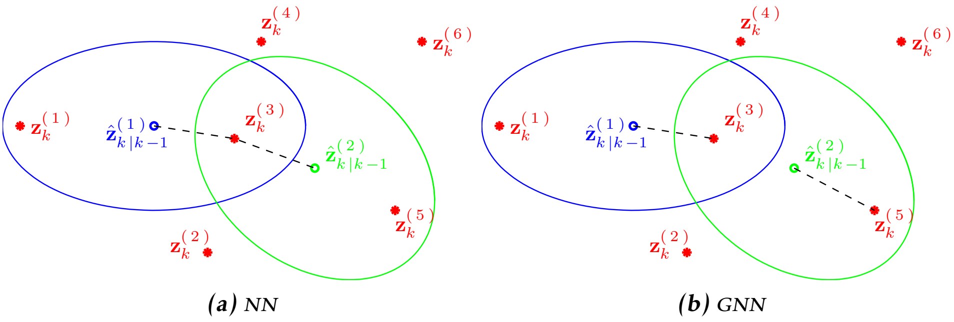

Figure 4.3: *An example with two targets (blue and green) and six measurements (in red). The ellipses are the gates and the two figures show the difference between the association methods* NN *and* GNN.

where the difference lies in that PDA considers each track separately, whereas JPDA forms global hypotheses to calculate the probabilities. Note that the number of targets is assumed fixed in the above mentioned association methods. These methods are not further discussed in this thesis, hence a detailed description is omitted at this place.

4.2.2 Track Management

The main task of the track management is to decide on how many true targets are observed. Only tracks of sufficient quality should be considered as valid tracks and used in the data association algorithms described above. According to their different life stages, tracks can be classified into three cases.

Tentative track: A track that is in the track initiation process. It is not sure that there is sufficient evidence that it is actually a target or not. A tentative track is started as soon as it is likely that a measurement originates from a new target. The tentative tracks can be associated to further measurements.

Confirmed track: A track that was decided to belong to a valid target in the surveillance area. If several sequential arriving observations indicate that the tentative track resembles a true target rather than noise or clutter it is decided to be a confirmed track.

Deleted track: At the other end of the initiation process, this is a track that is decided to come from all random false alarm. It can also be a track that is no longer visible to any sensor when the uncertainty of the target increases above a given threshold. All of its information should be deleted.

When starting a new track some initial guess about the properties of the track must be made. Put into a Bayesian wording, a *prior density* $p(\mathbf{x}_0)$, that contains the information of the state before any observation is made, must be designed. This can sometimes be a simple task, for instance if you expect targets to appear from a certain place, but in most cases it is not easy to know beforehand. A practical and straightforward method is to use the first measurement as the mean value of the prior distribution. Other statistics of the prior distribution are still considered as design variables. A better approach may be considered in the Kalman filter, where the prior distribution is Gaussian and may be chosen as $\mathbf{x}_0 \sim \mathcal{N}(0, P_0)$. If P_0 is chosen very large in comparison with the measurement uncertainty, the first updated state estimate will largely be based on the associated measurement.

In order to know if the first measurement stems from a true target or from clutter, the track management system must observe the tentative track for a number of samples. There exist different methods to decide if a tentative track shall be transformed into a confirmed track. One of the simplest and most well known is the so called M/N logic, where a track is confirmed if M measurements out of N possible are associated with the track. Other common methods are based on scoring measurements, with for example *sequential probability ratio test* (SPRT), which was first proposed by Wald (1945). The method is based on comparing the ratio between the likelihood of the hypothesis that a track describes a true target and the likelihood of the hypothesis that it is a false alarm. Furthermore, there exist combined validation and association methods. Integrated probabilistic data association (IPDA) expresses both the probability of target existence and data association based on PDA.

The track deletion methods are similar to the validation methods, both the M/N logic and the score based approaches, mentioned above, can be applied. More information and details about track management can be found in various books about target tracking, see e.g., Blackman and Popoli (1999).

4.3 Extended Target Tracking

In classical target tracking problems the objects are modeled as point sources and it is assumed that only one measurement is received from each target at each time step. In automotive applications, the targets are at a close distance and of such a large size that individual features can be resolved by the sensor. A target is denoted extended whenever the target extent is larger than the sensor resolution, and it is large enough to occupy multiple resolution cells of the sensor. Put in other words, if a target should be classified as extended does not only depend on its physical size, but rather on the physical size relative to the sensor resolution.

The relevant target characteristics that are to be estimated form the target's state vector $\mathbf{x}$. Generally, beside the kinematic variables as position, velocity and orientation, the state vector may also contain information about the target's spatial extension. However, when the target's state does not contain any variables related to the target extent, though the estimation is done as if the target was a point, the algorithms should still take care of the multiple measurements that originate from a target. In Paper E a generalized definition of an extended target is presented, and it is repeated below. This definition does not depend on whether the target extent is estimated or not.

4.2 Definition (Extended Target). A target which potentially gives rise to more than one measurement per time step irrespective of whether the target's extent is explicitly modeled (and/or estimated) or not is referred to as an extended target.

The methods used to track extended target are very similar to the ones used for tracking a group of targets moving in formation. Extended target tracking and group tracking are thoroughly described in e.g., Ristic et al. (2004). The bibliography of Waxman and Drummond (2004) provides a comprehensive overview of existing literature in the area of group and cluster tracking. There exist some different approaches to represent, i.e., to model, the extended targets, of which five methods are described in this section.

4.3.1 Point Features

The first and most traditional method is to model the target as a set of point features in a target reference frame, each of which may contribute at most one sensor measurement. The exact location of a feature in the target reference frame is often assumed uncertain. However, if the appearance of the target is known and especially if typical radar reflection points are known, then the location of the features in the target reference frame can be assumed known. The motion of an extended target is modeled through the process model in terms of the translation and rotation of the target reference frame relative to a world coordinate frame, see e.g., Dezert (1998).

For an application in two dimensions, the point features are defined as

$$\mathbf{P}^T = \left\{\mathbf{p}^{(i)}\right\}_{i=1}^{N_p} \quad \text{with} \quad \mathbf{p}^{(i)} = \begin{bmatrix} \mathsf{x}^{(i)} & \mathsf{y}^{(i)} \end{bmatrix}^{\mathrm{T}} \tag{4.8}$$

and these are usually expressed in a target fixed coordinate frame T. The position $\boldsymbol{d}_{TW}^{W} = \begin{bmatrix} \mathsf{x}_{TW}^{W} & \mathsf{y}_{TW}^{W} \end{bmatrix}^{\mathrm{T}}$ of the target's origin and the orientation ψ_T of the target's frame is tracked relative to the world coordinate frame. The state vector may be defined as

$$\mathbf{x} = \begin{bmatrix} \boldsymbol{d}_{TW}^{W} & \psi_T & \mathbf{P}^T \end{bmatrix}^{\mathrm{T}}. \tag{4.9}$$

The point features in the target's coordinate frame can be mapped into a point in the world frame through the transform

$$\mathbf{p}^{(i),W} = R^{WT}\mathbf{p}^{(i),T} + \boldsymbol{d}_{TW}^{W}. \tag{4.10}$$

The equation above constitutes the measurement model if the point measurements are expressed in the world coordinate frame W. The rotation matrix is given by

$$R^{WT} = \begin{bmatrix} \cos\psi_T & -\sin\psi_T \\ \sin\psi_T & \cos\psi_T \end{bmatrix}. \tag{4.11}$$

The uncertainty about the exact position of the point feature is modeled according to

$$p(\mathbf{P}^W | \boldsymbol{d}_{TW}^W, \psi_T) = \prod_{i=1}^{N_p} \mathcal{N}(p^{(i),W} | R^{WT}(\psi_T) p^{(i),T} + \boldsymbol{d}_{TW}^W, w_p I_2), \tag{4.12}$$

which means that the uncertainty is assumed isotropic around the mean location of the point and with known variance w_p.

At each time step a set of $N_\mathbf{z}$ measurements $\mathbf{Z} = \{\mathbf{z}_i\}_{i=1}^{N_\mathbf{z}}$ is received and has to be associated to the states. Not all measurements arise from a point feature, some are due to false detections (clutter). The association hypotheses are derived through some data association algorithm. In Vermaak et al. (2005) a method is proposed where the association hypotheses are included in the state vector and the output of the tracking filter is a joint posterior density function of the state vector and the association hypotheses. Furthermore, a multi-hypothesis likelihood is obtained by marginalizing over all the association hypotheses. An alternative solution is also proposed using a particle filter, where the unknown hypotheses are sampled from a well designed proposal density function.

An automotive radar sensor model developed for simulation purposes is proposed in Bühren and Yang (2006), where it is assumed that radar sensors often receive measurements from specific reflection centers on a vehicle. These reflection centers can be tracked in a filter and valuable information regarding the vehicle's orientation can be extracted as shown by Gunnarsson et al. (2007). A difficulty in solving the data association problem is the large number of association hypotheses available. To reduce the complexity Gunnarsson et al. (2007) proposes an approach where detections are associated with reflector groups. The spatial Poisson distribution, discussed in the subsequent section, is considered to be inappropriate, since the number of vehicle detections is assumed essentially known and not adequately modeled by a Poisson process.

In paper F the point features are denoted measurement generating points (MGP), and they are positioned on the surface of the target. In the referred publication, the MGPs are not considered having a fixed position on the surface, but they are instead defined as a random finite set of points on the one-dimensional surface of the target. The positions of the points on the surface are estimated in the target tracking filter, but they are of less importance, since they only serve as a means to estimate the position, shape and size of the entire target.

4.3.2 Spatial Distribution

Instead of modeling the target as a number of point features, which are assumed to be explicit measurement sources, the target may also be represented by a spatial probability distribution. It is more likely that a measurement comes from a region of high spatial density than from a sparse region. In Gilholm and Salmond (2005); Gilholm et al. (2005) it is assumed that the number of received target and clutter measurements are Poisson distributed, hence several measurements may originate from the same target. Each target related measurement is an independent sample from the spatial distribution. The spatial model could be a bounded distribution, such as a uniform PDF or an unbounded distribution, such as a Gaussian. The Poisson assumption allows the problem, or more specifically the evaluation of the likelihood, to be solved without association hypotheses. The spatial distribution is preferable where the point source models are poor representations of reality, that is in cases where the measurement generation is diffuse.

In Gilholm and Salmond (2005) two simple examples are given. One where the principle axis of the extended target is aligned with the velocity vector, i.e., the target is represented by a one dimensional uniform stick model. In the other example, a Gaussian mixture model is assumed for the target. A Kalman filter implementation with explicit constructions of assignment hypotheses is derived from the likelihood in Gilholm and Salmond (2005), whereas in Gilholm et al. (2005), a particle filter is applied directly given the likelihood which is represented by the Poisson spatial model of the stick. Hence, the need to construct explicit measurement-target assignment hypotheses is avoided in Gilholm et al. (2005). Swain and Clark (2010) proposes instead a standard measurement model but represents instead the extended targets as a spacial cluster process.

Boers et al. (2006) presents a similar approach, but since raw data is considered, no data association hypotheses are needed. The method to use raw data, i.e., consider the measurements without applying a threshold, is referred to as track before detect. A one dimensional stick target is assumed also by Boers et al. (2006), but unlike Gilholm and Salmond (2005), the target extent is assumed unknown. The state vector is given by the stick's center position and velocity as well as the stick's extension according to

$$\mathbf{x} = \begin{bmatrix} \mathsf{x} & \mathsf{y} & \dot{\mathsf{x}} & \dot{\mathsf{y}} & \mathsf{l} \end{bmatrix}^{\mathrm{T}}. \tag{4.13}$$

The process model is a simple constant velocity model and the length l is modeled as a random walk. The likelihood function is given by the probability distribution

$$p(\mathbf{z}|\mathbf{x}) = \int p(\mathbf{z}|\tilde{\mathbf{x}})p(\tilde{\mathbf{x}}|\mathbf{x})d\tilde{\mathbf{x}}, \tag{4.14}$$

where the spatial extension is modeled by the PDF $p(\tilde{\mathbf{x}}|\mathbf{x})$ and $\tilde{\mathbf{x}}$ is assumed to be a point source from an extended target with center given by the state vector $\mathbf{x}$. Hence, a measurement is received from a source $\tilde{\mathbf{x}}$ with likelihood $p(\mathbf{z}|\tilde{\mathbf{x}})$.

4.3.3 Elliptical Shaped Target

In many papers dealing with the shape of a target it is assumed that the sensor, e.g., radar, is also able to measure one or more dimensions of the target's extent. A high-resolution radar sensor may provide measurements of a targets down-range extent, i.e., the extension of the objects along the line-of-sight. The information of the target's extent is incorporated in the tracking filter and aids the tracking process to maintain track on the target when it is close to other objects.

An elliptical target model, to represent an extended target or a group of targets, is proposed in Drummond et al. (1990). The idea was improved by Salmond and

Parr (2003), where the sensor not only provides measurements of point observations, but rather range, bearing and down-range extent. The prime motivation of the study is to aid track retention for closely spaced moving targets. Furthermore, the state vector includes the position, velocity and the size of the ellipse. An EKF is used in Salmond and Parr (2003), but it is concluded that the filter may diverge under certain conditions, since the relation between the down-range extent measurement of the target and the position and velocity coordinates in the state vector is highly nonlinear. The same problem is studied in Ristic and Salmond (2004), where a UKF is implemented and tested. Even though the UKF shows better performance it is concluded that neither the EKF nor the UKF are suitable for this problem. The problem is further studied by Angelova and Mihaylova (2008), where other filter techniques, based on Monte Carlo algorithms, are proposed. In this paper the size of the ellipse takes values from a set of standard values, i.e., the algorithm estimates the type of object from a list, under the assumption that typical target sizes are known.

A group of objects moving collectively may also be modeled as an extended target. The ellipse model is used to model a formation of aircraft in Koch (2008). The object extension is represented by a symmetric positive definite random matrix, however, the measurement error is not considered in this publication. Improvements of this approach, including the consideration of sensor error, has been published by Feldmann et al. (2011). An alternative measurement model and an extesion using principal components is proposed by Degerman et al. (2011). Wieneke and Davey (2011) show how the random matrix approach can be used to track multiple extended targets directly from image data.

The concept of random hypersurface model, introduced by Baum and Hanebeck (2009), assumes that each measurement source is an element of a randomly generated hypersurface. In this publication an elliptical target shape is used to exemplify the approach. Improvements of the approach has been published in Baum et al. (2010), and a generalization which allows for tracking detail shapes, based on star convex shaped extended targets, is presented in Baum and Hanebeck (2011).

4.3.4 Curved Target

In Paper C the road borders are modeled as extended targets in the form of curved lines. A curved line is expressed as a third order polynomial in its coordinate frame. Since the road borders are assumed to be stationary, the frames are not included in the state vector. Furthermore, stationary points such as delineators and lamp posts are also modeled in Paper C. The nearest neighbor algorithm is used to associate measurements from stationary observations $\mathbf{z}^{(m)}$ to the targets. Here it is assumed that an extended line target $\mathrm{L}^{(j)}$ can give rise to several measurements, but a point target $\mathrm{P}^{(i)}$ can only contribute to one measurement. Since the likelihood of a line $\ell_{m,j}$ is a one dimensional spatial density function, but the likelihood of a point $\ell_{m,i}$ is given by a two dimensional density function, a likelihood ratio test is applied to determine the measurement-to-track association problem.

The likelihood ratio for a measurement $\mathbf{z}^{(m)}$ is given by

$$\Lambda(\mathbf{z}^{(m)}) \triangleq \frac{\sqrt{\ell_{m,i}}}{\ell_{m,j}}. \tag{4.15}$$

where the square root of the point likelihood is taken for unit matching, since the unit of the point likelihood is (distance)$^{-2}$ and the unit of the line likelihood is (distance)$^{-1}$. The corresponding *likelihood ratio test* is

$$\Lambda(\mathbf{z}^{(m)}) \underset{H_1}{\overset{H_0}{\gtrless}} \eta, \tag{4.16}$$

where H_0 and H_1 correspond to hypotheses that the measurement $\mathbf{z}^{(m)}$ is associated to the point P_i and to the line L_j, respectively. The threshold is selected experimentally. More theory about likelihood ratio test is given by e.g., van Trees (1968).

4.3.5 Extended Target Tracking and PHD filter

In the recent work Mahler (2009a) an extension of the (PHD) filter to also handle extended targets of the type presented in Gilholm et al. (2005) is given. The PHD filter is the topic of next section and therefore it will only be briefly summarized here. In Paper E a Gaussian-mixture implementation of the PHD-filter for extended targets called the extended target GM-PHD-filter (ET-GM-PHD) is presented. It is shown that this filter works well in most situation, but that it is sensitive in estimating the number of targets in a few situation e.g., when occlusion occurs. Therefore, generalization of Mahler's work has been made to derive the cardinalized PHD (CPHD) filter for extended targets, presented by Orguner et al. (2011). In addition to the derivation, a Gaussian mixture implementation for the derived CPHD filter is presented. This filter has less sensitive estimates of the number of targets. Early results on laser data are shown which illustrates robust characteristics of the CPHD filter compared to its PHD version.

Initial step have also been taken towards including estimation of target extent in the GM-PHD-filter, see Granström et al. (2011b). The state vector is augmented with a discrete state describing the type of object e.g., rectangle, ellipse etc. In Paper F a hybrid state space is introduced, where MGPs and the measurements are modeled by random finite sets and target states by random vectors. For each realization of the state vector, a PHD filter is utilized for estimating the conditional set of MGPs given the target states.

5

Probability Hypothesis Density Filter and Its Implementation

In the previous chapter it was shown how single target tracking filters can be extended and used to handle multiple targets by enclosing the filters with a target management framework. In this way measurements are associated to targets, which are tracked as isolated entities. To be able to perform the data association it is assumed that the number of present targets is known. This is rarely true, and therefore a track management logic estimated the number of valid and confirmed tracks. These methods explicitly separate the estimation of the number of targets and estimation of target states, which is suboptimal. *Random finite set* (RFS) formalism introduces a more rigorous approach to the multi target tracking problem. A set contains the random number of single target tracks, of which each is a random vector. The state vectors are elements of the RFS and their change in time is described with a motion model. The overall tracking problem is to compute the posterior density of the set-valued quantity, which also enables the approach to describe the uncertainty in the number of objects. The ordering of each single target state is not of importance in the the set notation; the estimation problem is reduced to capture the most essential part of the multi target tracking problem, estimating the number of objects and their individual states.

This chapter is split into three sections, which takes the estimation problem from a pure theoretical view into a practical implementation. The chapter begins in Section 5.1 with an introduction to the Bayes formulation of the RFS filter, which propagates the complete density of the RFS. This approach is not practically implementable, and therefore a solution is to only propagate the first order moment, called the *probability hypothesis density* (PHD), as described in Section 5.2. There exist a few practical representations of the PHD, of which the Gaussian mixture has turned out to be the most well-used during the last years. The *Gaussian mixture PHD* filter (GM-PHD) is the topic of Section 5.3. This chapter aims at sum-

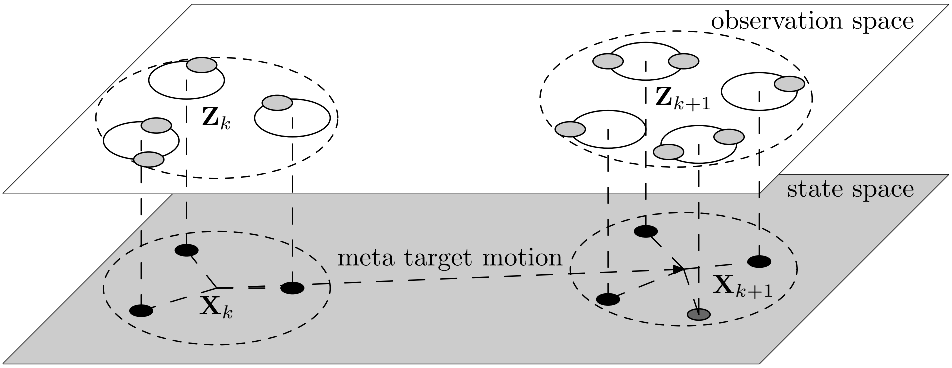

Figure 5.1: *Illustration of the RFS of states and measurements at time k and $k+1$. Note that this is the same setup as previously shown for the standard multitarget case in Figure 4.2.*

marizing the basic ideas and implementation methods, more details can be found in the textbook by Mahler (2007a), and other overviews are given by Mahler (2009b); Challa et al. (2011). Point process theory is described by e.g., Daley and Vere-Jones (2003); Streit (2010).

5.1 Introduction to Finite Set Statistics

The RFS estimation problem is in general solved in the same way as the single target tracking problem is approached, i.e., using Bayes' theorem. However, with the difference that the density is defined on a set rather than on a vector. *Finite set statistics* (FISST), introduced by Goodman et al. (1997); Mahler (2004), is a multisource-multitarget differential and integral calculus based on the so called belief-mass function, and the fact that it is the multisensor-multitarget counterpart of the probability-mass function for single target.

The conceptual idea of FISST is to redefine the target set as a single target, a so called meta target, with multitarget state

$$\mathbf{X} = \{\mathbf{x}^{(1)}, \mathbf{x}^{(2)}, \dots, \mathbf{x}^{(N_\mathbf{x})}\}, \tag{5.1}$$

a so called meta state; and similarly to redefine the observation set

$$\mathbf{Z} = \{\mathbf{z}^{(1)}, \mathbf{z}^{(2)}, \dots, \mathbf{z}^{(N_\mathbf{z})}\}, \tag{5.2}$$

as a single measurement, a meta measurement, of the observed meta targets. The concept is illustrated in Figure 5.1, where meta targets are shown in the state space in the lower layer and meta observations in the observation space in the upper layer. Furthermore, the multitarget multisensor data can be modeled using a multisensor-multitarget measurement model

$$\mathbf{Z}_k = H(\mathbf{X}_k) \cup \mathbf{C}_k, \tag{5.3}$$

where $H(\mathbf{X}_k)$ is the RFS of measurements originating from the true target and $\mathbf{C}$ is the clutter RFS. To see the similarity, compare this multitarget model with the single target measurement model (2.1a). The motion of the meta target can be modeled using a multitarget motion model

$$\mathbf{X}_{k+1} = F(\mathbf{X}_k) \cup \mathbf{B}_k \tag{5.4}$$

where $F(\cdot)$ models the change of a RFS from time k to $k+1$, and $\mathbf{B}$ is the RFS of born targets. Compare, also here, with the single target motion model (2.1b). Given this the multisensor, multitarget estimation problem can be reformulated into a single-sensor, single-target problem. The RFS is formally defined in Section 5.1.1, followed by a definition of the belief-mass function and multitarget density function in Section 5.1.2. The multisource multitarget Bayes filter is described in Section 5.1.3.

5.1.1 Random Finite Set

Before continuing describing the FISST and PHD a formal definition of a RFS is given below.

5.1 Definition (random finite set). A *random finite set* (RFS) Ψ is a random variable that has realizations $\Psi = Y \in \mathfrak{Y}$ where the hyperspace $\mathfrak{Y}$ is the set of all finite subsets of some underlying space $\mathfrak{Y}_0$.

Since the definition may seem a bit abstract it is illustrated with a simple example, related to target tracking.

5.2 Example: Target Tracking

Consider the target tracking example, which was introduced in Example 1.2. In the example the state vector represents the Cartesian position of a target, i.e., $n_x = 2$. The state space is defined as an Euclidean vector space, i.e., $\mathbf{x} \in \mathbb{R}^2$. This state space is the underlying space $\mathfrak{Y}_0$ in the definition above. The hyperspace $\mathfrak{Y}$ includes all finite subsets of $\mathfrak{Y}_0 = \mathbb{R}^{n_x}$. Let the state variable vectors be $\mathbf{x}^{(i)} \in \mathfrak{Y}_0 = \mathbb{R}^2$ for $i = 1, \ldots, \infty$, then some realizations X of the random set $\mathbf{X}$ can be $X = \emptyset$ (no targets), $X = \{\mathbf{x}^{(1)}, \mathbf{x}^{(2)}\}$ (two targets with states $\mathbf{x}^{(1)}$ and $\mathbf{x}^{(2)}$), or $X = \{\mathbf{x}^{(1)}, \ldots, \mathbf{x}^{(N_\mathbf{x})}\}$ ($N_\mathbf{x}$ targets with states $\mathbf{x}^{(1)}, \ldots, \mathbf{x}^{(N_\mathbf{x})}$).

5.1.2 Belief-Mass and Multitarget Density Function

The reformulation of the multisensor multitarget estimation problem as a single-metasensor, single-metatarget problem is based on the concept of belief-mass. Belief-mass functions are nonadditive generalizations of probability-mass function. In order to let the content be more easily digested, the multitarget notation is accompanied with the single target analogous notation.

Starting with some simple notation taken from single target tracking (cf. Section 4.1). For a random vector $\mathbf{y}$ the *probability mass function* $p_\mathbf{y}(\mathbb{S})$ gives the probability of $\mathbf{y}$ being in some subset of the region $\mathbb{S} \subseteq \mathfrak{Y}_0$, i.e.,

$$p_\mathbf{y} = \Pr(\mathbf{y} \in \mathbb{S}). \tag{5.5}$$

The probability density function $p_{\mathbf{y}}(y)$ describes the likelihood of $\mathbf{y}$ to occur at a given point y. The relation between the mass function and the density function is given by

$$p_{\mathbf{y}}(y) = \frac{dp_{\mathbf{y}}}{dy}. \tag{5.6}$$

The probability mass function for a random vector can be generalized to the belief-mass function for RFS. The belief-mass function is denoted $\beta_{\Psi}(\mathbb{S})$, and is defined as the probability that the random finite set Ψ on $\mathfrak{Y}_0$ is within some region $\mathbb{S}$, $\beta_{\Psi}(\mathbb{S}) = \Pr(\Psi \subseteq \mathbb{S})$. Similarly, the probability density function for a random vector can be generalized to the probability density function $p_{\Psi}(Y)$ of a random finite set Ψ. The relation between the probability density function $\Psi p_{\Psi}(Y)$ of a random finite set and the belief-mass function $\beta_{\Psi}(S)$ is given by

$$\beta_{\Psi}(S) \int_{\mathbb{S}} p_{\Psi}(Y)\,\delta Y = \Pr(\Psi \subseteq \mathbb{S}) \tag{5.7}$$

and

$$p_{\Psi}(Y) = \frac{\delta \beta_{\Psi}}{\delta Y}(\emptyset). \tag{5.8}$$

Here, $\int \cdot \,\delta Y$ denotes the *set integral*, and $\frac{\delta \cdot}{\delta Y}$ denotes the *set derivative*. The definitions of the set integral and the set derivative are too complicated to present here, the interested reader can consult Mahler (2007a).

These definitions have the following practical use when applied to the likelihood function and the Markov transition density

- In the single target case the probabilistic-mass function of the sensor model $p(\mathbb{S}|\mathbf{x}) = \Pr(\mathbf{z} \in S|\mathbf{x})$ is the probability that the random observation $\mathbf{z}$ will be found in a given region $\mathbb{S}$ if the target state is $\mathbf{x}$. Analogously, in the multitarget case the belief-mass function $\beta(\mathbb{S}|\mathbf{X}) = \Pr(\mathbf{Z} \subseteq \mathbb{S}|\mathbf{X})$ is the total probability that all observations will be found in any given region $\mathbb{S}$, if the multitarget state is $\mathbf{X}$. In the single target case the likelihood function is obtained by differentiation of the probabilistic-mass function. The same concept holds for the multitarget case, i.e., the true multitarget likelihood function $p(\mathbf{Z}|\mathbf{X})$ can, using FISST, be derived from $\beta(\mathbb{S}|\mathbf{X})$ according to

$$p_{k|k}(\mathbf{Z}_k|\mathbf{X}_k) = \frac{\delta \beta_{k|k}(\emptyset|\mathbf{X}_k)}{\delta \mathbf{Z}_k} \tag{5.9}$$

  where $\frac{\delta}{\delta \mathbf{Z}_k}$ is the set derivative.

- Similarly, the probability-mass $p_{k+1|k}(\mathbb{S}|\mathbf{x}) = \Pr(\mathbf{x}_{k+1} \in \mathbb{S}|\mathbf{x}_k)$ of a single target motion model is the probability that the target will be found in region $\mathbb{S}$ at time step $k+1$, given that it had state $\mathbf{x}_k$ at time step k. In the multitarget case the belief-mass function $\beta_{k+1|k}(\mathbb{S}|\mathbf{X}) = \Pr(\mathbf{X}_{k+1} \subseteq \mathbb{S}|\mathbf{X}_k)$ of a multitarget motion model is the total probability of finding all targets in region $\mathbb{S}$ at time $k+1$, if at time k they had a multi object state $\mathbf{X}_k$. By differentiating $p(\mathbb{S}|\mathbf{x}_k)$ the Markov transition density $p_{k+1|k}(\mathbf{x}_{k+1}|\mathbf{x}_k)$ can be derived in the single target case. Using FISST the multitarget Markov density can be derived by taking the set derivative of the belief-mass function

$$p_{k+1|k}(\mathbf{X}_{k+1}|\mathbf{X}_k) = \frac{\delta\beta_{k+1|k}(\emptyset|\mathbf{X}_k)}{\delta\mathbf{X}_{k+1}} \tag{5.10}$$

5.1.3 The Multitarget Bayes Filter

Consider the single target state propagation summarized in Section 4.1. The filter recursion is extended to the multitarget case under the FISST assumptions in this section. The single target random state variables $\mathbf{x}$ are substituted with the RFS of a set of targets. Before giving the filter recursion, the interpretation of a set probability function is discussed. Consider the multitarget state propagation

$$\cdots \to \underline{p_{k|k}(\mathbf{X}_k|\mathbf{Z}_{1:k})} \overset{\text{predictor}}{\to} p_{k+1|k}(\mathbf{X}_{k+1}|\mathbf{Z}_{1:k}) \overset{\text{corrector}}{\to} p_{k+1|k+1}(\mathbf{X}_{k+1}|\mathbf{Z}_{1:k+1}) \to \cdots$$

The meaning of the underlined prior is exemplified below,

$p(\emptyset\|\mathbf{Z}_{1:k})$	probability that there are no targets present
$p(\{\mathbf{x}_k^{(1)}\}\|\mathbf{Z}_{1:k})$	likelihood of one target with state $\mathbf{x}_k^{(1)}$
$p(\{\mathbf{x}_k^{(1)},\mathbf{x}_k^{(2)}\}\|\mathbf{Z}_{1:k})$	likelihood of two targets with state $\mathbf{x}_k^{(1)},\mathbf{x}_k^{(2)}$
$\vdots$	
$p(\{\mathbf{x}_k^{(1)},\ldots,\mathbf{x}_k^{(N_\mathbf{x})}\}\|\mathbf{Z}_{1:k})$	likelihood of $N_\mathbf{x}$ targets with state $\mathbf{x}_k^{(1)},\ldots,\mathbf{x}_k^{(N_\mathbf{x})}$

i.e., the set density is not only a function of the state variable values, but also a function of the number of targets $N_\mathbf{x}$ in the set.

The single target Bayes filter equations were stated in (3.13), the multitarget Bayes filter counterpart has the form

$$p_{k|k}\left(\mathbf{X}_k|\mathbf{Z}_{1:k}\right) = \frac{p_k\left(\mathbf{Z}_{1:k}|\mathbf{X}_k\right)\cdot p_{k|k-1}\left(\mathbf{X}_k|\mathbf{Z}_{1:k-1}\right)}{\int p_k\left(\mathbf{Z}_{1:k}|\mathbf{X}_k\right)\cdot p_{k|k-1}\left(\mathbf{X}_k|\mathbf{Z}_{1:k-1}\right)\delta\mathbf{X}_k} \tag{5.11a}$$

$$p_{k+1|k}(\mathbf{X}_{k+1}|\mathbf{Z}_{1:k}) = \int p_{k+1|k}(\mathbf{X}_{k+1}|\mathbf{X}_k)\cdot p_{k|k}(\mathbf{X}_k|\mathbf{Z}_{1:k})\delta\mathbf{X}_k \tag{5.11b}$$

where $p_k\left(\mathbf{Z}_k|\mathbf{X}_k\right)$ is the multisource likelihood function, $p_{k+1|k}(\mathbf{X}_{k+1}|\mathbf{X}_k)$ is the multitarget Markov transition function, $p_{k|k-1}\left(\mathbf{X}_k|\mathbf{Z}_{k-1}\right)$ is the multitarget prior, $p_{k|k}(\mathbf{X}_k|\mathbf{Z}_k)$ is the multitarget posterior and $p_{k+1|k}(\mathbf{X}_{k+1}|\mathbf{Z}_k)$ is the multitarget prediction. The filter recursion is given by,

$$
\begin{array}{ccccc}
\cdots \to p_{k|k}(\mathbf{X}_k|\mathbf{Z}_{1:k}) & \xrightarrow{\text{predictor}} & p_{k+1|k}(\mathbf{X}_{k+1}|\mathbf{Z}_{1:k}) & \xrightarrow{\text{corrector}} & p_{k+1|k+1}(\mathbf{X}_{k+1}|\mathbf{Z}_{1:k+1}) \to \quad \cdots \\
 & & \uparrow & & \uparrow \\
 & & \text{Markov density} & & \text{Likelihood function} \\
 & & p(\mathbf{X}_{k+1}|\mathbf{X}_k) & & p(\mathbf{Z}_{k+1}|\mathbf{X}_{k+1}) \\
 & & \uparrow & & \uparrow \\
 & & \text{Motion Model} & & \text{Measurement Model} \\
 & & \mathbf{X}_{k+1} = \underbrace{F(\mathbf{X}_k)}_{\text{persisting}} \bigcup \underbrace{\mathbf{B}_k}_{\text{new}} & & \mathbf{Z}_{k+1} = \underbrace{H(\mathbf{X}_{k+1})}_{\substack{\text{generated} \\ \text{observations}}} \bigcup \underbrace{\mathbf{C}_{k+1}}_{\text{clutter}}
\end{array}
$$

compare with the single target filter recursions given on the same form in Section 3.2. Note that the motion model describes a union of the set of persisting targets and the set of new born, or detected, targets. In the same manner, the measurement model describes a union of the set of target generated observations and the set of clutter measurement. Here, the measurement set $\mathbf{Z}$ is the set of all observations received by the sensor.

The conclusions of this section can be summarized in a few items, which will be furher addressed in the next section:

- The Bayesian filter on sets is very similar to standard Bayesian density recursion.
- Related single target densities and operations are replaced with their set equivalents, compare (5.11) with (3.13).
- A set integral $\int \cdot \, \delta\mathbf{X}$ is necessary to derive the posterior

$$p(\mathbf{X}_k|\mathbf{Z}_{1:k}) \propto p(\mathbf{Z}_k|\mathbf{X}_k) \int p(\mathbf{X}_k|\mathbf{X}_{k-1}) p(\mathbf{X}_{k-1}|\mathbf{Z}_{1:k-1}) \delta\mathbf{X}_{k-1}$$

- Therefore, the filter is computationally prohibitive.

5.2 Introduction to the PHD filter

The multisource multitarget filter as described in the last section is computationally demanding to implement. This section describes a new approach, first proposed by Mahler (2003), for approximate multitarget nonlinear filters called the *probability hypothesis density* (PHD) filter. The PHD is a first order moment approximation of the RFS. To describe this approximation the single target case will first be repeated in Section 5.2.1 and then compared with the multitarget case in Section 5.2.2, where also the PHD is defined. The PHD filter recursion is explained in Section 5.2.3. The section is concluded in Section 5.2.4 with a short literature survey of generalizations and extensions of the PHD filter.

5.2.1 Approximations in Single-Target Tracking

The single target density propagation is illustrated below

$$
\begin{array}{ccccc}
\cdots \to p_{k|k}(\mathbf{x}_k|\mathbf{z}_{1:k}) & \overset{\text{predictor}}{\to} & p_{k+1|k}(\mathbf{x}_{k+1}|\mathbf{z}_{1:k}) & \overset{\text{corrector}}{\to} & p_{k+1|k+1}(\mathbf{x}_{k+1}|\mathbf{z}_{1:k+1}) \to \cdots \\
\downarrow & & \downarrow & & \downarrow \\
\hat{\mathbf{x}}_{k|k} & \overset{\text{predictor}}{\to} & \hat{\mathbf{x}}_{k+1|k} & \overset{\text{corrector}}{\to} & \hat{\mathbf{x}}_{k+1|k+1}
\end{array}
$$

At each time step the first order moment, i.e., the expected value may be collapsed from the density function. In the so called constant-gain filter, of which the alpha-beta filter is the most well known, only the expected value is propagated over time. This makes the filter computationally faster. Both the first and the second order moments are propagated in the standard Kalman filter, compare with Section 3.2.1. If the density functions are Gaussian, the first and second order moments are the sufficient statistics, hence propagating these variables describes the density functions sufficiently. However, if the density functions are not Gaussian, propagating the moments is only an approximation of the density.

5.2.2 Approximations in Multitarget Tracking

Based on the same analogy as with the single target tracking the density of the RFS my be compressed to the first order moments, and these may be propagated as follows:

$$
\begin{array}{ccccc}
\cdots \to p_{k|k}(\mathbf{X}_k|\mathbf{Z}_{1:k}) & \overset{\text{predictor}}{\to} & p_{k+1|k}(\mathbf{X}_{k+1}|\mathbf{Z}_{1:k}) & \overset{\text{corrector}}{\to} & p_{k+1|k+1}(\mathbf{X}_{k+1}|\mathbf{Z}_{1:k+1}) \to \cdots \\
\downarrow & & \downarrow & & \downarrow \\
D_{k|k}(\mathbf{x}_k|\mathbf{Z}_{1:k}) & \overset{\text{predictor}}{\to} & D_{k+1|k}(\mathbf{x}_{k+1}|\mathbf{Z}_{1:k}) & \overset{\text{corrector}}{\to} & D_{k+1|k+1}(\mathbf{x}_{k+1}|\mathbf{Z}_{1:k+1})
\end{array}
$$

The first order moment is called a PHD and denoted D. However, it is not obvious what the multitarget counterpart of an expected value is; a naïve defininition would be

$$
\mathrm{E}(\Psi) = \int X \cdot p_\Psi(X)\delta X, \tag{5.12}
$$

where $p_\Psi(X)$ is the multitarget probability density of a RFS Ψ. However, this integral is not mathematically defined, since addition of finite subsets is not usefully defined. A strategy is to transform subsets X into vectors T_X in some vector space. It is important that this transformation $X \to T_X$ preserves set-theoretic structures, i.e., transforming unions into sums $T_{X\cup X'} = T_X + T_{X'}$, whenever $X \cap X' = \emptyset$. An indirect expected value can now be defined according to

$$
\mathrm{E}(\Psi) = \int T_X \cdot p_\Psi(X)\delta X. \tag{5.13}
$$

The vector is commonly chosen as $T_X = \delta_X(\mathbf{x})$ with

$$
T_X = \begin{cases} 0 & \text{if } X = \emptyset \\ \sum_{\mathbf{y}\in\mathbf{X}} \delta_{\mathbf{y}}(\mathbf{x}) & \text{otherwise} \end{cases} \tag{5.14}
$$

where $\delta_{\mathbf{y}}(\mathbf{x})$ is the Dirac delta function with peak at $\mathbf{y}$. Given these assumptions, the multitarget analog of the expected value is given by

$$D_\Psi(\mathbf{x}) = \int \delta_X(\mathbf{x}) \cdot p_\Psi(X)\delta X. \tag{5.15}$$

To exemplify this rather theoretical discussion, consider a realization X_k of the RFS $\mathbf{X}_k = \{\mathbf{x}_k^{(1)}, \mathbf{x}_k^{(2)}, \dots, \mathbf{x}_k^{(N_\mathbf{x})}\}$. Define a scalar valued function of X_k according to

$$\delta_{X_k} = \sum_{i=1}^{N} \delta_{\mathbf{x}_k^{(i)}}(\mathbf{x}), \tag{5.16}$$

as illustrated in Figure 5.2a. Then, the probability hypothesis density (PHD) is the expectation of δ_{X_k} with respect to X_k

$$D_{k|k}(\mathbf{x}) = \mathrm{E}(\delta_{X_k}) = \int \delta_{X_k} \cdot p_\Psi(X)\delta X. \tag{5.17}$$

The expected value is illustrated in Figure 5.2b. Note also that the expected number of targets in the volume $\mathbb{S}$ is

$$\widehat{N}_\mathbf{x} = \int_{\mathbb{S}} D_{k|k}(\mathbf{x})d\mathbf{x} \tag{5.18}$$

In fact one can define the PHD using the expected number of targets as follows: Given any region $\mathbb{S}$ of single target state space $\mathfrak{X}_0$ the integral $\int_{\mathbb{S}} D_{k|k}(\mathbf{x})d\mathbf{x}$ is the expected number of targets in $\mathbb{S}$.

The PHD is an *intensity function*, which models the joint density over the states. The PHD is multi-modal, with peaks near the actual targets, see Figure 5.3. This figure shows the PHD approximation of the RFS in Figure 5.1. The intensity function is used in Paper D to represent the density of stationary targets along the edges of a road. An autonomous driving vehicle should avoid areas with high intensity and the objective should be to keep the vehicle in the valleys of the intensity function.

5.2.3 The PHD Filter

The PHD filter consists of two equations, the predictor equation, which extrapolates the current PHD to the predicted PHD at the time of the new observation, and the corrector equation, which updates the predicted PHD with the new observations.

The PHD predictor equations takes care of the motion of existing targets, birth and spawn of new targets and the death of existing targets. The components of the prediction model are summarized below:

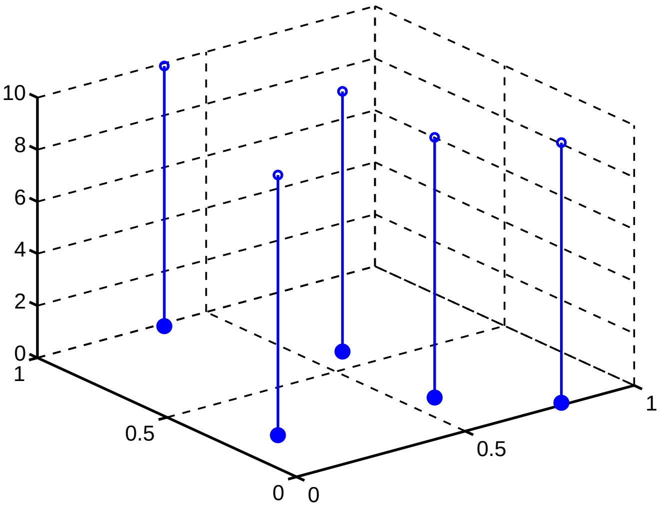

(a) Sum of Dirac functions δ_{X_k}

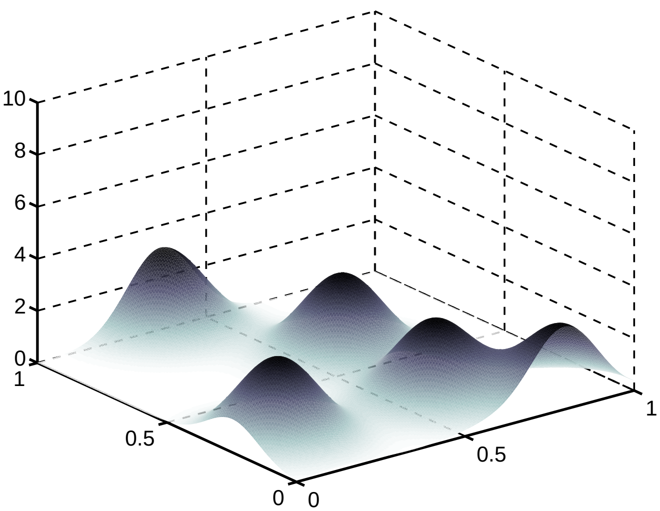

(b) Expectation $\mathrm{E}(\delta_{X_k})$

Figure 5.2: *Definition and example of the PHD, the Dirac functions represents the RFS and the surface the first order moment, i.e., the PHD.*

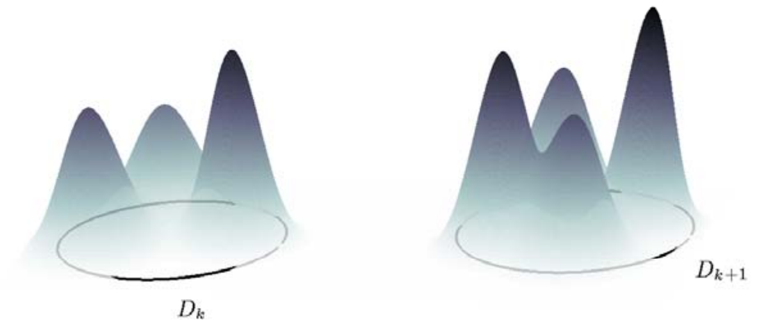

Figure 5.3: *Illustration of the PHD for the time steps k and $k+1$. This is the PDF of the RFS in Figure 5.1.*

	model	time step	description
motion:	$p(\mathbf{x}_{k+1} \mid \mathbf{x}_k)$	$\mathbf{x}_k \to \mathbf{x}_{k+1}$	likelihood that target will have state $\mathbf{x}_{k+1}$ if it had state $\mathbf{x}_k$
death:	$1 - P_S(\mathbf{x}_k)$	$\mathbf{x}_k \to \emptyset$	probability that target will vanish if it had state $\mathbf{x}_k$
spawn:	$b(\mathbf{X}_{k+1} \mid \mathbf{x}_k)$	$\mathbf{x}_k \to \mathbf{X}_{k+1}$	likelihood that a target will spawn target set $\mathbf{X}_{k+1}$ if it had state $\mathbf{x}_k$
birth:	$b(\mathbf{X}_{k+1})$	$\emptyset \to \mathbf{X}_{k+1}$	likelihood that a target set $\mathbf{X}_{k+1}$ will appear in scene

In the table above $P_S(\mathbf{x})$ denotes the probability that a target with state $\mathbf{x}$ at time k will survive at time $k+1$, $p(\mathbf{x}_{k+1}|\mathbf{x}_k)$ is the single target Markov transition density, $b(\mathbf{X}_{k+1}|\mathbf{x}_k)$ is the PHD of targets spawned by other targets with state $\mathbf{x}$, and $b(\mathbf{X}_{k+1})$ is the PHD of new appearing targets. The PHD predictor equation is given by

$$\underbrace{D_{k+1|k}(\mathbf{x}_{k+1}|\mathbf{z}_{1:k})}_{\text{time updated PHD}} =$$

$$= \underbrace{b_{k+1|k}(\mathbf{x}_{k+1})}_{\text{target birth PHD}} + \int \Big[\underbrace{P_S(\xi_k)}_{\substack{\text{probability of}\\ \text{survival}}} \underbrace{p(\mathbf{x}_{k+1}|\xi_k)}_{\substack{\text{Markov transition}\\ \text{density}}} + \underbrace{b(\mathbf{x}_{k+1}|\xi_k)}_{\substack{\text{target spawn by}\\ \text{existing targets}}} \Big] \underbrace{D_{k|k}(\xi_k|\mathbf{z}_{1:k})}_{\text{PHD from previous } k} \, d\xi_k. \tag{5.19}$$

The parts of the model are illustrated with a number of plots in Figure 5.4. One example of a PHD $D_{k|k}(\xi|\mathbf{z}_{1:k})$ from the previous time step k is illustrated in Figure 5.4a. The magnitude of the PHD is reduced a bit when multiplied with the probability of survival $P_S(\xi)$ in Figure 5.4b. Thereafter, multiplying with the Markov transition density and then integrating changes the mean value and the covariance, see Figure 5.4c. Note, that all target motions are assumed statistically independent. In Figure 5.4d, the spawn PHD $b(\mathbf{x}_{k+1}|\xi_k)$ is added in red, and in Figure 5.4e the birth PHD $b_{k+1|k}(\mathbf{x}_{k+1})$ in green. Finally, the total predicted PHD $D_{k+1|k}(\mathbf{x}_{k+1}|\mathbf{z}_{1:k})$, after time update, is shown in Figure 5.5a.

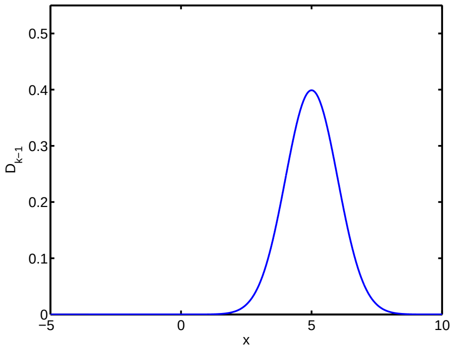

(a) *PHD from previous k*

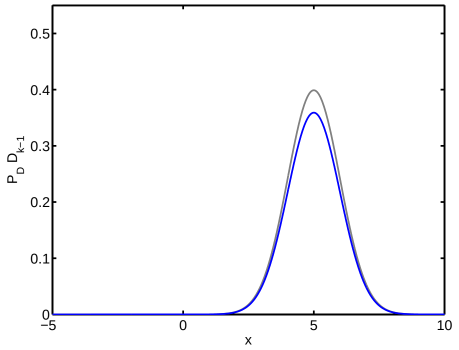

(b) *multiplied with P_S*

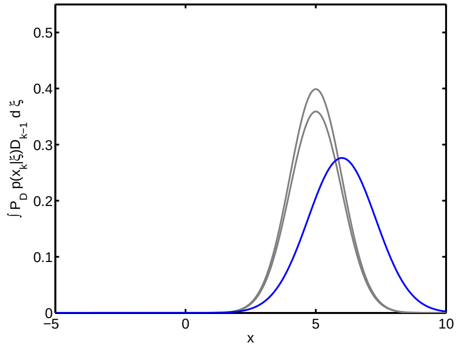

(c) *multiplied with transition density and integrated*

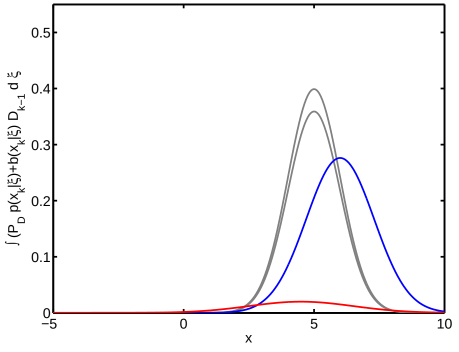

(d) *adding spawn PHD*

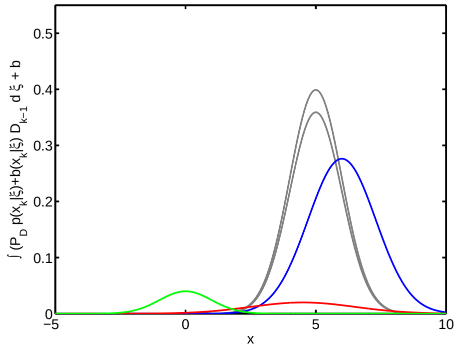

(e) *adding birth PHD*

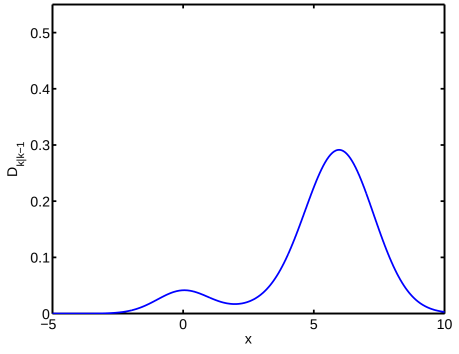

(f) *predicted PHD*

Figure 5.4: *An example showing the components of the predictor equation* (5.19) *of PHD filter.*

The PHD corrector equations takes care of the likelihood of the existing targets, misdetection of targets and clutter. The components of the prediction model are summarized below:

	model	**update**	**description**
likelihood:	$p(\mathbf{z}_k \vert \mathbf{x}_k)$	$\mathbf{x}_k \rightarrow \mathbf{z}_k$	likelihood that target will generate observation $\mathbf{z}_k$ if it has state $\mathbf{x}_k$
misdetection:	$(1 - P_D(\mathbf{x}_k))$	$\mathbf{x}_k \rightarrow \emptyset$	state dependent probability that target will not generate an observation
clutter:	$c(\mathbf{Z}_k)$	$\emptyset \rightarrow \mathbf{Z}_k$	likelihood that a set $\mathbf{Z}_k = \{\mathbf{z}_k^{(1)}, \ldots, \mathbf{z}_k^{(M)}\}$ of clutter observations will be generated

In the table above $P_D(\mathbf{x}_k)$ is the probability of detection of a target with the state $\mathbf{x}$ at time step k, $p(\mathbf{z}_k|\mathbf{x}_k)$ is the single target likelihood function and $c(\mathbf{Z}_k)$ is the density of Poisson false alarms, due to clutter. The modeling is done under the assumption that the observations and the clutter are statistically independent. Furthermore it is assumed that the multitarget prediction is approximately Poisson. Given a new scan of data $\mathbf{Z}_k = \{\mathbf{z}_k^{(1)}, \ldots, \mathbf{z}_k^{(M)}\}$ the corrector equation is given by

$$\underbrace{D_{k|k}(\mathbf{x}|\mathbf{Z}_{1:k})}_{\text{updated PHD}} \approx \underbrace{\sum_{\mathbf{z}\in\mathbf{Z}_k} \frac{\Lambda_{k|k}(\mathbf{x}|\mathbf{z})}{\lambda_k c_k(\mathbf{z}) + \int \Lambda_{k|k}(\mathbf{x}|\mathbf{z}) d\mathbf{x}} + (1 - P_D(\mathbf{x}))}_{\text{pseudo-likelihood}} \underbrace{D_{k|k-1}(\mathbf{x}|\mathbf{Z}_{1:k-1})}_{\text{predicted PHD}} \tag{5.20}$$

where λ_k is the average number of false alarms. Furthermore

$$\Lambda_{k|k}(\mathbf{x}|\mathbf{z}) = P_D(\mathbf{x})p(\mathbf{z}|\mathbf{x})D_{k|k-1}(\mathbf{x}|\mathbf{z}_{1:k}). \tag{5.21}$$

The corrector equation is again exemplified by a series of plots in Figure 5.5. Figure 5.5a shows the predicted PHD. The non-detected targets are modeled by multiplying the predicted PHD with $(1 - P_D(\mathbf{x}))$, as illustrated in red in Figure 5.5b. Assume that two detections are made; the likelihood functions $p(\mathbf{z}|\mathbf{x})$ of these individual observations are shown in Figure 5.5c. The pseudo-likelihood function of the detections multiplied with the predicted PHD is shown in blue in Figure 5.5d. Finally, the updated posterior PHD is illustrated in Figure 5.5e.

In Paper E, the pseudo-likelihood function is modified to handle extended targets. This modification is one of the major contributions of that paper.

5.2.4 Generalizations of the PHD filter

There exists an improvement of the PHD filter, called the *cardinalized probability hypothesis density* (CPHD) filter, which also propagates the probability distribution on the target number. This filter generally performs better, but with increased computational load. The CPHD filter is too complex to be described in

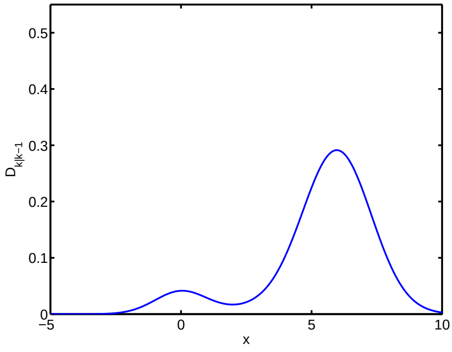

(a) PHD *from prediction*

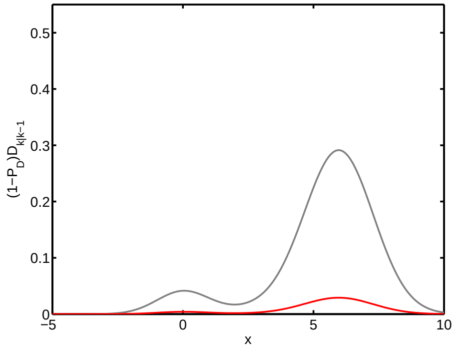

(b) Non-detected targets

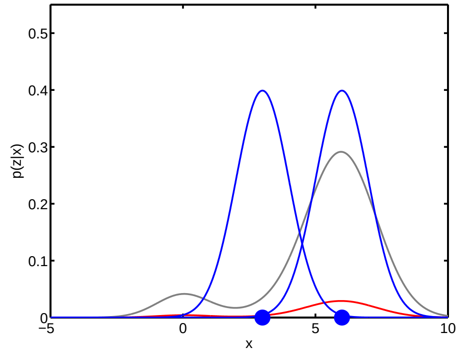

(c) likelihood functions of two measurements

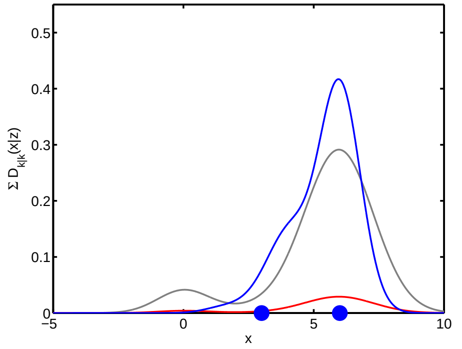

(d) Detected and non-detected targets

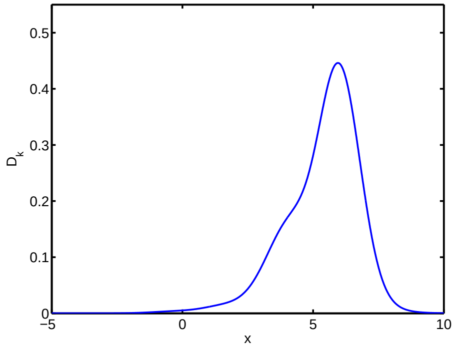

(e) Updated PHD

Figure 5.5: *Steps in the* PHD *update and corrector equations* (5.20).

the present chapter, and it is also not used in any of the publications in Part II. Details about the CPHD filter can be found in Mahler (2007b,a), and a Gaussian mixture implementation is described in Vo et al. (2007).

The standard PHD filter as described in this section does not maintain track labels from time step to time step. A so called peak to track association technique has been proposed by Lin et al. (2004); Panta et al. (2004) in order to maintain track labels.

Furthermore, PHD smoother has been studied in Mahler et al. (2010); Clark (2010), and a Gaussian mixture implementation is presented by Vo et al. (2010, 2011). Again, since the smoother is not further used in Part II, it is also not described here.

The so called *intensity filter*, developed by Streit, is another generalization of the PHD filter. The difference is that in the PHD filter certain prior assumptions regarding target birth and measurement clutter are made. More specifically the intensity filter uses an augmented single target state space, while the PHD filter uses only the standard single target state space. The augmented state space represents the absent target hypothesis, and it therefore allows the filter to on-line estimate the intensities of the target birth and measurement clutter Poisson point processes. Note that the PHD is an intensity function, and in the PHD filter the birth and clutter intensities are known *a priori*. A thorough description of the intensity filter is given in the textbook by Streit (2010) and a summary is given in the publications Streit and Stone (2008); Streit (2008).

5.3 Gaussian Mixture Implementation

There exist primarily two different implementations of the PHD filter, the SMC approximation, see Vo et al. (2003); Sidenbladh (2003); Zajic and Mahler (2003), and the Gaussian mixture (GM) approximation, introduced in Vo and Ma (2006), and hence called GM-PHD filter. A physical interpretation of the PHD filter is proposed by Erdinc et al. (2009). Both approximations of the PHD are exemplified in Figure 5.6.

The advantage of the SMC approximation is that it can accommodate highly non-linear motion and measurement models. The disadvantages are that it is computational demanding. The SMC based approximation is not further used in this thesis and it is therefore not described in further detail here, the interested reader is referred to Vo et al. (2003) or the textbook Mahler (2007a). The GM implementation is discussed in more detail in this section.

The GM-PHD filter has the following properties,

- It is less computationally demanding than the SMC solution.
- It is exact, i.e., it provides a true closed-form algebraic solution.
- It is easy to implement,

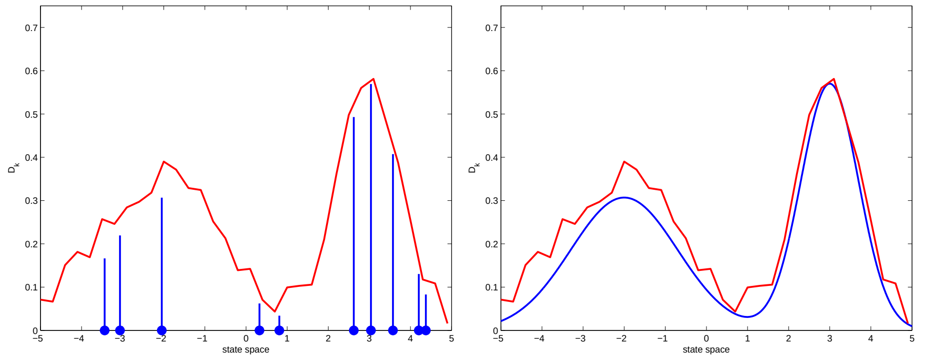

(a) *Sequential Monte Carlo* PHD *approximations (*SMC-PHD*)*

(b) *Gaussian mixture* PHD *approximation (*GM-PHD*)*

Figure 5.6: *Practical implementation methods of the* PHD*.*

- however, measurement and motion models must be linear-Gaussian.

This section is outlined as follows. The approximations made in the GM-PHD filter are summarized in Section 5.3.1 and the algorithm is given in Section 5.3.2. Some practical details regarding the implementation, e.g., target extraction are described in Section 5.3.3.

5.3.1 Gaussian Mixture PHD Approximation

Similarly, as first shown for the theoretical Bayesian multitarget filter in Section 5.1.3 and then for the more practical standard PHD filter in Section 5.2.2, the easily implementable filter recursion of the GM-PHD filter is summarized below:

$$
\begin{array}{ccccc}
\cdots \rightarrow \quad D_{k|k}(\mathbf{x}|\mathbf{Z}_{1:k}) & \overset{\text{predictor}}{\rightarrow} & D_{k+1|k}(\mathbf{x}|\mathbf{Z}_{1:k}) & \overset{\text{corrector}}{\rightarrow} & D_{k+1|k+1}(\mathbf{x}|\mathbf{Z}_{1:k+1}) \\
\downarrow & & \downarrow & & \downarrow \\
\cdots \rightarrow \sum_{i=1}^{J_{k|k}} w_{k|k}^{(i)} \mathcal{N}\left(\mathbf{x}; \mu_{k|k}^{(i)}, P_{k|k}^{(i)}\right) & \rightarrow & \sum_{i=1}^{J_{k+1|k}} w_{k+1|k}^{(i)} \mathcal{N}\left(\mathbf{x}; \mu_{k+1|k}^{(i)}, P_{k+1|k}^{(i)}\right) & \rightarrow & \sum_{i=1}^{J_{k+1|k+1}} w_{k+1|k+1}^{(i)} \mathcal{N}\left(\mathbf{x}; \mu_{k+1|k+1}^{(i)}, P_{k+1|k+1}^{(i)}\right) \\
\downarrow & & \downarrow & & \downarrow \\
\mu_{k|k}^{(1)}, \ldots, \mu_{k|k}^{(J_{k|k})} & \rightarrow & \mu_{k+1|k}^{(1)}, \ldots, \mu_{k+1|k}^{(J_{k+1|k})} & \rightarrow & \mu_{k+1|k+1}^{(1)}, \ldots, \mu_{k+1|k+1}^{(J_{k+1|k+1})} \\
P_{k|k}^{(1)}, \ldots, P_{k|k}^{(J_{k|k})} & \rightarrow & P_{k+1|k}^{(1)}, \ldots, P_{k+1|k}^{(J_{k+1|k})} & \rightarrow & P_{k+1|k+1}^{(1)}, \ldots, P_{k+1|k+1}^{(J_{k+1|k+1})} \\
w_{k|k}^{(1)}, \ldots, w_{k|k}^{(J_{k|k})} & \rightarrow & w_{k+1|k}^{(1)}, \ldots, w_{k+1|k}^{(J_{k+1|k})} & \rightarrow & w_{k+1|k+1}^{(1)}, \ldots, w_{k+1|k+1}^{(J_{k+1|k+1})}
\end{array}
$$

The PHD is represented by a Gaussian mixture and the summary statistics of the Gaussian components, i.e., the mean value μ and the covariance P are propagated together with a weight w for each Gaussian component. The number of Gaussian components at each time step is denoted J. The prior, predicted and posterior GM-PHD are shown above.

When deriving the GM-PHD filter some assumptions are made, see Vo and Ma (2006). Since these assumptions are formally repeated in Paper E, on Page 230, these are only summarized here. It is assumed that each target follows a linear Gaussian motion model,

$$p_{k+1|k}(\mathbf{x}_{k+1}|\mathbf{x}_k) = \mathcal{N}(\mathbf{x}_{k+1}; F_k\mathbf{x}_k, Q_k), \tag{5.22}$$

where F_k is the state transition matrix and Q_k is the process noise covariance, and it is assumed that all target motions are statistically independent. Observations and clutter are assumed statistically independent and the sensor is assumed to have a linear Gaussian measurement model, i.e.,

$$p_{k|k}(\mathbf{z}_k|\mathbf{x}_k) = \mathcal{N}(\mathbf{z}_k; H_k\mathbf{x}_k, R_k), \tag{5.23}$$

where H_k is the measurement model matrix and R_k is the observation noise covariance. Furthermore it is assumed that the survival and detection probabilities are state independent, i.e., $P_S(\mathbf{x}) = P_S$ and $P_D(\mathbf{x}) = P_D$. The PHD of the birth and the spawn are Gaussian mixtures

$$b(\mathbf{X}_{k+1}) = \sum_{i=1}^{J_{b,k}} w_{b,k}^{(i)} \mathcal{N}(\mathbf{x}; \mu_{b,k}^{(i)}, P_{b,k}^{(i)}), \tag{5.24}$$

$$b(\mathbf{X}_{k+1}|\mathbf{x}_k^{(i)}) = \sum_{\ell=1}^{J_{\beta,k+1}} w_{\beta,k+1}^{(\ell)} \mathcal{N}(\mathbf{x}; \mu_{\beta,k+1|k}^{(i,\ell)}, P_{\beta,k+1|k}^{(i,\ell)}), \tag{5.25}$$

where $w_{b,k}^{(i)}$, $\mu_{b,k}^{(i)}$ and $P_{b,k}^{(i)}$ are the weight, the mean and the covariance of the ith born component, $i = 1, \dots, J_{b,k}$, and $J_{b,k}$ is the number of components. Further, $w_{\beta,k+1}^{(\ell)}$, $\mu_{\beta,k+1|k}^{(i,\ell)}$ and $P_{\beta,k+1|k}^{(i,\ell)}$ are the weight, mean and covariance of the ℓth component $\ell = 1, \dots, J_{\beta,k+1}$ at time $k+1$ spawned from the ith component at time k, and $J_{\beta,k+1}$ is the total number of components spawned from component i. It is also assumed that the predicted multitarget RFS are Poisson.

5.3.2 GM-PHD Filter Algorithm

In this section the GM-PHD filter algorithm including the predictor and the corrector equations, are given. The prediction equation is an approximation of the general PHD prediction equation (5.19), with the difference that the PHD components are substituted with Gaussian mixtures according to

$$\begin{aligned} D_{k|k-1}(\mathbf{x}|\mathbf{Z}_{1:k-1}) = &\sum_{j=1}^{J_{b,k}} w_{b,k}^{(j)} \mathcal{N}(\mathbf{x}; \mu_{b,k}^{(j)}, P_{b,k}^{(j)}) + P_S \sum_{j=1}^{J_{k-1}} w_{k-1}^{(j)} \mathcal{N}(\mathbf{x}; \mu_{k|k-1}^{(j)}, P_{k|k-1}^{(j)}) \\ &+ \sum_{j=1}^{J_{k-1}} \sum_{\ell=1}^{J_{\beta,k}} w_{\beta,k|k-1}^{(j,\ell)} \mathcal{N}(\mathbf{x}; \mu_{\beta,k|k-1}^{(j,\ell)}, P_{\beta,k|k-1}^{(j,\ell)}). \end{aligned} \tag{5.26}$$

In the case when the motion and sensor models are linear, the Gaussian components can be predicted using the prediction step of the Kalman filter (3.16). The illustration in Figure 5.4 still holds for this Gaussian case, and the discussion is therefore not repeated again. The corrector equation is an approximation of the general PHD corrector equation (5.20), with the difference that the PHD components are substituted with Gaussian mixtures according to

$$D_{k|k}(\mathbf{x}|\mathbf{Z}_{1:k}) \approx \underbrace{\sum_{i=1}^{J_{k|k-1}} w_{k|k}^{(i)} \mathcal{N}\left(\mu_{k|k}^{(i)}, P_{k|k}^{(i)}\right)}_{\text{not detected targets}} + \underbrace{\sum_{j=1}^{N_{\mathbf{z}}} \sum_{i=1}^{J_{k|k-1}} w_{k|k}^{(i,j)} \mathcal{N}\left(\mu_{k|k}^{(i,j)}, P_{k|k}^{(i,j)}\right)}_{\text{detected targets}} \tag{5.27}$$

The complete filter recursion, as it is presented by Vo and Ma (2006), is given in Algorithm 7.

Algorithm 7 Gaussian Mixture PHD filter

Require: the Gaussians $\{w_{k-1}^{(i)}, \mu_{k-1}^{(i)}, P_{k-1}^{(i)}\}_{i=1}^{J_{k-1}}$ and the measurement set $\mathbf{Z}_k$

Prediction for birth and spawn targets

i = 0
for $j = 1$ **to** $J_{b,k}$ **do**
  $i = i + 1$
  $w_{k|k-1}^{(i)} = w_{b,k}^{(j)}, \quad \mu_{k|k-1}^{(i)} = \mu_{b,k}^{(j)}, \quad P_{k|k-1}^{(i)} = P_{b,k}^{(j)}$
end for
for $j = 1$ **to** $J_{\beta,k}$ **do**
  for $\ell = 1$ **to** J_{k-1} **do**
    $i = i + 1$
    $w_{k|k-1}^{(i)} = w_{k-1}^{(\ell)} w_{\beta,k}^{(j)}$
    $\mu_{k|k-1}^{(i)} = F_{\beta,k-1}^{(j)} \mu_{k-1}^{(\ell)} + d_{\beta,k-1}^{(j)}, \quad P_{k|k-1}^{(i)} = Q_{\beta,k-1}^{(j)} + F_{\beta,k-1}^{(j)} P_{\beta,k-1}^{(\ell)} (F_{\beta,k-1}^{(j)})^{\mathrm{T}}$
  end for
end for

Prediction for existing targets

for $j = 1$ **to** J_{k-1} **do**
  $i = i + 1$
  $w_{k|k-1}^{(i)} = P_S w_{k-1}^{(j)}$
  $\mu_{k|k-1}^{(i)} = F_{k-1} \mu_{k-1}^{(j)}, \quad P_{k|k-1}^{(i)} = F_{k-1} P_{k-1}^{(j)} F_{k-1}^{\mathrm{T}} + Q_{k-1}$
end for
$J_{k|k-1} = i$

Construction of PHD update components

for $j = 1$ **to** $J_{k|k-1}$ **do**
  $\eta_{k|k-1}^{(j)} = H_k \mu_{k|k-1}^{(j)}, \quad S_k^{(j)} = R_k + H_k P_{k|k-1}^{(j)} H_k^{\mathrm{T}}$
  $K_k^{(j)} = P_{k|k-1}^{(j)} H_k^{\mathrm{T}} (S_k^{(j)})^{-1}, \quad P_{k|k}^{(j)} = (I - K_k^{(j)} H_k) P_{k|k-1}^{(j)}$
end for

Update non-detected targets

for $j = 1$ **to** $J_{k|k-1}$ **do**
  $w_k^{(j)} = (1 - P_D) w_{k|k-1}^{(j)}$
  $\mu_k^{(j)} = \mu_{k|k-1}^{(j)}, P_k^{(j)} = P_{k|k-1}^{(j)}$
end for

Update detected targets

$\ell = 0$

for each $\mathbf{z} \in \mathbf{Z}_k$ **do**

  $\ell = \ell + 1$

  for $j = 1$ **to** $J_{k|k-1}$ **do**

    $w_k^{(\ell J_{k|k-1}+j)} = P_D w_{k|k-1} \mathcal{N}(\mathbf{z}; \eta_{k|k-1}^{(j)}, S_k^{(j)})$

    $\mu_k^{(\ell J_{k|k-1}+j)} = \mu_{k|k-1}^{(j)} + K_k^{(j)}(\mathbf{z}_k - \eta_{k|k-1}^{(j)})$

    $P_k^{(\ell J_{k|k-1}+j)} = P_{k|k}^{(j)}$

  end for

  for $j = 1$ **to** $J_{k|k-1}$ **do**

    $w_k^{(\ell J_{k|k-1}+j)} = \frac{w_k^{(\ell J_{k|k-1}+j)}}{\lambda c(\mathbf{z}) + \sum_{i=1}^{J_{k|k-1}} w_k^{(\ell J_{k|k-1}+i)}}$

  end for

end for

$J_k = \ell J_{k|k-1} + J_{k|k-1}$

return $\{w_k^{(i)}, \mu_k^{(i)}, P_k^{(i)}\}_{i=1}^{J_k}$

To allow for nonlinear motion and sensor models, the EKF or UKF can be utilized, in that case the prediction and update of the single Gaussian components are instead performed as described in Algorithm 4 and 5, respectively. The UKF version of the GM-PHD filter is used in Paper D to track the edges of a road and thereby to create an intensity map of the environment. An extension of the KF based GM-PHD used to track extended targets, is presented Paper E. In that paper modifications are made to the update step to account for the extended targets, which may give rise to more than one measurement per target and time step. In Paper F the GM-PHD filter is used as an inner core in a tracking filter which aims at estimating the size and shape of targets. The outer shell of the approach represents the position and motion of the target, whereas the PHD is defined on the surface of the target as a means to estimate its shape.

5.3.3 Merge, Prune and Extract Targets

A few approximations and modifications to the GM-PHD filter must be made in order to obtain a computationally realizable filter. The number of Gaussian components grows rapidly, since each predicted Gaussian component is updated with each measurement. To handle this situation components with low weights are pruned and similar components are merged. The procedure is described in Vo and Ma (2006) and in Algorithm 8. A model based approach to merge components is presented in Paper D.

The extraction of multiple-target state estimates is straightforward from the posterior PHD. It can be assumed that closely spaced components are reasonable well separated after the prune and merge step of the algorithm. The means of the remaining Gaussian components are the local maxima of the PHD. The states are extracted by selecting the means of the Gaussians that have weights greater

Algorithm 8 Merging and Pruning for GM-PHD filter

Require: the Gaussian components $\{w_k^{(i)}, \mu_k^{(i)}, P_k^{(i)}\}_{i=1}^{J_{k|k}}$, the truncation threshold δ_{t} and the merging threshold δ_{m}

initiate: by setting $\ell = 0$, $I = \{i = 1, \ldots, J_{k|k} | w_k^{(i)} > \delta_{\mathrm{t}}\}$ and then
repeat
$\quad \ell := \ell + 1$
$\quad j := \arg\max_{i \in I} \; w_k^{(i)}$
$\quad L := \left\{ i \in I \middle| \left(\mu_k^{(i)} - \mu_k^{(j)}\right)^{\mathrm{T}} \left(P_k^{(i)}\right)^{-1} \left(\mu_k^{(i)} - \mu_k^{(j)}\right) \leq \delta_{\mathrm{m}} \right\},$
$\quad \tilde{w}_k^{(\ell)} = \sum_{i \in L} w_k^{(i)}$
$\quad \tilde{\mu}_k^{(\ell)} = \frac{1}{\tilde{w}_k^{(\ell)}} \sum_{i \in L} w_k^{(i)} \mu_k^{(i)}$
$\quad \tilde{P}_k^{(\ell)} = \frac{1}{\tilde{w}_k^{(\ell)}} \sum_{i \in L} w_k^{(i)} \left(P_k^{(i)} + \left(\tilde{\mu}_k^{(\ell)} - \mu_k^{(i)}\right)\left(\tilde{\mu}_k^{(\ell)} - \mu_k^{(i)}\right)^{\mathrm{T}} \right)$
$\quad I := I \setminus L$
until $I = \emptyset$
if $\ell > J_{\max}$, the then chose the Gaussians $\{\tilde{w}_k^{(i)}, \tilde{\mu}_k^{(i)}, \tilde{P}_k^{(i)}\}_{i=1}^{\ell}$ with the largest weights.
return the Gaussian components $\{\tilde{w}_k^{(i)}, \tilde{\mu}_k^{(i)}, \tilde{P}_k^{(i)}\}_{i=1}^{\ell}$

than some threshold, see Algorithm 9. An advantage with the PHD filter is that a hard decision, i.e., extraction of targets, is only performed for obtaining an output from the filter at each time step. The extracted targets are not used within the filter; the information about the intensity of targets remains in the filter without the need to make hard decisions, which would destroy information.

Algorithm 9 Multitarget State Extraction

Require: $\{w_k^{(i)}, \mu_k^{(i)}, P_k^{(i)}\}_{i=1}^{J_k}$ and a threshold δ_e

1: Set $\widehat{\mathbf{X}}_k = \emptyset$
2: **for** $i = 1$ **to** J_k **do**
3:     **if** $w_k^{(i)} > \delta_\mathrm{e}$ **then**
4:         **for** $j = 1$ **to** round$(w_k^{(i)})$ **do**
5:             update $\widehat{\mathbf{X}}_k = \begin{bmatrix} \widehat{\mathbf{X}}_k & \mu_k^{(i)} \end{bmatrix}$
6:         **end for**
7:     **end if**
8: **end for**
9: **return** the multitarget state estimate $\widehat{\mathbf{X}}_k$

6

Concluding Remarks

In the first part an overview of the basics behind the research reported in this thesis has been presented. This part also aims at explaining how the papers in Part II relate to each other and to the existing theory. A conclusion of the results presented in this thesis is given in Section 6.1 and ideas for future work are discussed in Section 6.2.

6.1 Conclusion

The work presented in this thesis has dealt with the problem of estimating the motion and parameters of a vehicle, as well as representing and estimating its surroundings. In this context the surroundings consist of other vehicles, stationary objects, and the road. Here, a major part of the work is not only the estimation problem itself, but also the way in which to represent the environment, i.e., building maps of stationary objects and describing the size of other vehicles.

The second part of the thesis begins in Paper A with an overview of mapping techniques used to describe a road and its closer environment. Four different types of mapping philosophies are described; beginning with so called feature based maps, where each element of the map both described the properties and location of the specific map-element. In location based maps each map-element already corresponds to a certain location and the value of the element describes only the properties in that position. Hence, feature based maps are usually rather sparse. Furthermore, road maps and intensity based maps are also summarized. The intensity based map is the main topic of paper D.

Paper B is concerned with estimating the lane geometry. The lane markings are described by a polynomial and the coefficients are the states to estimate. This problem can be solved with a camera and computer vision, but by fusing the data obtained from the image processing with information about the ego vehicle's motion and the other vehicles' movement on the road, the road geometry estimate can be improved. The other vehicles are tracked primarily by using measurements from a radar. The motion of the ego vehicle is estimated by combining measurements from the vehicle's IMU, steering wheel angle sensor and wheel velocity sensors in a model based filter. The model is in this case the so called single track model or bicycle model.

Paper C and D both deal with the problems of estimating and representing stationary objects along the edges of a road. Paper C, associates the radar measurements to extended stationary objects in the form of curved lines and tracks these lines as extended targets. The lines are modeled as polynomials and one novelty in this paper is that the approach leads to a so called errors in variables problem when noisy point measurements are associated to polynomials. The standard approach is to assume that the measurements are only noisy in one direction when associated to a line, here however noise is assumed to be present in all directions. This assumption is of course more realistic and the results are more accurate.

Paper D describes a new type of map, the intensity based map. In this paper the environment, i.e., the stationary objects, is represented by an intensity function or probability hypothesis density (PHD) as it is also called. The intensity function is described by a Gaussian mixture. This makes the representation very sparse, since only a number of sufficient statistics must be tracked, but also very rich since the extension of the Gaussian components can cover and model larger areas. It is shown how prior knowledge of the road construction can be used to both improve the update of the filter and to simplify the map representation.

Paper E and F deal with the tracking of extended moving targets. In Paper E the target is still modeled as a point target, however, it allows for obtaining more than one measurement per target. A modification of the pseudo-likelihood function used in the update step of the so called PHD filter is presented. In the standard filter one measurement can only be obtained from each target per time step. The novelty of the paper is the practical implementation of the pseudo-likelihood function and partitioning of the measurement data. In a number of simulations and experiments the advantages of the modifications are shown. A drawback is that the wrong number of targets is estimated in some rare cases, this is further discussed in the next section outlining some possible directions of future work.

In Paper F, the size and the shape of an extended target are also estimated. It is still assumed that the sensor obtains a number of point measurements. In order to associate the point measurements to the shaped target it is assumed that the measurements have been produced by a number of measurement generating points on the surface of the target. The measurement generating points are represented by a random finite set and these are only used as a means to estimate the size and the shape of the target. Only one simple simulation example is shown and also here future work will cover more situations.

The last paper, Paper G, aims at estimating the wheel radii of a vehicle. This is made under the assumption that a change in the wheel radii is related to a change in tire pressure, and that tire pressure losses can be detected using this approach. The proposed method is only based on measurements from the wheel speed sensors and the GPS position information. The wheel radii are represented with noise parameters in the state space model. The novelty lies in a Bayesian approach to estimate these time-varying noise parameters on-line using a marginalized particle filter. Experimental results of the proposed approach show many advantages, both regarding the accuracy and the reduced computational complexity, when it is compared with other methods.

The approaches in Papers A-D, and G have been evaluated on real data from both freeways and rural roads in Sweden. In Paper E data of moving pedestrians has been used. Of the seven publications in Part II six are journal papers and one is a peer-reviewed conference paper. Five of the papers are published and two are still under review.

6.2 Future Research

The radar and camera data used in this thesis is generally preprocessed. However, the preprocessing is not covered in this thesis. Specifically, more effort can be spent on the image processing to increase the information content. For example within the area of odometry the estimate could be more accurate if the camera information is used in addition to the IMU measurements. This is called visual odometry and it would probably improve the estimate of the body side slip angles, especially during extreme maneuvers where the tire road interaction is strongly nonlinear. Since only one camera is used, the inverse depth parametrization introduced by Civera et al. (2008) is an interesting approach, see e.g., Schön and Roll (2009); Nilsson et al. (2011) for automotive examples on visual odometry. To verify the state estimates, more accurate reference values are needed as well. Furthermore, the methods presented in Paper G could possibly be used as a basis to more accurately describe the road-tire interaction and thereby improve the estimate of the slip of the vehicle.

Different aspects to estimate extended objects have been discussed in this thesis, however an efficient solution on how to estimate the shape of any possible objects has not been found. Paper F, is closest to this goal, but more experimental studies must be performed and the computational time must be reduced by finding more efficient forms of representation. Also, as concluded in Paper E, the number of targets is falsely estimated in some rare cases, e.g., in the case of occlusion or not well separated targets. In that specific case, the so called cardinalized PHD filter (CPHD) is assumed to improve the results drastically, see Orguner et al. (2011). However, more experimental results must be obtained before conclusions can be drawn.

Currently there is a lot of activity within the computer vision community to enable non-planar road models, making use of parametric road models similar to the ones used in this thesis. A very interesting avenue for future work is to combine the ideas presented in this thesis with information from a camera about the height differences on the road side within a sensor fusion framework. This would probably improve the estimates, especially in situations when there are too few radar measurements available.

Bibliography

A. Abdulle and G. Wanner. 200 years of least squares method. *Elemente der Mathematik*, 57:45–60, May 2002.

M. Adams, W. S. Wijesoma, and A. Shacklock. Autonomous navigation: Achievements in complex environments. *IEEE Instrumentation & Measurement Magazine*, 10(3):15–21, June 2007.

M. Ahrholdt, F. Bengtsson, L. Danielsson, and C. Lundquist. SEFS – results on sensor data fusion system development. In *Proceedings of the World Congress on Intelligent Transportation Systems and Services*, Stockholm, Sweden, September 2009.

B. D. O. Anderson and J. B. Moore. *Optimal Filtering*. Information and system science series. Prentice Hall, Englewood Cliffs, NJ, USA, 1979.

D. Angelova and L. Mihaylova. Extended object tracking using Monte Carlo methods. *IEEE Transactions on Signal Processing*, 56(2):825–832, February 2008.

T. Ardeshiri, F. Larsson, F. Gustafsson, T. B. Schön, and M. Felsberg. Bicycle tracking using ellipse extraction. In *Proceedings of the International Conference on Information Fusion*, pages 1–8, Chicago, IL, USA, July 2011.

M. S. Arulampalam, S. Maskell, N. Gordon, and T. Clapp. A tutorial on particle filters for online nonlinear/non-Gaussian Bayesian tracking. *IEEE Transactions on Signal Processing*, 50(2):174–188, February 2002.

T. Bailey and H. Durrant-Whyte. Simultaneous localization and mapping (SLAM): Part II. *IEEE Robotics & Automation Magazine*, 13(3):108–117, September 2006.

Y. Bar-Shalom and T. E. Fortmann. *Tracking and Data Association*. Mathematics in science and engineering. Academic Press, Orlando, FL, USA, 1988.

Y. Bar-Shalom and E. Tse. Tracking in a cluttered environment with probabilistic data association. *Automatica*, 11(5):451–460, September 1975.

Y. Bar-Shalom, X. Rong Li, and T. Kirubarajan. *Estimation with Applications to Tracking and Navigation*. John Wiley & Sons, New York, NY, USA, 2001.

M. Baum and U. D. Hanebeck. Random hypersurface models for extended object tracking. In *IEEE International Symposium on Signal Processing and Information Technology*, pages 178–183, Ajman, United Arab Emirates, December 2009.

M. Baum and U. D. Hanebeck. Shape tracking of extended objects and group targets with star-convex RHMs. In *Proceedings of the International Conference on Information Fusion*, pages 338–345, Chicago, IL, USA, July 2011.

M. Baum, B. Noack, and U. D. Hanebeck. Extended object and group tracking with elliptic random hypersurface models. In *Proceedings of the International Conference on Information Fusion*, pages 1–8, Edinburgh, UK, July 2010.

T. Bayes. An essay towards solving a problem in the doctrine of chances. *The Philosophical Transactions*, 53:370–418, 1763.

R. Behringer. *Visuelle Erkennung und Interpretation des Fahrspurverlaufes durch Rechnersehen für ein autonomes Straßenfahrzeug*, volume 310 of *Fortschrittsberichte VDI, Reihe 12*. VDI Verlag, Düsseldorf, Germany, 1997. Also as: PhD Thesis, Universität der Bundeswehr, 1996.

F. Bengtsson. *Models for tracking in automotive safety systems*. Licentiate Thesis No R012/2008, Department of Signals and Systems, Chalmers University of Technology, 2008.

F. Bengtsson and L. Danielsson. Designing a real time sensor data fusion system with application to automotive safety. In *Proceedings of the World Congress on Intelligent Transportation Systems and Services*, New York, USA, November 2008.

D. P. Bertsekas. The auction algorithm for assignment and other network flow problem: a tutorial. *Interfaces*, 20(4):133–149, July 1990.

S. S. Blackman and R. Popoli. *Design and Analysis of Modern Tracking Systems*. Artech House, Norwood, MA, USA, 1999.

Y. Boers, H. Driessen, J. Torstensson, M. Trieb, R. Karlsson, and F. Gustafsson. Track-before-detect algorithm for tracking extended targets. *IEE Proceedings of Radar, Sonar and Navigation*, 153(4):345–351, August 2006.

M. Bühren and B. Yang. Simulation of automotive radar target lists using a novel approach of object representation. In *Proceedings of the IEEE Intelligent Vehicles Symposium*, pages 314–319, Tokyo, Japan, 2006.

O. Cappe, S. J. Godsill, and E. Moulines. An overview of existing methods and recent advances in sequential Monte Carlo. *Proceedings of the IEEE*, 95(5): 899–924, May 2007.

S. Challa, M. R. Morelande, D. Musicki, and R. J. Evans. *Fundamentals of Object Tracking*. Cambridge University Press, Cambridge, UK, 2011.

J. Civera, A. J. Davison, and J. Montiel. Inverse depth parametrization for monocular SLAM. *IEEE Transactions on Robotics*, 24(5):932–945, October 2008.

D. E. Clark. First-moment multi-object forward-backward smoothing. In *Proceedings of the International Conference on Information Fusion*, pages 1–6, Edinburgh, UK, July 2010.

D. J. Daley and D. Vere-Jones. *An introduction to the theory of point processes. Vol. 1 , Elementary theory and method*. Springer, New York, NY, USA, 2 edition, 2003.

L. Danielsson. *Tracking Theory for Preventive Safety Systems*. Licentiate Thesis No R004/2008, Department of Signals and Systems, Chalmers University of Technology, 2008.

L. Danielsson. *Tracking and radar sensor modelling for automotive safety systems*. PhD thesis No 3064, Department of Signals and Systems, Chalmers University of Technology, 2010.

J. Degerman, J. Wintenby, and D. Svensson. Extended target tracking using principal components. In *Proceedings of the International Conference on Information Fusion*, pages 1–8, Chicago, IL, USA, July 2011.

J. C. Dezert. Tracking maneuvering and bending extended target in cluttered environment. In *Proceedings of Signal and Data Processing of Small Targets*, volume 3373, pages 283–294, Orlando, FL, USA, April 1998. SPIE.

E. D. Dickmanns. *Dynamic Vision for Perception and Control of Motion*. Springer, London, UK, 2007.

P. M. Djuric, J. H. Kotecha, J. Zhang, Y. Huang, T. Ghirmai, M. F. Bugallo, and J. Miguez. Particle filtering. *Signal Processing Magazine, IEEE*, 20(5):19–38, September 2003.

A. Doucet, S. J. Godsill, and C. Andrieu. On sequential Monte Carlo sampling methods for Bayesian filtering. *Statistics and Computing*, 10(3):197–208, 2000.

A. Doucet, N. de Freitas, and N. Gordon, editors. *Sequential Monte Carlo Methods in Practice*. Springer Verlag, New York, USA, 2001.

O. E. Drummond, S. S. Blackman, and G. C. Pretrisor. Tracking clusters and extended objects with multiple sensors. In *Proceedings of Signal and Data Processing of Small Targets*, volume 1305, pages 362–375, Orlando, FL, USA, January 1990. SPIE.

H. Durrant-Whyte and T. Bailey. Simultaneous localization and mapping (SLAM): Part I. *IEEE Robotics & Automation Magazine*, 13(2):99–110, June 2006.

A. Eidehall. *Tracking and threat assessment for automotive collision avoidance*.

PhD thesis No 1066, Linköping Studies in Science and Technology, Linköping, Sweden, January 2007.

A. Eidehall and F. Gustafsson. Obtaining reference road geometry parameters from recorded sensor data. In *Proceedings of the IEEE Intelligent Vehicles Symposium*, pages 256–260, Tokyo, Japan, June 2006.

A. Eidehall, J. Pohl, and F. Gustafsson. Joint road geometry estimation and vehicle tracking. *Control Engineering Practice*, 15(12):1484–1494, December 2007.

O. Erdinc, P. Willett, and Y. Bar-Shalom. The bin-occupancy filter and its connection to the PHD filters. *IEEE Transactions on Signal Processing*, 57(11): 4232–4246, November 2009.

M. Feldmann, D. Fränken, and W. Koch. Tracking of extended objects and group targets using random matrices. *IEEE Transactions on Signal Processing*, 59(4): 1409–1420, April 2011.

R. A. Fisher. On an absolute criterion for fitting frequency curves. *Messenger of Mathematics*, 41:155–160, 1912.

R. A. Fisher. On the mathematical foundations of theoretical statistics. *Philosophical Transactions of the Royal Society Series A*, 222:309–368, 1922.

T. Fortmann, Y. Bar-Shalom, and M. Scheffe. Sonar tracking of multiple targets using joint probabilistic data association. *IEEE Journal of Ocean Engineering*, 8(3):173–184, July 1983.

A. Gern, U. Franke, and P. Levi. Advanced lane recognition - fusing vision and radar. In *Proceedings of the IEEE Intelligent Vehicles Symposium*, pages 45–51, Dearborn, MI, USA, October 2000.

A. Gern, U. Franke, and P. Levi. Robust vehicle tracking fusing radar and vision. In *Proceedings of the international conference of multisensor fusion and integration for intelligent systems*, pages 323–328, Baden-Baden, Germany, August 2001.

K. Gilholm and D. Salmond. Spatial distribution model for tracking extended objects. *IEE Proceedings of Radar, Sonar and Navigation*, 152(5):364–371, October 2005.

K. Gilholm, S. Godsill, S. Maskell, and D. Salmond. Poisson models for extended target and group tracking. In *Proceedings of Signal and Data Processing of Small Targets*, volume 5913, pages 230–241, San Diego, CA, USA, August 2005. SPIE.

T. D. Gillespie. *Fundamentals of Vehicle Dynamics*. SAE Society of Automotive Engineers, Warrendale, PA, USA, 1992.

I. R. Goodman, R. P. S. Mahler, and H. T. Nguyen. *Mathematics of data fusion*. Kluwer Academic, Dordrecht, 1997.

N. J. Gordon, D. J. Salmond, and A. F. M. Smith. Novel approach to nonlinear/non-Gaussian Bayesian state estimation. *IEE Proceedings on Radar and Signal Processing*, 140(5):107–113, April 1993.

K. Granström, C. Lundquist, and U Orguner. A Gaussian mixture PHD filter for extended target tracking. In *Proceedings of the International Conference on Information Fusion*, Edinburgh, UK, July 2010.

K. Granström, C. Lundquist, and U. Orguner. Extended target tracking using a Gaussian-mixture PHD filter. *IEEE Transactions on Aerospace and Electronic Systems*, 2011a. Under review.

K. Granström, C. Lundquist, and U Orguner. Tracking rectangular and elliptical extended targets using laser measurements. In *Proceedings of the International Conference on Information Fusion*, Chicago, IL, USA, July 2011b.

J. Gunnarsson. *Models and Algorithms - with applications to vehicle tracking and frequency estimation*. PhD thesis No 2628, Department of Signals and Systems, Chalmers University of Technology, June 2007.

J. Gunnarsson, L. Svensson, E Bengtsson, and L. Danielsson. Joint driver intention classification and tracking of vehicles. In *IEEE Nonlinear Statistical Signal Processing Workshop*, pages 95–98, September 2006.

J. Gunnarsson, L. Svensson, L. Danielsson, and F. Bengtsson. Tracking vehicles using radar detections. In *Proceedings of the IEEE Intelligent Vehicles Symposium*, pages 296–302, Istanbul, Turkey, June 2007.

F. Gustafsson. *Adaptive Filtering and Change Detection*. John Wiley & Sons, New York, USA, 2000.

F. Gustafsson. Automotive safety systems. *IEEE Signal Processing Magazine*, 26 (4):32–47, July 2009.

F. Gustafsson. Particle filter theory and practice with positioning applications. *IEEE Transactions on Aerospace and Electronic Systems*, 25(7):53–82, July 2010.

G. Hendeby. *Performance and Implementation Aspects of Nonlinear Filtering*. PhD thesis No 1161, Linköping Studies in Science and Technology, Linköping, Sweden, February 2008.

J. Jansson. *Collision Avoidance Theory with Applications to Automotive Collision Mitigation*. PhD thesis No 950, Linköping Studies in Science and Technology, Linköping, Sweden, June 2005.

A. H. Jazwinski. *Stochastic processes and filtering theory*. Mathematics in science and engineering. Academic Press, New York, USA, 1970.

K. H. Johansson, M. Törngren, and L. Nielsen. Vehicle applications of controller area network. In D. Hristu-Varsakelis and W. S. Levine, editors, *Handbook of Networked and Embedded Control Systems*, pages 741–765. Birkhäuser, 2005.

S. J. Julier. The scaled unscented transformation. In *Proceedings of the American Control Conference*, volume 6, pages 4555–4559, 2002.

S. J. Julier and J. K. Uhlmann. New extension of the Kalman filter to nonlinear systems. In *Signal Processing, Sensor Fusion, and Target Recognition VI*, volume 3068, pages 182–193, Orlando, FL, USA, 1997. SPIE.

S. J. Julier and J. K. Uhlmann. Reduced sigma point filters for the propagation of means and covariances through nonlinear transformations. In *Proceedings of the American Control Conference*, volume 2, pages 887–892, 2002.

S. J. Julier and J. K. Uhlmann. Unscented filtering and nonlinear estimation. *Proceedings of the IEEE*, 92(3):401–422, March 2004.

S. J. Julier, J. K. Uhlmann, and H. F. Durrant-Whyte. A new approach for filtering nonlinear systems. In *American Control Conference, 1995. Proceedings of the*, volume 3, pages 1628–1632, Jun 1995.

T. Kailath. *Linear systems*. Prentice Hall, Englewood Cliffs, NJ, USA, 1980.

T. Kailath, A. H. Sayed, and B. Hassibi. *Linear Estimation*. Information and System Sciences Series. Prentice Hall, Upper Saddle River, NJ, USA, 2000.

R. E. Kalman. A new approach to linear filtering and prediction problems. *Transactions of the ASME, Journal of Basic Engineering*, 82:35–45, 1960.

R. Karlsson. *Particle Filtering for Positioning and Tracking Applications*. PhD thesis No 924, Linköping Studies in Science and Technology, Linköping, Sweden, March 2005.

S. M. Kay. *Fundamentals of Statistical Signal Processing, Volume I: Estimation Theory*. Prentice Hall Signal Processing. Prentice Hall, Upper Saddle River, NJ, USA, 1993.

U. Kiencke, S. Dais, and M. Litschel. Automotive serial controller area network. Technical Report 860391, SAE International Congress, 1986.

J. W. Koch. Bayesian approach to extended object and cluster tracking using random matrices. *IEEE Transactions on Aerospace and Electronic Systems*, 44 (3):1042–1059, July 2008.

M. E. Liggins, D. L. Hall, and J. Llinas. *Handbook of multisensor data fusion : theory and practice*. CRC Press, Boca Raton, FL, USA, 2 edition, 2009.

L. Lin, Y. Bar-Shalom, and T. Kirubarajan. Data association combined with the probability hypothesis density filter for multitarget tracking. In *Proceedings of Signal and Data Processing of Small Targets*, volume 5428, pages 464–475, Orlando, FL, USA, 2004. SPIE.

L. Ljung. *System identification, Theory for the user*. System sciences series. Prentice Hall, Upper Saddle River, NJ, USA, 2 edition, 1999.

C. Lundquist. *Automotive Sensor Fusion for Situation Awareness*. Licentiate Thesis No 1422, Department of Electrical Engineering, Linköping University, Sweden, 2009.

C. Lundquist. Method for stabilizing a vehicle combination. U.S. Patent US 8010253 August 30, 2011 and German Patent Application DE 102007008342 August 21, 2008, Priority date February 20, 2007.

C. Lundquist and R. Großheim. Method and device for determining steering angle information. German Patent Application DE 10 2007 000 958 Mai 14, 2009, International Patent Application WO 2009 047 020 April 16, 2009 and European Patent Application EP 2205478 April 16, 2009, Priority date October 2, 2007.

C. Lundquist and W. Reinelt. Back driving assistant for passenger cars with trailer. In *Proceedings of the SAE World Congress*, SAE paper 2006-01-0940, Detroit, MI, USA, April 2006a.

C. Lundquist and W. Reinelt. Rückwärtsfahrassistent für PKW mit Aktive Front Steering. In *Proceedings of the AUTOREG (Steuerung und Regelung von Fahrzeugen und Motoren*, VDI Bericht 1931, pages 45–54, Wiesloch, Germany, March 2006b.

C. Lundquist and W. Reinelt. Electric motor rotor position monitoring method for electrically aided steering system e.g. steer by wire, for motor vehicle, involves outputting alarm when difference between measurement value and estimated value of motor exceeds threshold. German Patent Application DE 102005016514 October 12, 2006, Priority date April 8, 2006.

C. Lundquist and T. B. Schön. Road geometry estimation and vehicle tracking using a single track model. In *Proceedings of the IEEE Intelligent Vehicles Symposium*, pages 144–149, Eindhoven, The Netherlands, June 2008.

C. Lundquist and T. B. Schön. Estimation of the free space in front of a moving vehicle. In *Proceedings of the SAE World Congress*, SAE paper 2009-01-1288, Detroit, MI, USA, April 2009a.

C. Lundquist and T. B. Schön. Recursive identification of cornering stiffness parameters for an enhanced single track model. In *Proceedings of the IFAC Symposium on System Identification*, pages 1726–1731, Saint-Malo, France, July 2009b.

C. Lundquist and T. B. Schön. Joint ego-motion and road geometry estimation. *Information Fusion*, 12:253–263, October 2011.

C. Lundquist, U. Orguner, and T. B. Schön. Tracking stationary extended objects for road mapping using radar measurements. In *Proceedings of the IEEE Intelligent Vehicles Symposium*, pages 405–410, Xi'an, China, June 2009.

C. Lundquist, L. Danielsson, and F. Gustafsson. Random set based road mapping using radar measurements. In *Proceedings of the European Signal Processing Conference*, pages 219–223, Aalborg, Denmark, August 2010a.

C. Lundquist, U. Orguner, and F Gustafsson. Estimating polynomial structures from radar data. In *Proceedings of the International Conference on Information Fusion*, Edinburgh, UK, July 2010b.

C. Lundquist, K. Granström, and U. Orguner. Estimating the shape of targets with a PHD filter. In *Proceedings of the International Conference on Information Fusion*, Chicago, IL, USA, July 2011a.

C. Lundquist, L. Hammarstrand, and F. Gustafsson. Road intensity based mapping using radar measurements with a probability hypothesis density filter. *IEEE Transactions on Signal Processing*, 59(4):1397–1408, April 2011b.

C. Lundquist, U. Orguner, and F. Gustafsson. Extended target tracking using polynomials with applications to road-map estimation. *IEEE Transactions on Signal Processing*, 59(1):15–26, January 2011c.

C. Lundquist, E. Özkan, and F. Gustafsson. Tire radii estimation using a marginalized particle filter. *IEEE Transactions on Intelligent Transportation Systems*, 2011d. Submitted.

C. Lundquist, T. B. Schön, and F. Gustafsson. Situational awareness and road prediction for trajectory control applications. In A. Eskandarian, editor, *Handbook of Intelligent Vehicles*, chapter 24. Springer, November 2011e.

C. Lundquist, M. Skoglund, K. Granström, and T. Glad. How peer-review affects student learning. In *Utvecklingskonferens för Sveriges ingenjörsutbildingar*, Norrköping, Sweden, November 2011f.

R. P. S. Mahler. Multitarget Bayes filtering via first-order multitarget moments. *IEEE Transactions on Aerospace and Electronic Systems*, 39(4):1152–1178, October 2003.

R. P. S. Mahler. Statistics 101 for multisensor, multitarget data fusion. *IEEE Transactions on Aerospace and Electronic Systems*, 19(1):53–64, January 2004.

R. P. S. Mahler. *Statistical Multisource-Multitarget Information Fusion*. Artech House, Boston, MA, USA, 2007a.

R. P. S. Mahler. PHD filters of higher order in target number. *IEEE Transactions on Aerospace and Electronic Systems*, 43(4):1523–1543, October 2007b.

R. P. S. Mahler. PHD filters for nonstandard targets, I: Extended targets. In *Proceedings of the International Conference on Information Fusion*, pages 915–921, Seattle, WA, USA, July 2009a.

R. P. S. Mahler. Random set theory for multisource-multitarget information fusion. In M. E. Liggins, D. L. Hall, and J. Llinas, editors, *Handbook of multisensor data fusion: theory and practice*, chapter 16. CRC Press, Boca Raton, FL, 2 edition, November 2009b.

R. P. S. Mahler, B.-N. Vo, and B.-T. Vo. The forward-backward probability hypothesis density smoother. In *Proceedings of the International Conference on Information Fusion*, pages 1–8, Edinburgh, UK, July 2010.

S. Malinen, C. Lundquist, and W. Reinelt. Fault detection of a steering wheel sensor signal in an active front steering system. In *Preprints of the IFAC Symposium on SAFEPROCESS*, pages 547–552, Beijing, China, August 2006.

M. Mitschke and H. Wallentowitz. *Dynamik der Kraftfahrzeuge*. Springer, Berlin, Heidelberg, 4 edition, 2004.

E. Nilsson, C. Lundquist, T. B. Schön, D. Forslund, and J. Roll. Vehicle motion estimation using an infrared camera. In *Proceedings of the World Congress of the International Federation of Automatic Control*, Milan, Italy, August 2011.

U. Orguner, C. Lundquist, and K. Granström. Extended target tracking with a cardinalized probability hypothesis density filter. In *Proceedings of the International Conference on Information Fusion*, pages 65–72, Chicago, IL, USA, July 2011.

E. Özkan, C. Lundquist, and F. Gustafsson. A Bayesian approach to jointly estimate tire radii and vehicle trajectory. In *Proceedings of the IEEE Conference on Intelligent Transportation Systems*, Washington DC, USA, October 2011.

K. Panta, B.-N. Vo, S. Singh, and A. Doucet. Probability hypothesis density filter versus multiple hypothesis tracking. In *Signal Processing, Sensor Fusion, and Target Recognition XIII*, volume 5429, pages 284–295, Orlando, FL, USA, 2004. SPIE.

R. Rajamani. *Vehicle Dynamics and Control*. Springer, Boston, MA, USA, 2006. ISBN 978-0-387-28823-9.

G. Reimann and C. Lundquist. Method for operating electronically controlled servo steering system of motor vehicle, involves determining steering wheel angle as measure for desired steering handle angle by steering handle for steering wheels of motor vehicle. German Patent Application DE 102006053029 May 15, 2008, Priority date November 10, 2006.

W. Reinelt and C. Lundquist. Observer based sensor monitoring in an active front steering system using explicit sensor failure modeling. In *Proceedings of the IFAC World Congress*, Prague, Czech Republic, July 2005.

W. Reinelt and C. Lundquist. Mechatronische Lenksysteme: Modellbildung und Funktionalität des Active Front Steering. In R. Isermann, editor, *Fahrdynamik Regelung - Modellbildung, Fahrassistenzsysteme, Mechatronik*, pages 213–236. Vieweg Verlag, September 2006a.

W. Reinelt and C. Lundquist. Controllability of active steering system hazards: From standards to driving tests. In Juan R. Pimintel, editor, *Safety Critical Automotive Systems*, pages 173–178. SAE International, 400 Commonwealth Drive, Warrendale, PA, USA, August 2006b.

W. Reinelt and C. Lundquist. Method for assisting the driver of a motor vehicle with a trailer when reversing. German Patent DE 10 2006 002 294 February 24, 2011, European Patent Application EP 1810913 July 25, 2007 and Japanese Patent Application JP 2007191143 August 2, 2007, Priority date January 18, 2006.

W. Reinelt, W. Klier, G. Reimann, C. Lundquist, W. Schuster, and R. Großheim. Active front steering for passenger cars: System modelling and functions. In *Proceedings of the IFAC Symposium on Advances in Automotive Control*, Salerno, Italy, April 2004.

W. Reinelt, C. Lundquist, and H. Johansson. On-line sensor monitoring in an active front steering system using extended Kalman filtering. In *Proceedings of the SAE World Congress*, SAE paper 2005-01-1271, Detroit, MI, USA, April 2005.

W. Reinelt, W. Schuster, R. Großheim, and C. Lundquist. Motor vehicle's electronically regulated servo steering system operating method, involves comparing actual value of measured value with stored practical value of corresponding measured value. German Patent DE 10 2006 040 443 January 27, 2011, Priority date August 29, 2006.

W. Reinelt, W. Schuster, R. Großheim, and C. Lundquist. Operating method for electronic servo steering system of vehicle, involves presetting steering wheel angle by steering mechanism as measure for desired wheel turning angle for steering wheel of vehicle. German Patent Application DE 102006052092 May 8, 2008, Priority date November 4, 2006.

W. Reinelt, C. Lundquist, and S. Malinen. Automatic generation of a computer program for monitoring a main program to provide operational safety. German Patent Application DE 102005049657 April 19, 2007, Priority date October 18, 2005.

W. Reinelt, W. Schuster, R. Großheim, and C. Lundquist. Electronic servo steering system operating method for motor vehicle, involves recognizing track misalignment of vehicle when forces differentiate around preset value from each other at preset period of time in magnitude and/or direction. German Patent DE 102006043069 December 3, 2009, Priority date September 14, 2006.

W. Reinelt, W. Schuster, R. Großheim, and C. Lundquist. Operating method for electronic power-assisted steering system of vehicle, involves overlapping additional angle, which is disabled after re-start of utility function. German Patent Application DE 102006041236 Mars 6, 2008, Priority date September 2, 2006a.

W. Reinelt, W. Schuster, R. Großheim, and C. Lundquist. Operating method for electronic power-assisted steering system of vehicle, involves re-starting utility function, and after re-start of utility function superimposition of additional angle is unlatched. German Patent DE 102006041237 December 3, 2009, Priority date September 2, 2006b.

B. Ristic and D. J. Salmond. A study of a nonlinear filtering problem for tracking an extended target. In *Proceedings of the International Conference on Information Fusion*, pages 503–509, Stockholm, Sweden, June 2004.

B. Ristic, S. Arulampalam, and N. Gordon. *Beyond the Kalman Filter: Particle filters for tracking applications*. Artech House, London, UK, 2004.

X. Rong Li and V. P. Jilkov. Survey of maneuvering target tracking: Part III. Measurement models. In *Proceedings of Signal and Data Processing of Small Targets*, volume 4473, pages 423–446, San Diego, CA, USA, 2001. SPIE.

X. Rong Li and V. P. Jilkov. Survey of maneuvering target tracking: Part I. Dynamic models. *IEEE Transactions on Aerospace and Electronic Systems*, 39(4): 1333–1364, October 2003.

M. Roth and F. Gustafsson. An efficient implementation of the second order extended Kalman filter. In *Proceedings of the International Conference on Information Fusion*, pages 1–6, July 2011.

W. J. Rugh. *Linear System Theory*. Information and system sciences series. Prentice Hall, Upper Saddle River, NJ, USA, 2 edition, 1996.

D. J. Salmond and M. C. Parr. Track maintenance using measurements of target extent. *IEE Proceedings of Radar, Sonar and Navigation*, 150(6):389–395, December 2003.

S. F. Schmidt. Application of state-space methods to navigation problems. *Advances in Control Systems*, 3:293–340, 1966.

B. Schofield. *Model-Based Vehicle Dynamics Control for Active Safety*. PhD thesis, Department of Automatic Control, Lund University, Sweden, September 2008.

T. B. Schön. *Estimation of Nonlinear Dynamic Systems – Theory and Applications*. PhD thesis No 998, Linköping Studies in Science and Technology, Department of Electrical Engineering, Linköping University, Sweden, February 2006.

T. B. Schön and J. Roll. Ego-motion and indirect road geometry estimation using night vision. In *Proceedings of the IEEE Intelligent Vehicles Symposium*, pages 30–35, Xi'an, China, June 2009.

T. B. Schön, F. Gustafsson, and P.-J. Nordlund. Marginalized particle filters for mixed linear/nonlinear state-space models. *IEEE Transactions on Signal Processing*, 53(7):2279–2289, July 2005.

T. B. Schön, A. Eidehall, and F. Gustafsson. Lane departure detection for improved road geometry estimation. In *Proceedings of the IEEE Intelligent Vehicles Symposium*, pages 546–551, Tokyo, Japan, June 2006.

T. B. Schön, D. Törnqvist, and F. Gustafsson. Fast particle filters for multi-rate sensors. In *Proceedings of the 15th European Signal Processing Conference*, Poznań, Poland, September 2007.

H. Sidenbladh. Multi-target particle filtering for the probability hypothesis density. In *Proceedings of the International Conference on Information Fusion*, volume 2, pages 800–806, Cairns, Australia, March 2003.

G. L. Smith, S. F. Schmidt, and L. A. McGee. Application of statistical filter theory to the optimal estimation of position and velocity on board a circumlunar vehicle. Technical Report TR R-135, NASA, 1962.

J. Sörstedt, L. Svensson, F. Sandblom, and L. Hammarstrand. A new vehicle motion model for improved predictions and situation assessment. *IEEE Transactions on Intelligent Transportation Systems*, 2011. ISSN 1524-9050. doi: 10.1109/TITS.2011.2160342.

R. L. Streit. Multisensor multitarget intensity filter. In *Proceedings of the International Conference on Information Fusion*, pages 1–8, Cologne, Germany, July 2008.

R. L. Streit. *Poisson Point Processes*. Springer, 1 edition, 2010.

R. L. Streit and L. D. Stone. Bayes derivation of multitarget intensity filters. In *Proceedings of the International Conference on Information Fusion*, pages 1–8, Cologne, Germany, July 2008.

L. Svensson and J. Gunnarsson. A new motion model for tracking of vehicles. In *Proceedings of the 14th IFAC Symposium on System Identification*, Newcastle, Australia, 2006.

A. Swain and D. Clark. Extended object filtering using spatial independent cluster processes. In *Proceedings of the International Conference on Information Fusion*, pages 1–8, Edinburgh, UK, July 2010.

S. Thrun. Robotic mapping: A survey. In *Exploring Artificial Intelligence in the New Millenium*. Morgan Kaufmann, 2002.

H. L. van Trees. *Detection, Estimation, and Modulation Theory*. John Wiley & Sons, New York, NY, USA, 1968.

J. Vermaak, N. Ikoma, and S. J. Godsill. Sequential Monte Carlo framework for extended object tracking. *IEE Proceedings of Radar, Sonar and Navigation*, 152 (5):353–363, October 2005.

B.-N. Vo and W.-K. Ma. The Gaussian mixture probability hypothesis density filter. *IEEE Transactions on Signal Processing*, 54(11):4091–4104, November 2006.

B.-N. Vo, S. Singh, and A. Doucet. Random finite sets and sequential Monte Carlo methods in multi-target tracking. In *Proceedings of the International Radar Conference*, pages 486–491, Adelaide, Australia, September 2003.

B.-N. Vo, B.-T. Vo, and R. P. S. Mahler. A closed form solution to the probability hypothesis density smoother. In *Proceedings of the International Conference on Information Fusion*, pages 1–8, Edinburgh, UK, July 2010.

B.-N. Vo, B.-T. Vo, and R. P. S. Mahler. Closed form solutions to forward-backward smoothing. *IEEE Transactions on Signal Processing*, 2011. doi: 10.1109/TSP.2011.2168519.

B.-T. Vo, B.-N. Vo, and A. Cantoni. Analytic implementations of the cardinalized probability hypothesis density filter. *IEEE Transactions on Signal Processing*, 55(7):3553–3567, July 2007.

N. Wahlström, J. Callmer, and F. Gustafsson. Single target tracking using vector magnetometers. In *IEEE Conference on Acoustics, Speech and Signal Processing*, pages 4332–4335, Prague, Czech Republic, May 2011.

A. Wald. Sequential tests of statistical hypotheses. *The Annals of Mathematical Statistics*, 16(2):117–186, June 1945.

M. J. Waxman and O. E. Drummond. A bibliography of cluster (group) tracking. In *Proceedings of Signal and Data Processing of Small Targets*, volume 5428, pages 551–560, Orlando, FL, USA, April 2004. SPIE.

M. Wieneke and S. J. Davey. Histogram PMHT with target extent estimates based on random matrices. In *Proceedings of the International Conference on Information Fusion*, pages 1–8, Chicago, IL, USA, July 2011.

J. Y. Wong. *Theory Of Ground Vehicles*. John Wiley & Sons, New York, USA, 3 edition, 2001.

T. Zajic and R. P. S. Mahler. Particle-systems implementation of the PHD multitarget-tracking filter. In *Signal Processing, Sensor Fusion, and Target Recognition XII*, volume 5096, pages 291–299, Orlando, FL, USA, April 2003. SPIE.

Z. Zomotor and U. Franke. Sensor fusion for improved vision based lane recognition and object tracking with range-finders. In *Proceedings of the IEEE Conference on Intelligent Transportation Systems*, pages 595–600, Boston, MA, USA, November 1997.